Degradation and Stability of Polymers: The Role of Aggregation Structure and a New Stabilization Method

Guangxian Li

College of polymer science and engineering, State key laboratory of polymer materials engineering, Sichuan University, Chengdu 610065, China

Outline

四川大學 Sichuan University

- ☐ Introduction
- ☐ Effects of aggregation structures on the degradation:
  - Crystallization
  - Orientation
  - Phase domain
- ☐ New stabilization method
- ☐ Outdoor degradation behaviors of different polymers under typical climatic regions in China

Introduction

四川大學 Sichuan University

☐ Degradation of polymers

- There are **two critical factors** governing the degradation of polymers:
  (1) **Permeability of environmental medium** (Light, oxygen, solvent etc.)
  (2) **formation of free radicals**

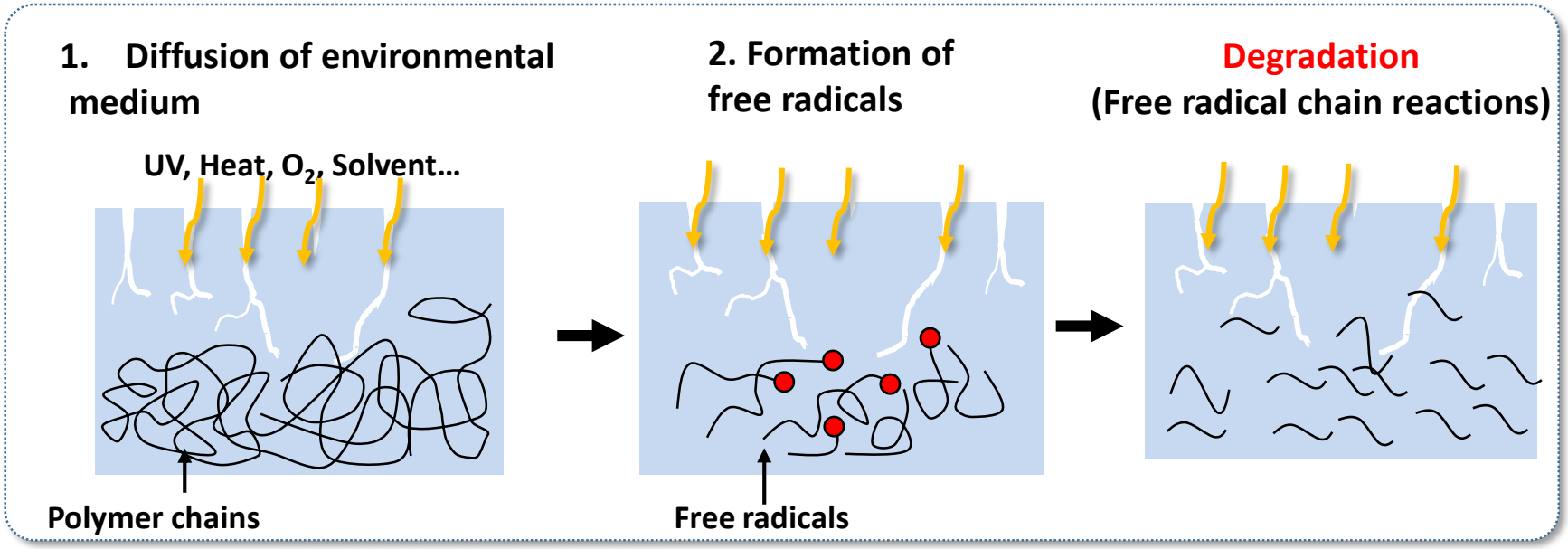

☐ Major efforts so far focused on the elimination of free radicals by using anti-aging additives

➢ Scavenge radicals

✓ **Alkyl radicals**

- **Hindered Amine Stabilizers (HAS)**

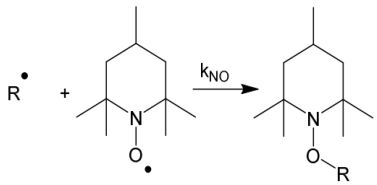

✓ **Peroxy radicals** O—O

- **Primary antioxidant (phenolic antioxidant)**
- **HAS**

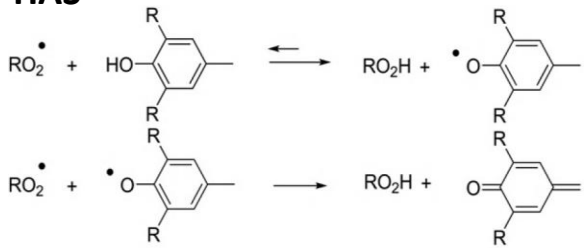

➢ Forestall hydroperoxides

✓ **Hydroperoxide** O—OH

- **Secondary antioxidant (trivalent phosphorous, thioethers)**
- **HAS**

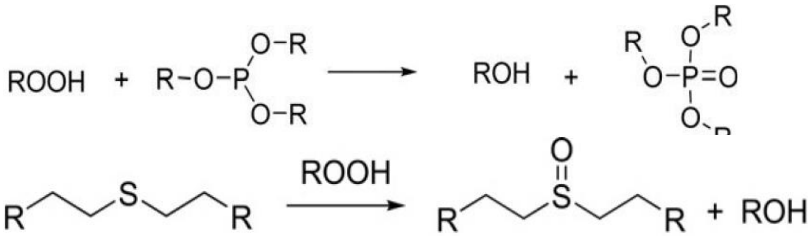

- **To prevent the degradation of polymers, small-molecule stabilizers are widely used which act by interrupting in the free radicals reaction cycle**

Smith, Accounts of Chemical Research, 2018, 51, 2006; Gijsman, Polymer Degradation and Stability, 2017, 145, 2

Is there any way else to control the degradation? block the channel of permeability of environment factors

Structuring of aggregation of polymers

- **Crystallization**

Crystallinity (%)	Free volume radius (nm)
5 ↓	0.35 ↓
27	0.33

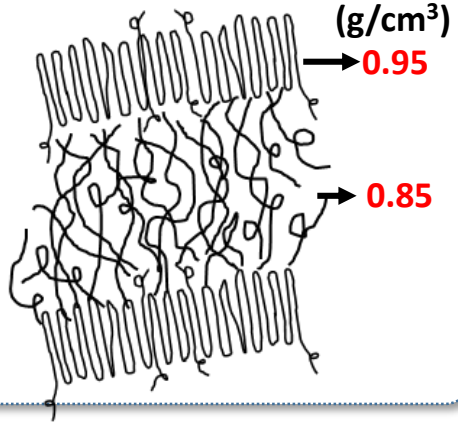

- **Crosslinking**

Crosslinking density x 10^4 (mol/cm³)	Free volume radius (nm)
0 ↓	0.34 ↓
3.4	0.32

- **Orientation of polymer chains**

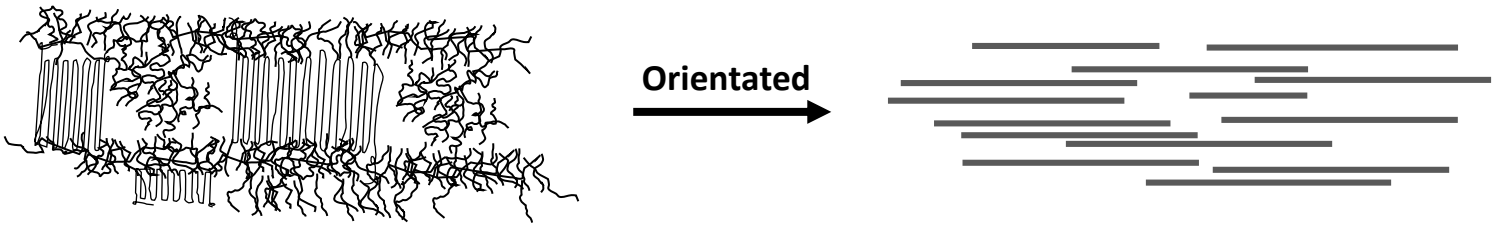

Lin, Macromolecules 2005; S. Zekriardehani, Macromolecules 50(7) (2017) 2845-2855. K. Bandzierz, Materials 9(7) (2016) 607.

- **Adding barring fillers in polymer matrix ; or producing multiphase materials**

✓ **Nano sheet filler (Graphene)**

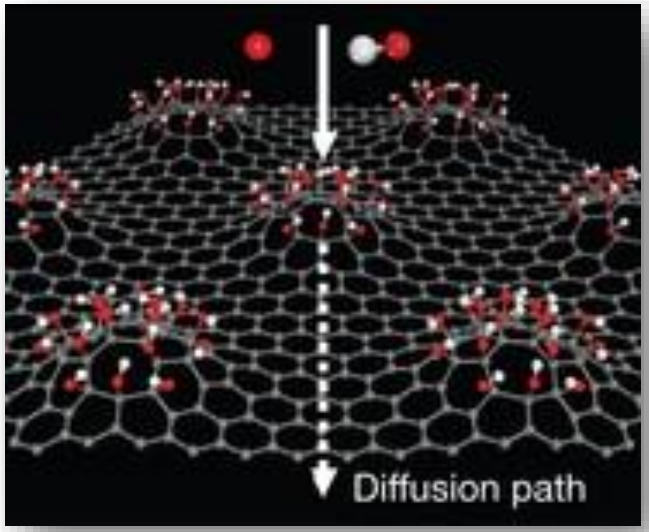

O_2 size: 0.30 nm; Mesh size: 0.28 nm

✓ **Phase separated structure**

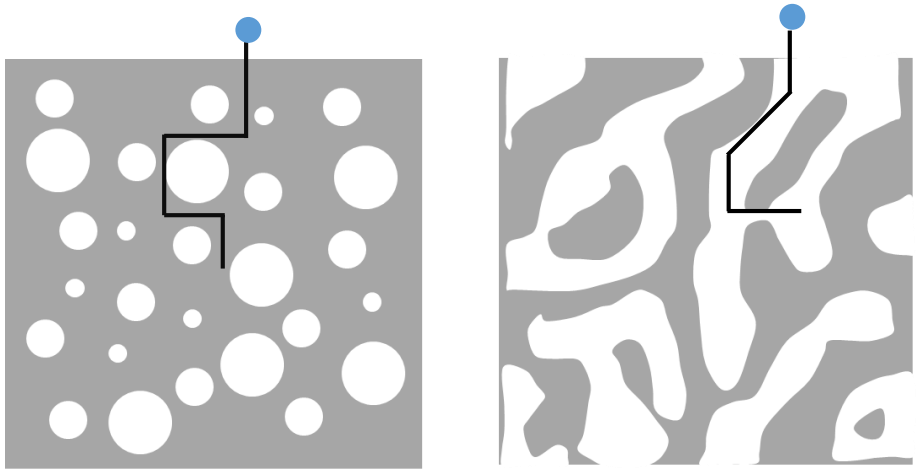

Dispersed Co-continuous

Phase size: 100 nm – 100 µm

- **Aggregation structures might be used for governing the diffusion of environmental factors, by changing the available space for diffusing channel**

Adv. Mater. 2010, 22, 4759; Nanoscale, 2010, 2, 373

Case 1:
Crystallized polymers

Controlling the permeability by adjusting crystallization (crystallinity, lamellae size and crystal forms)

- Crystallinity

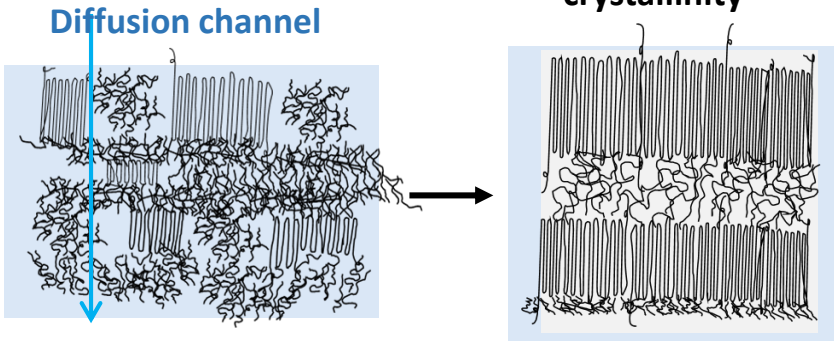

- Lamellae size

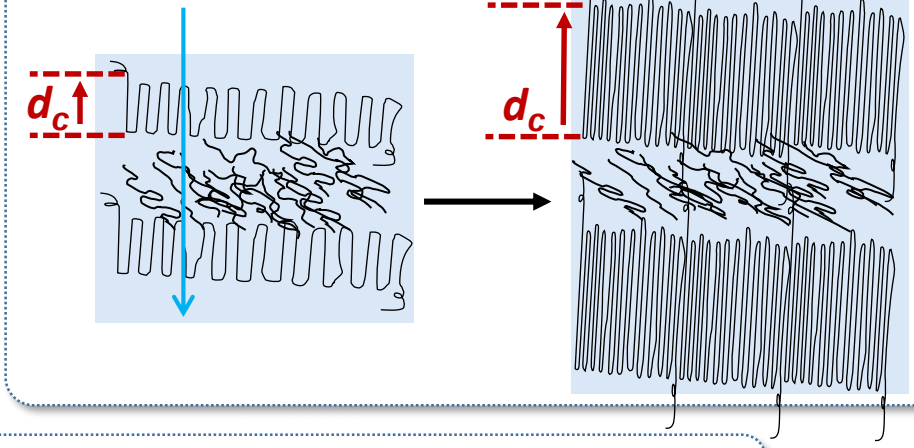

- Crystal forms
  - ✓ α spherulites (~100 um)
  - ✓ β sheet (~10 um)

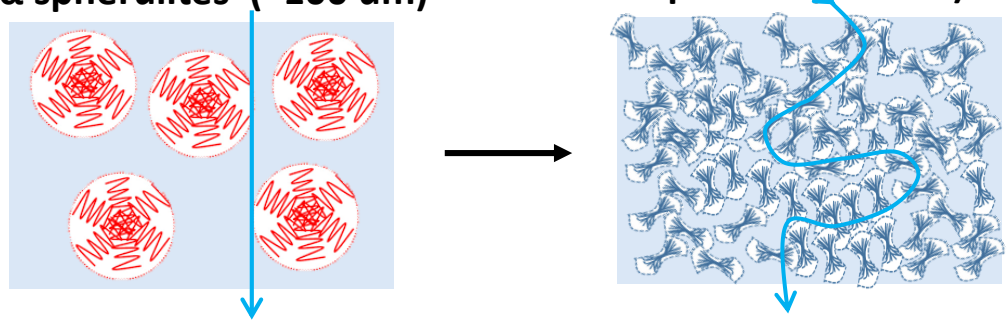

- **Crystalline structures** would decline the diffusion probability of environmental factors, which play critical roles in the degradation of polymers

1. iPP: Annealing changes the crystallinity and lamellae size

➢ **Effects of annealing time on crystal structures at different temperatures**

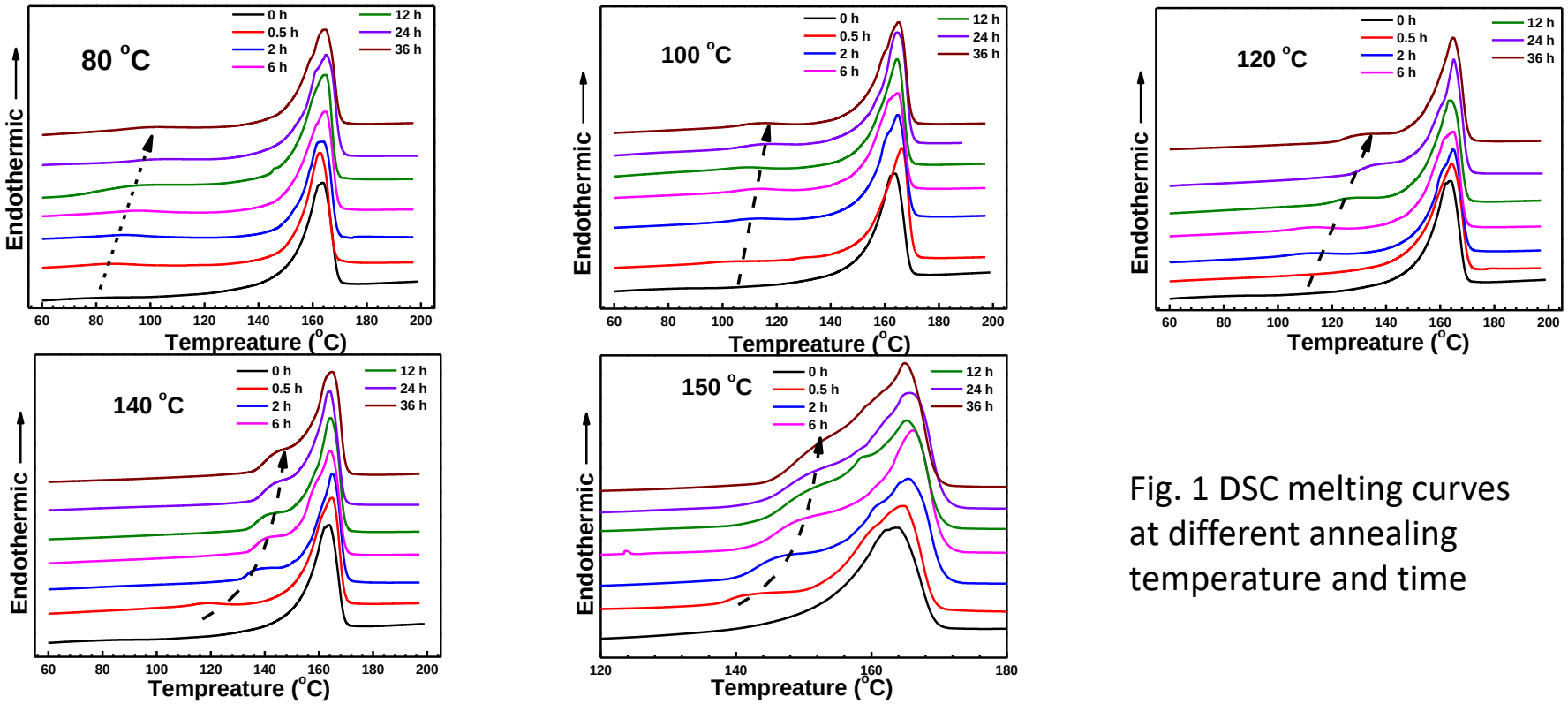

Fig. 1 DSC melting curves at different annealing temperature and time

- **Annealing induced secondary crystallization: increase in crystallinity; thickening of crystals**

Q Liu, GX Li, Polymer Degradation and Stability, 2019, 162, 180

➢ Effects of annealing time on crystal structures

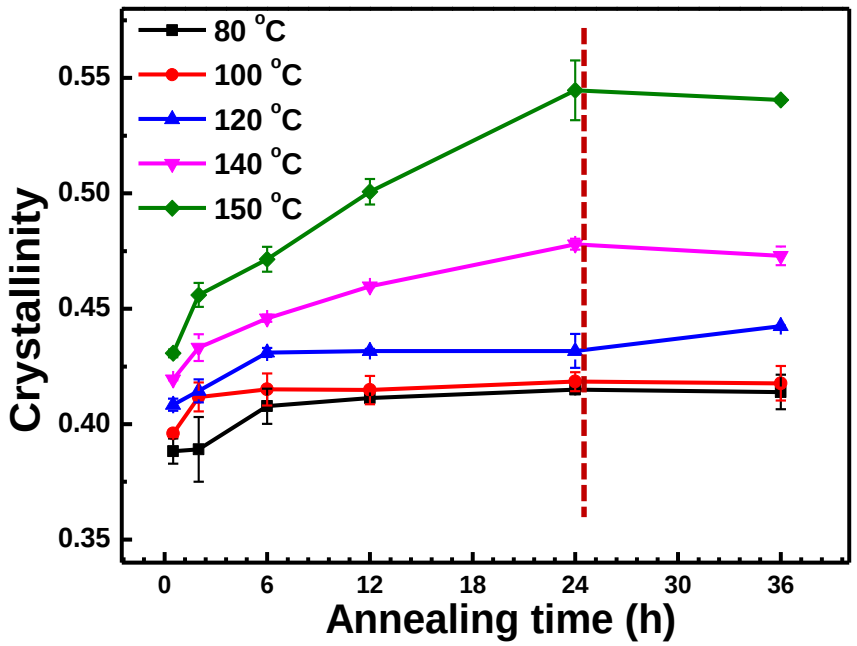

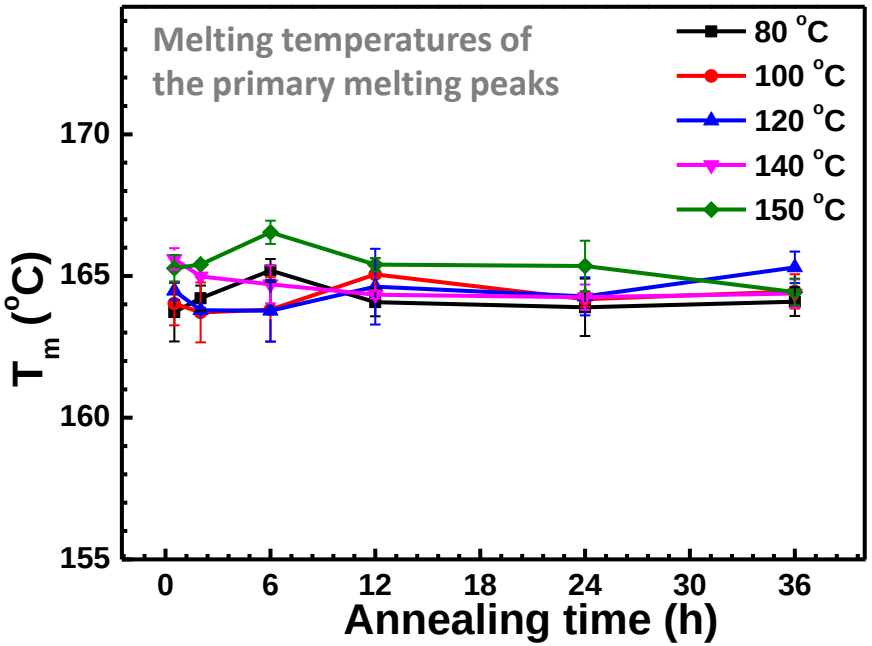

Fig. 2 Crystallinity and T_m vs. annealing time

- **Crystallinity increases with increasing annealing time due to the secondary crystallization, which becomes stable after 24 h**
- **Primary melting temperature does not change too much**

➢ Effects of annealing temperature on crystal structure

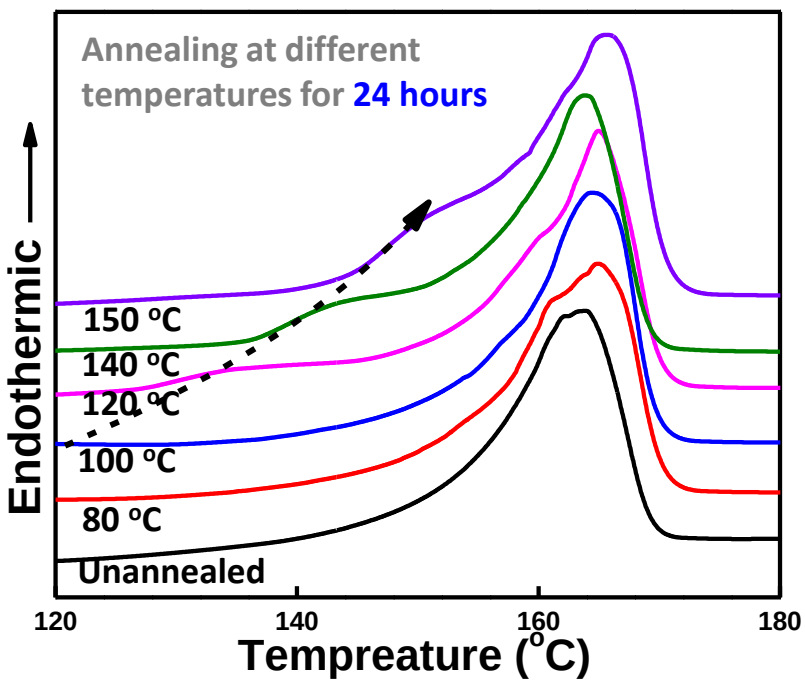

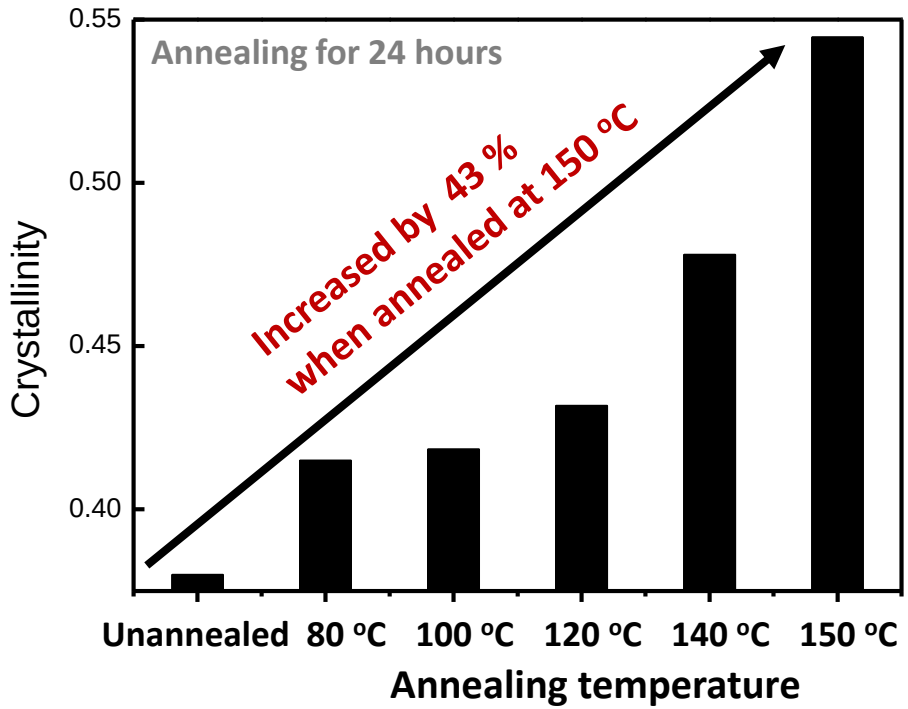

Fig. 3 DSC melting curves at different annealing temperature, and crystallinity vs. annealing temperature

- **Increasing temperature will enhance crystallinity remarkably (up to 55%)**

➢ Effects of annealing temperature on lamellae size

$$K(z) = \frac{\int I(q)q^2 \cos(qz)dq}{\int I(q)q^2 dq}$$

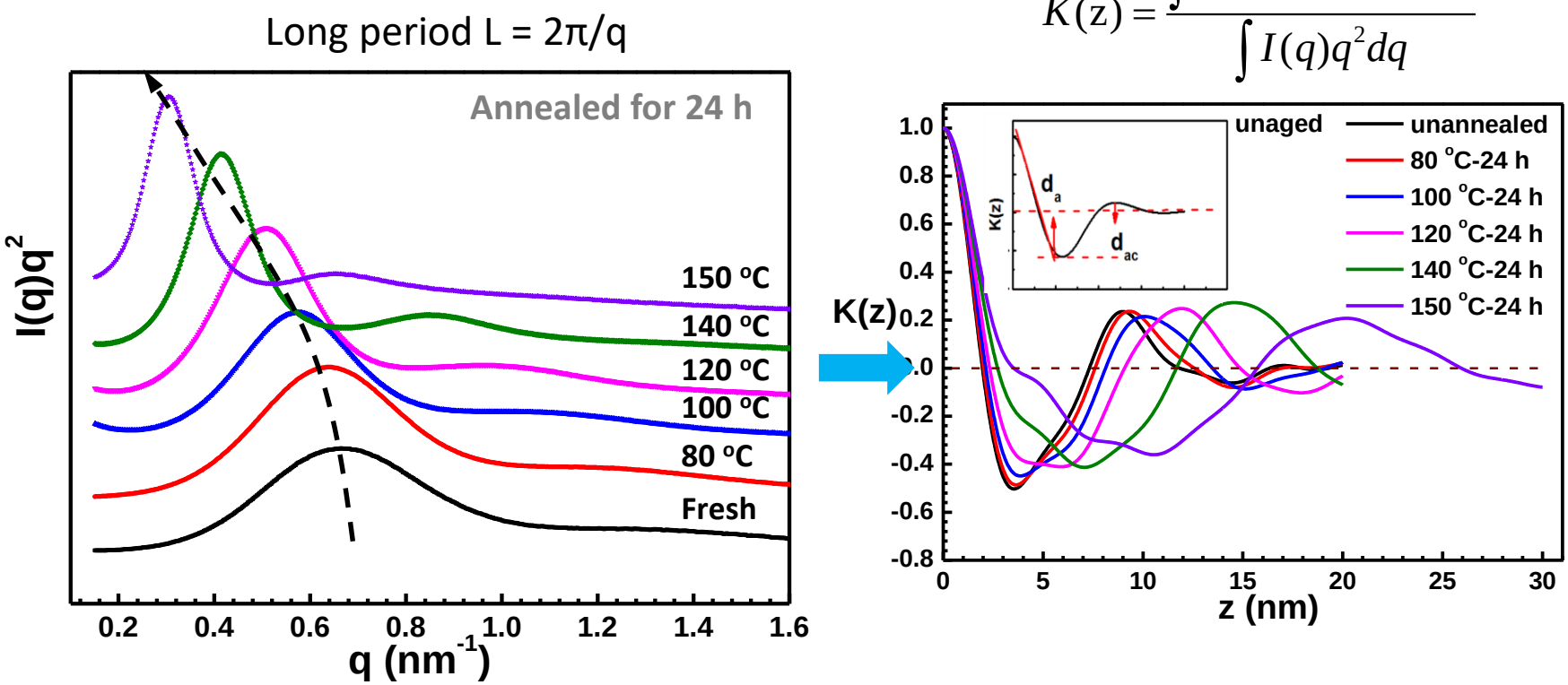

Fig. 4 **SAXS curves** and corresponding correlation function at different annealing temperature

- **Annealing induced SAXS curves shift to lower q, the thickening of lamellae**

➢ Effects of annealing temperature on lamellae size

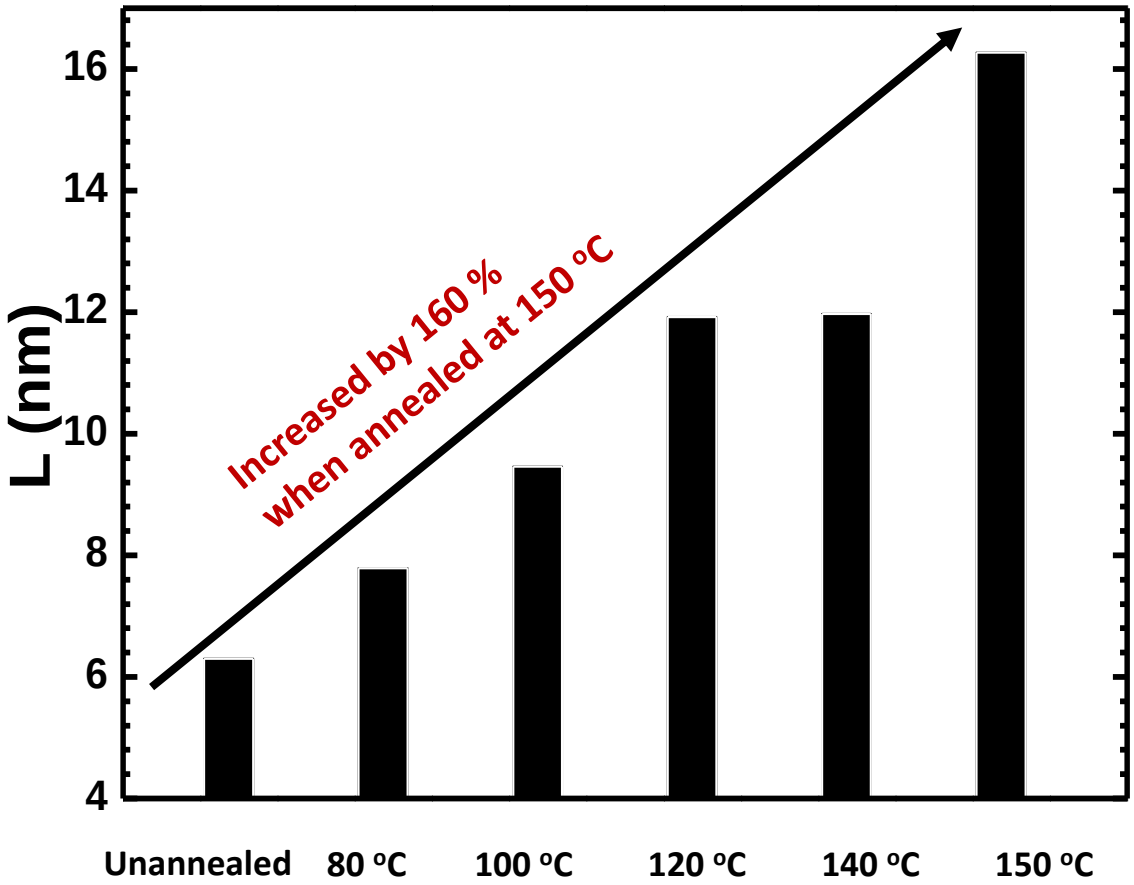

Fig. 5 Lamellae size calculated based on SAXS data vs. annealing temperature

- **Annealing leads to the thickening of lamellae up to ~ 16 µm**

➢ Effects of annealing on storage modulus

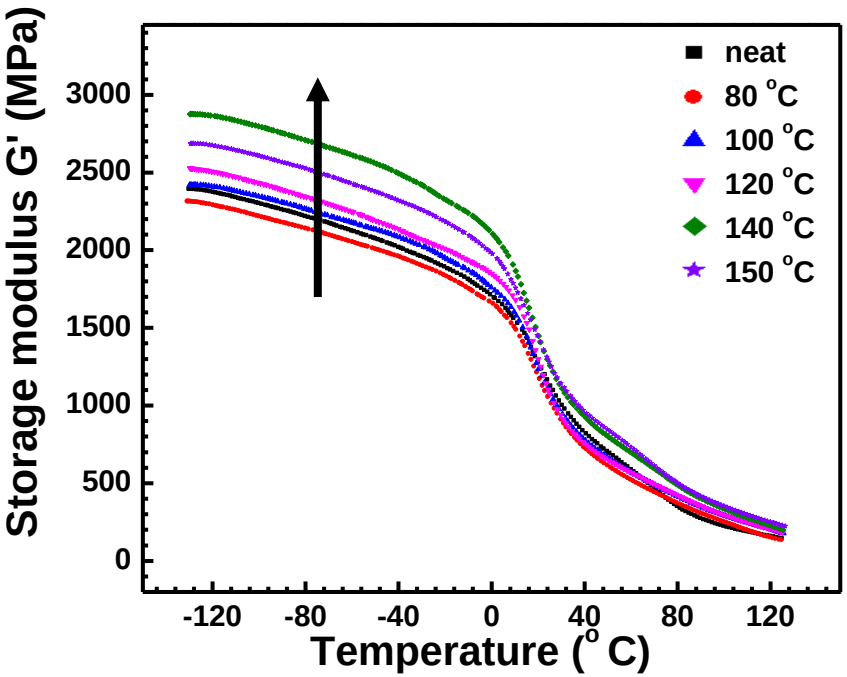

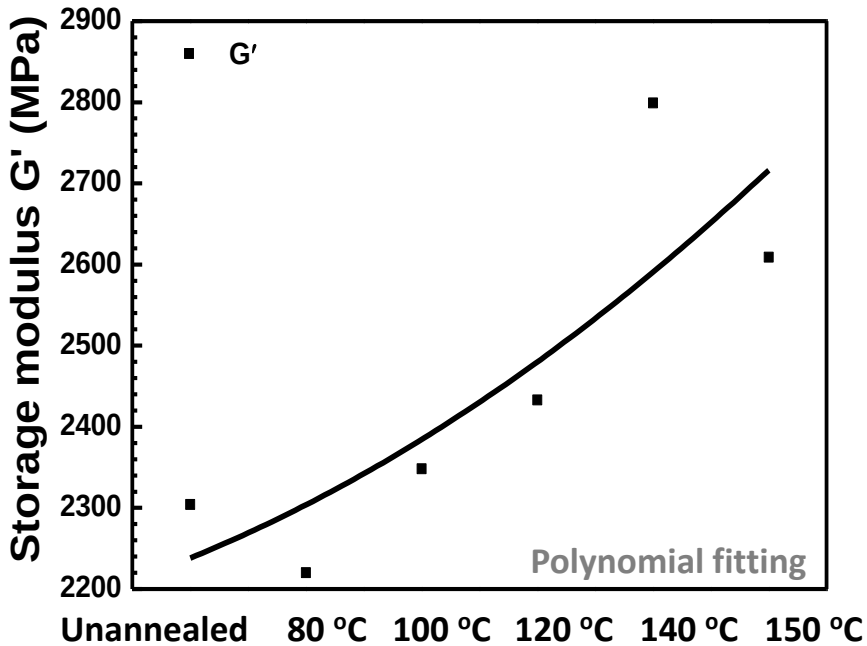

Fig. 6 (a) Storage modulus vs. annealing temperature measured by DMA

- **Annealing enhances the storage modulus, resisting deterioration in mechanical properties induced by polymer degradation**

➢ Effects of annealing on glass transition temperature

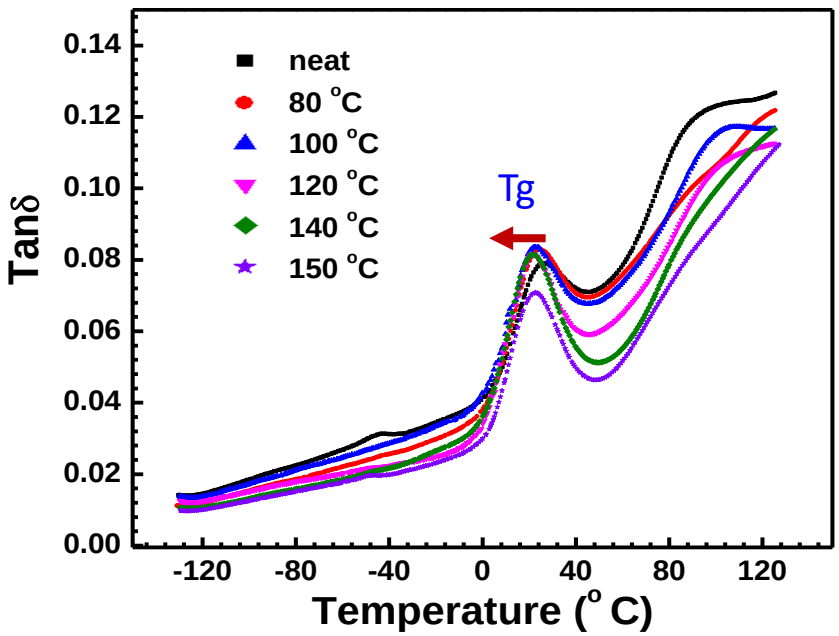

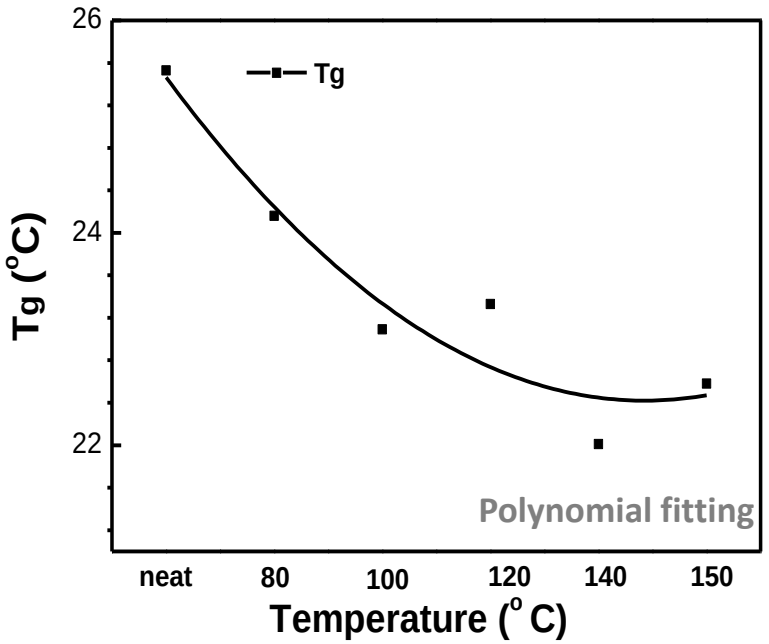

Fig. 6 (b) Glass transition temperature vs. annealing temperature measured by DMA

- **Annealing reduces the entanglement of polymer chains and the concentration of polymer segments in amorphous phase, leading to the decrease of Tg**

➢ Effects of crystallization on the oxygen permeability

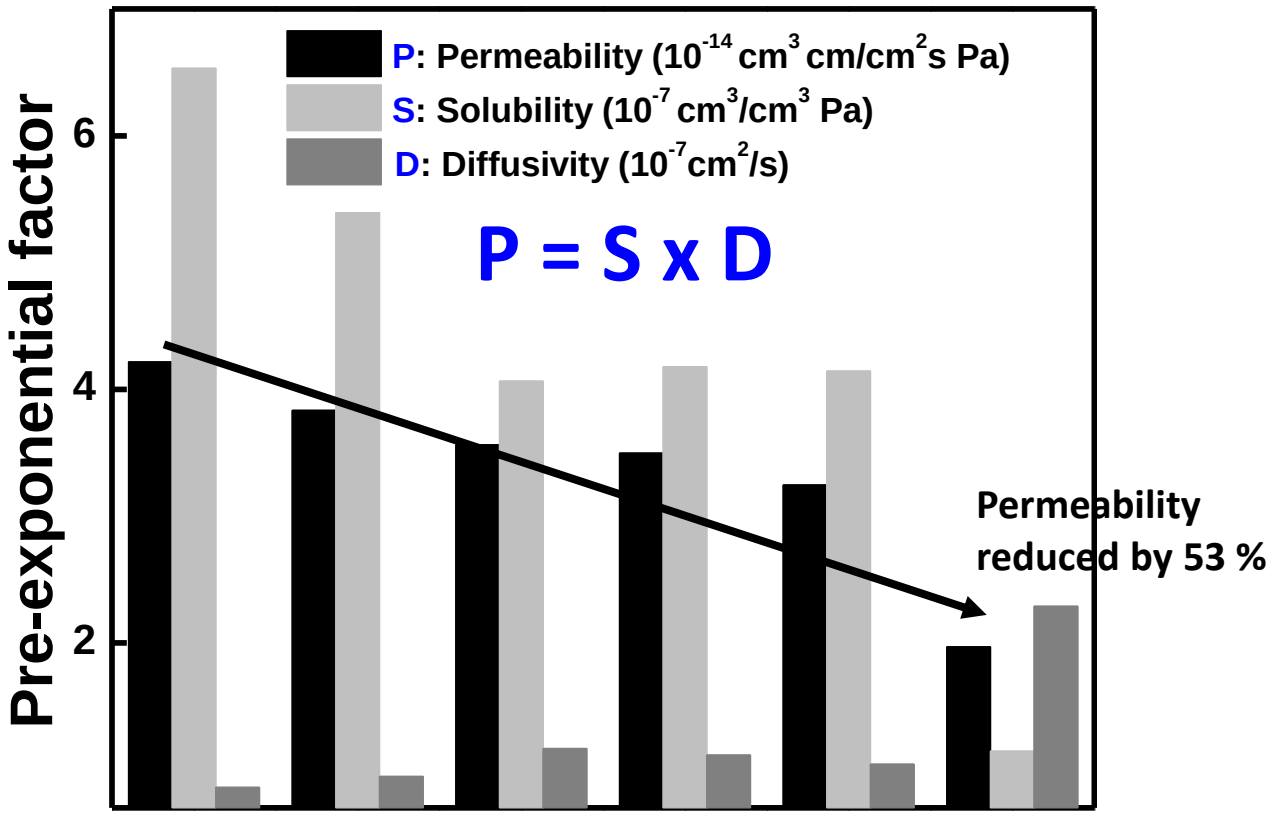

Fig. 7 Permeability, solubility and diffusivity vs. annealing temperature, measured by gas permeability tester using film samples with thickness of 500 μm

- **Oxygen permeability of annealed samples is reduced significantly by the increase of crystallinity and lamellae thickness**

➢ Effects of crystallization on the concentration of free radicals

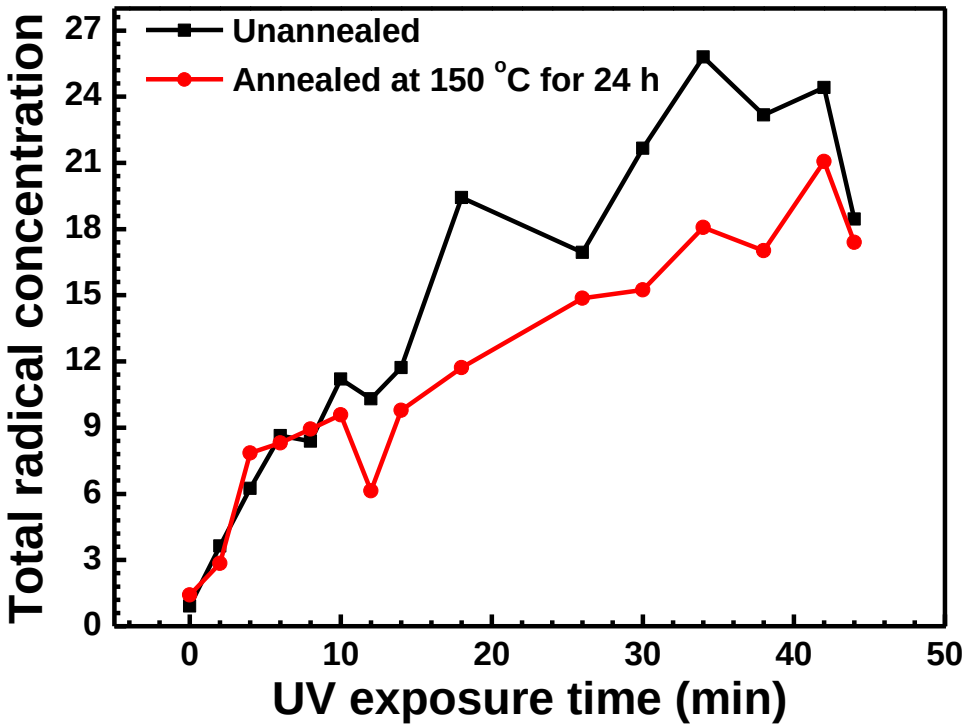

Fig. 8 Concentration of free radicals measured by Electron Paramagnetic Resonance (EPR) under UV light

- **Concentration of free radicals decreased significantly after annealing**

➢ Effect of crystallization on the oxidation of PP

- **Formation of C=O during UV degradation**

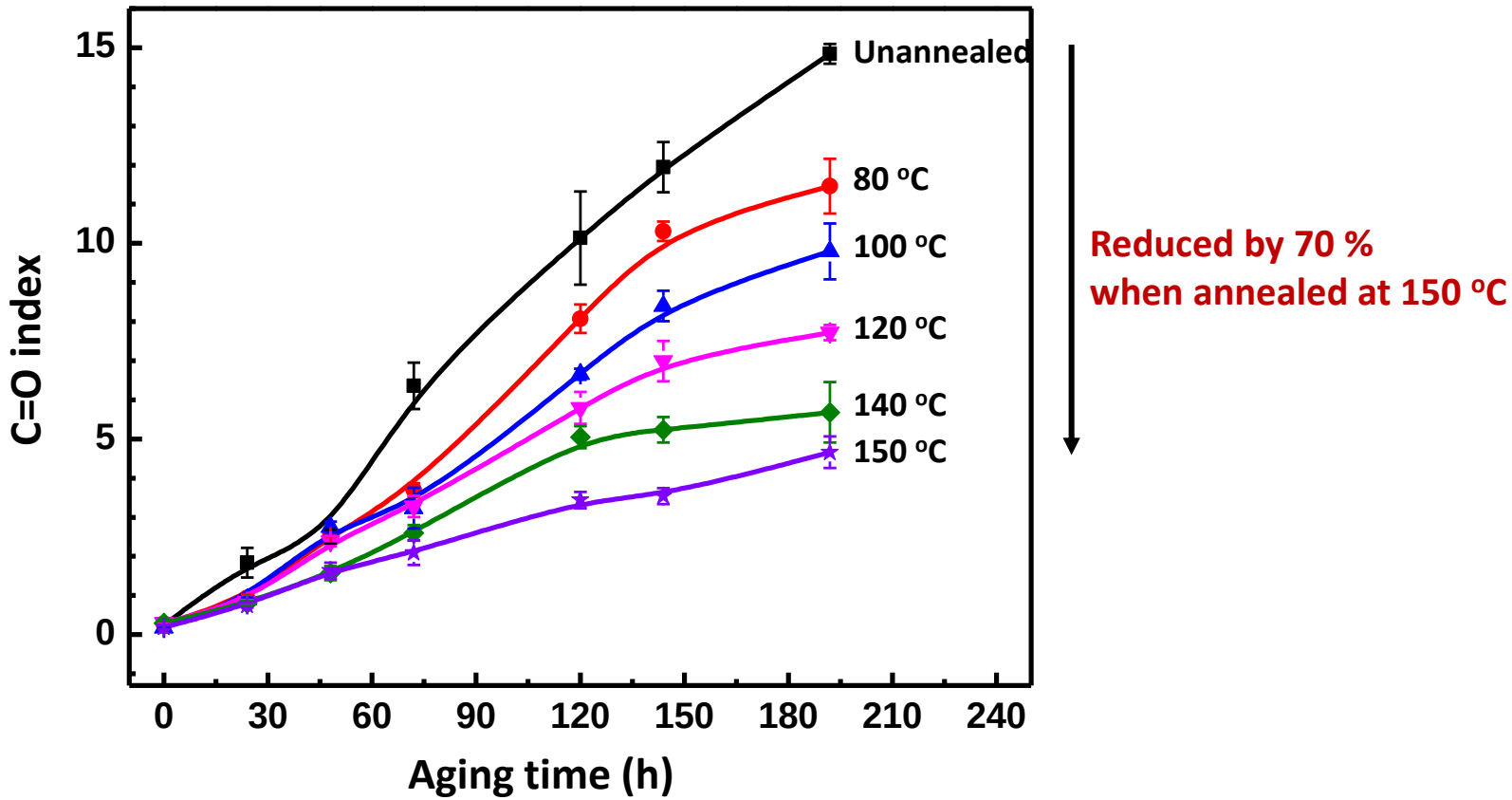

Fig. 9 C=O index vs. photooxidation time measured by FTIR

- **Annealing reduced the concentration of carbonyl group by up to 70 %**

➢ UV caused damage of surface morphology

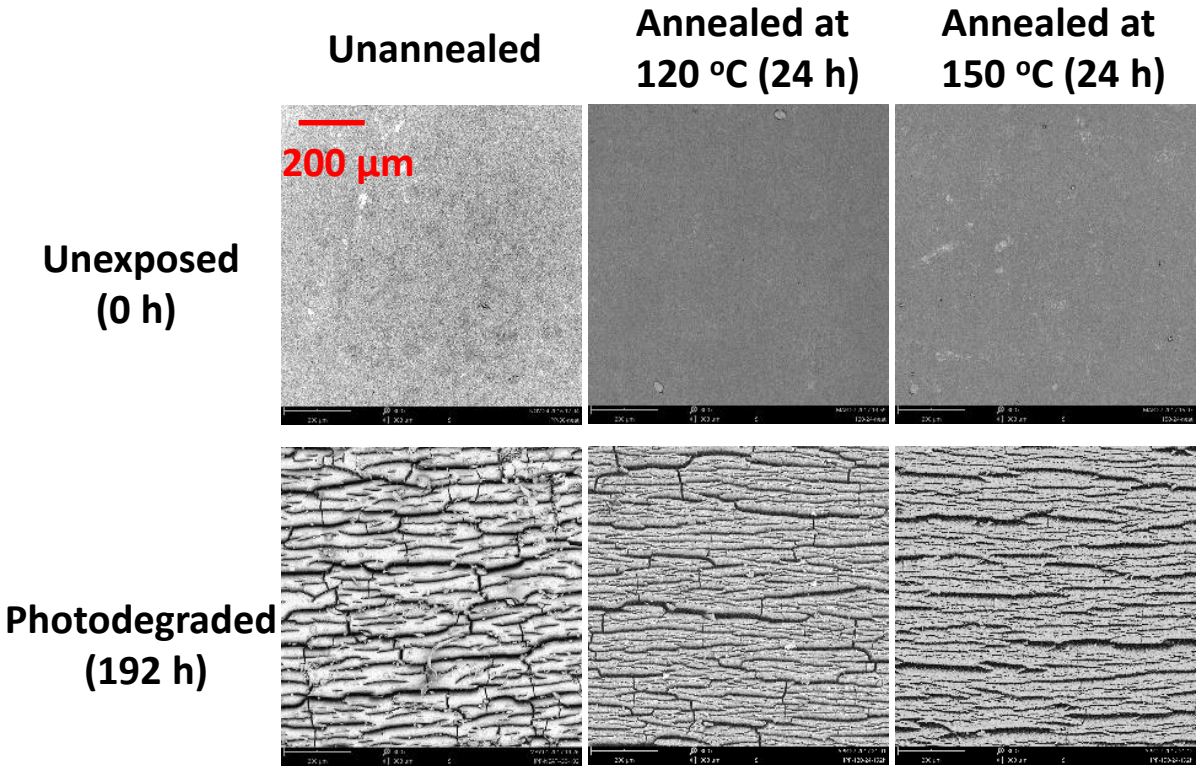

Fig. 10 Surface morphology of annealed samples after photooxidation measured by SEM

Table 1 Area percentage of cracks (APC)

	APC（%）
unannealed	27.1
120 °C	24.0
150 °C	21.0

- **Annealing suppressed the formation of microcracks after UV exposure**

➢ Effect of UV irradiation on the melting point after annealing

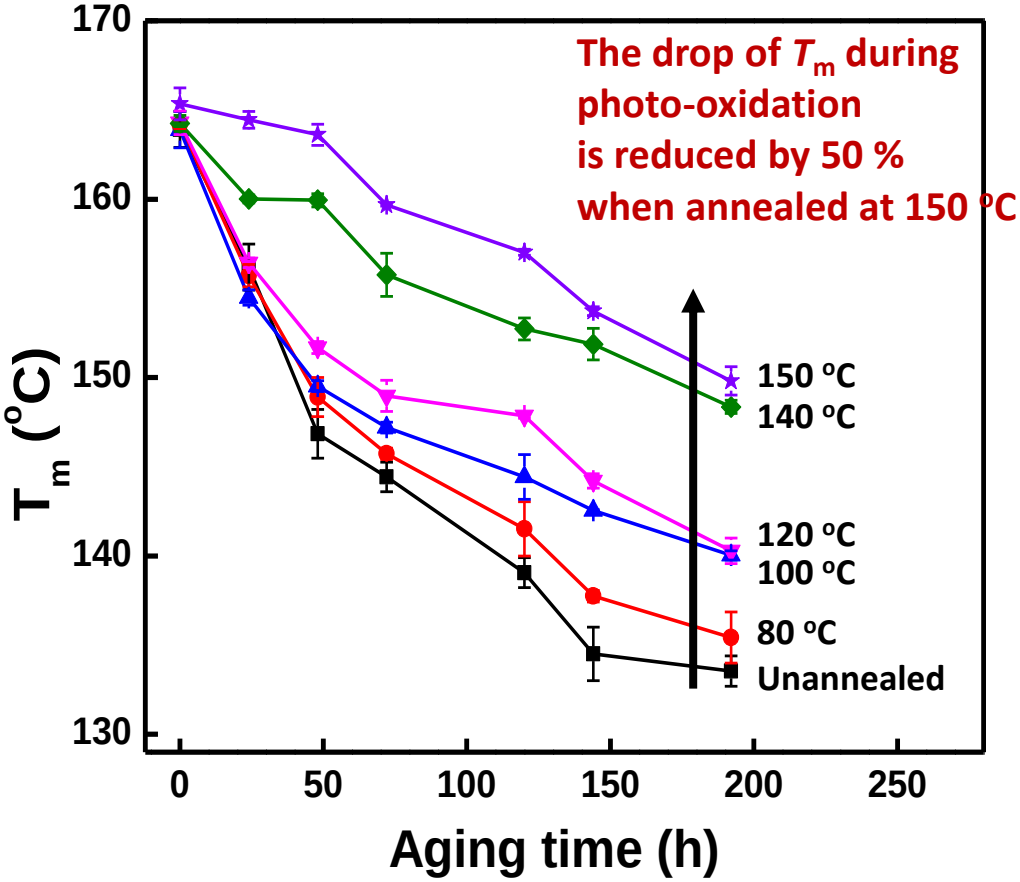

Fig. 11 T_m vs. photooxidation time for unannealed and annealed samples

- **The better crystal structure had the better effects in preventing the UV degradation**

Permeable channel of oxygen, H_2O, UV, …

Block the permeable channel of oxygen

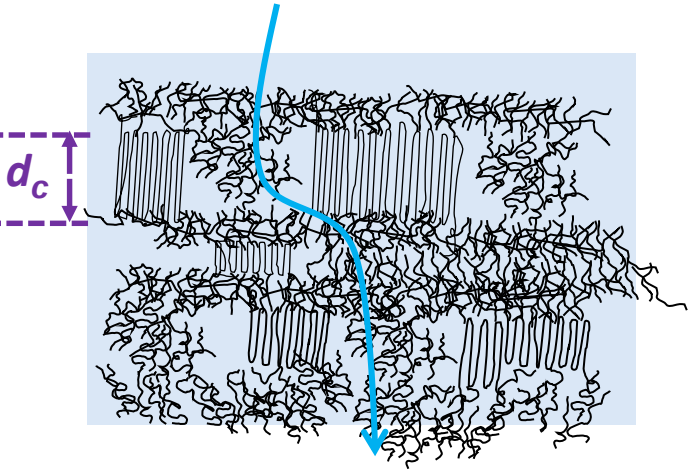

Annealing

- Increases crystallinity
- Increases lamellae dimension

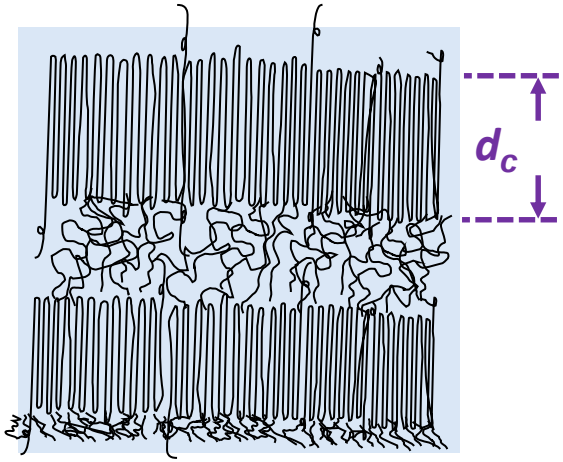

- Lower oxygen permeability
- Lower oxygen solubility

- **Higher crystallinity and thicker lamellae size of annealed PP lowers the oxygen permeability, and enhances its resistance to photo-oxidation**

2. iPP: Using β-nucleating agent → crystal forms

➢ α → β

α-iPP,
crystallinity = 48 %

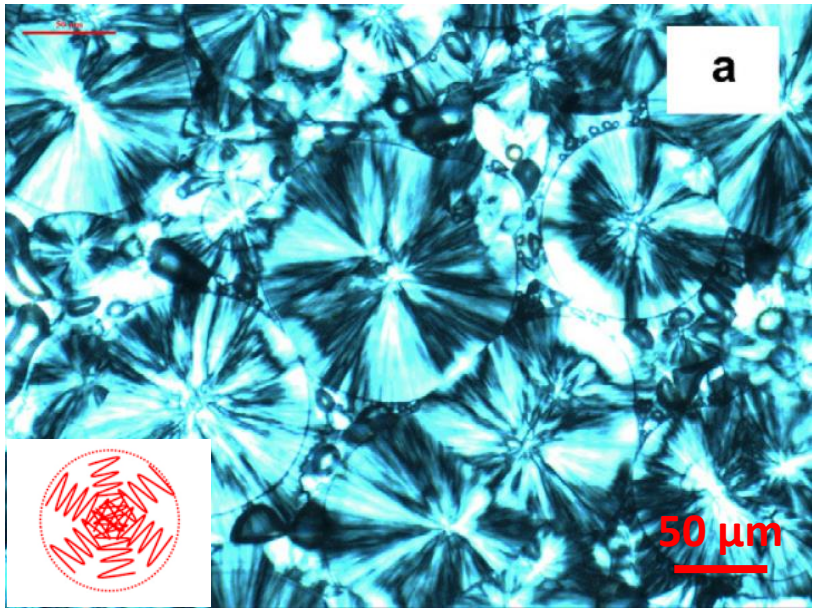

Large spherulites with an average diameter of ~100 μm

β-nucleated iPP (β-iPP)
(0.05 wt.% β-NA), crystallinity = 49 %

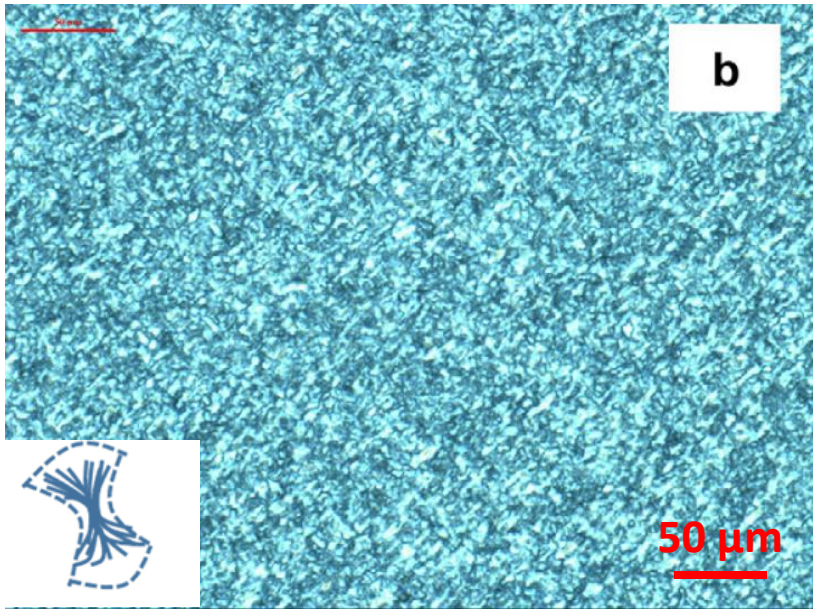

Size of β-crystal reduced significantly to ~10 μm

Fig. 12 Polarized optical images of α-iPP and β-PP

- β-sheet crystals have a better fine structure and higher density, which reduced the oxygen permeability

YD Lv, GX Li, Polymer Testing, 2013, 32, 179

➢ Effects of crystal form types on oxygen permeability

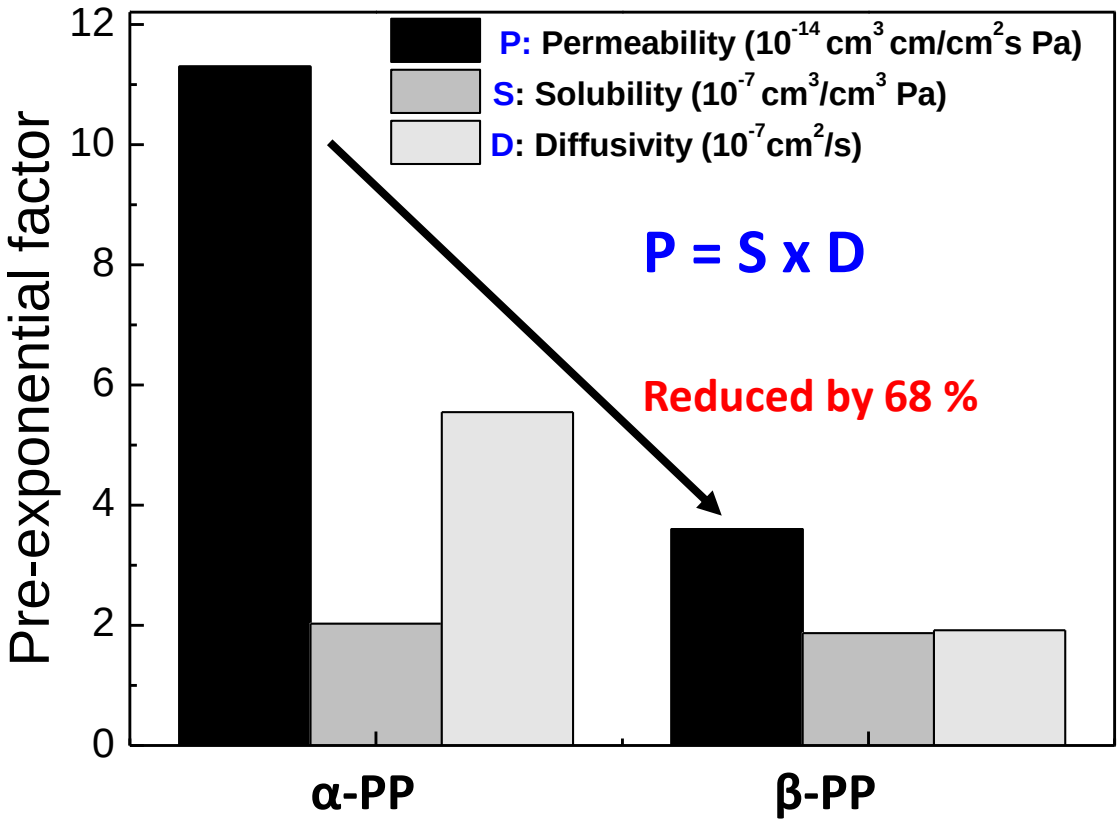

Fig. 13 Permeability, solubility and diffusivity for α-PP and β-PP, measured by gas permeability tester using film samples with thickness of 150 μm

- **With a similar crystallinity (48 - 49%), β-PP has much lower oxygen permeability; it is very effective in controlling the diffusion channel of oxygen**

➢ Effects of crystal form types on oxidation (C=O)

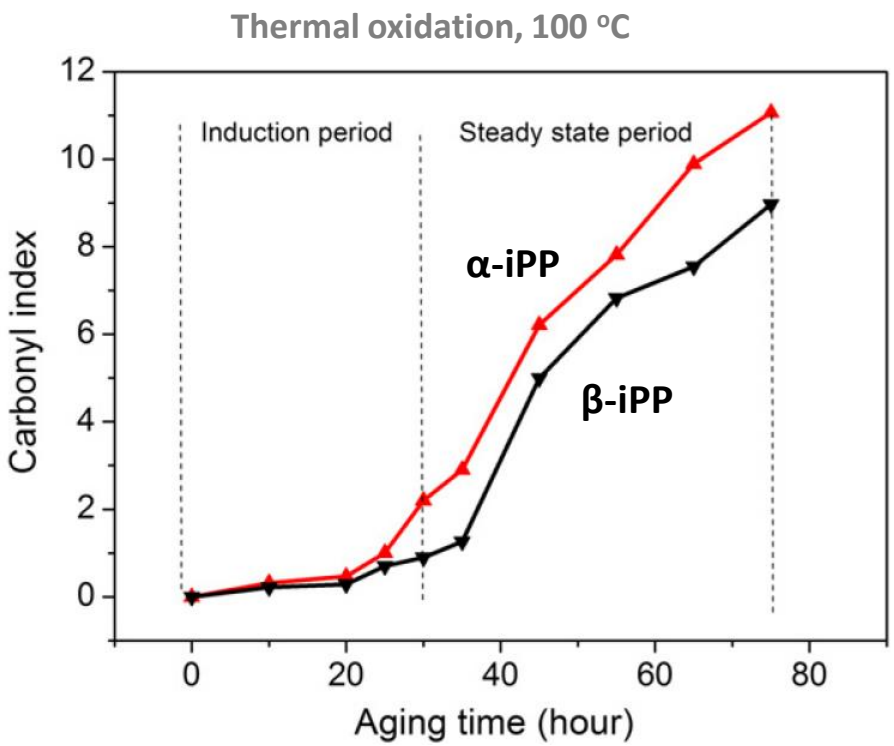

Fig. 14 C=O index for neat PP and β-PP during thermal oxidation

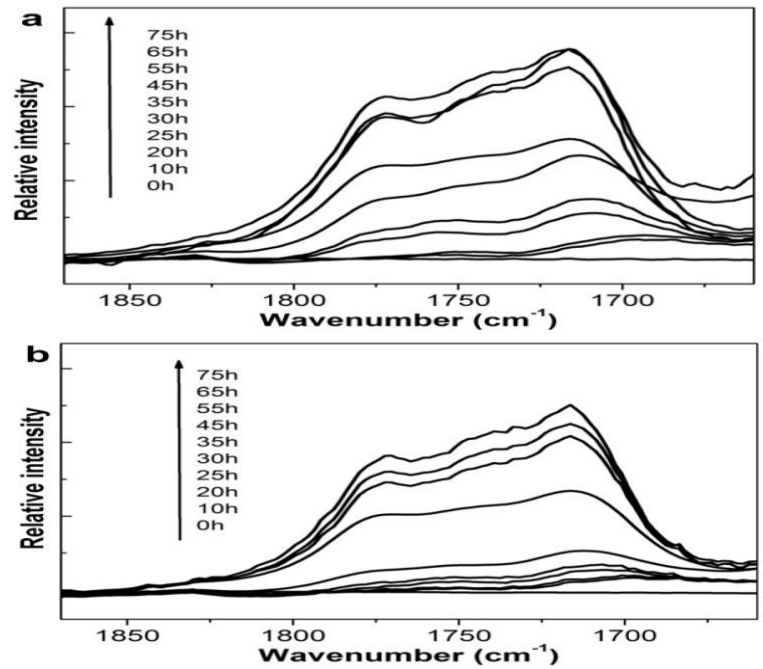

Similar degradation products

Fig. 15 FTIR curves for neat PP and β-PP during thermal oxidation

- **β-iPP has much lower carbonyl concentration ascribed to its better oxygen barrier ability**

➢ Mechanisms of the size of crystals on the degradation(the higher density and lower permeability)

Diffusion channel of oxygen

✓ α spherulites

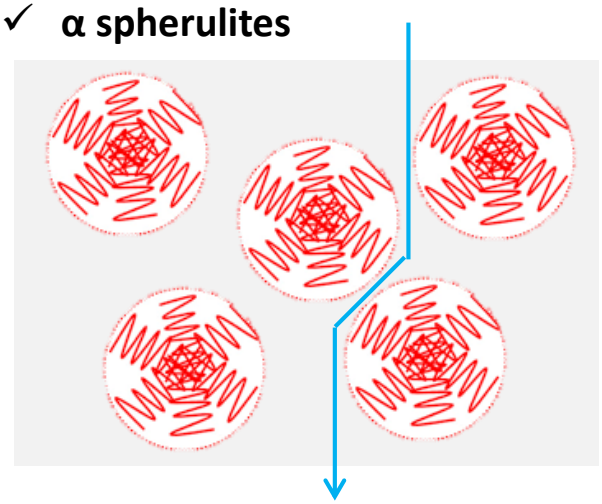

β-nucleating agent

➢Formation of β crystal form

Reduce the diffusion channels of oxygen

✓ β sheet

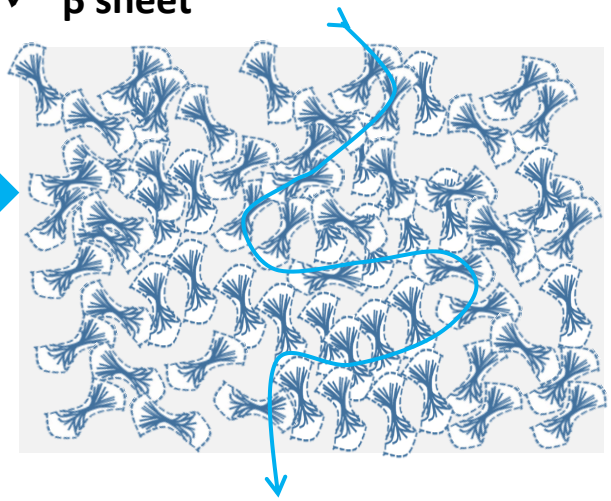

➢Lower oxygen permeability and solubility

- **Tiny and small diffusion channels of β-PP lower the oxygen permeability, which enhances its resistance to thermal-oxidation**

3. PC: Solvent induced surface crystallization

➢ Condensed states on surface to hinder diffusion channels

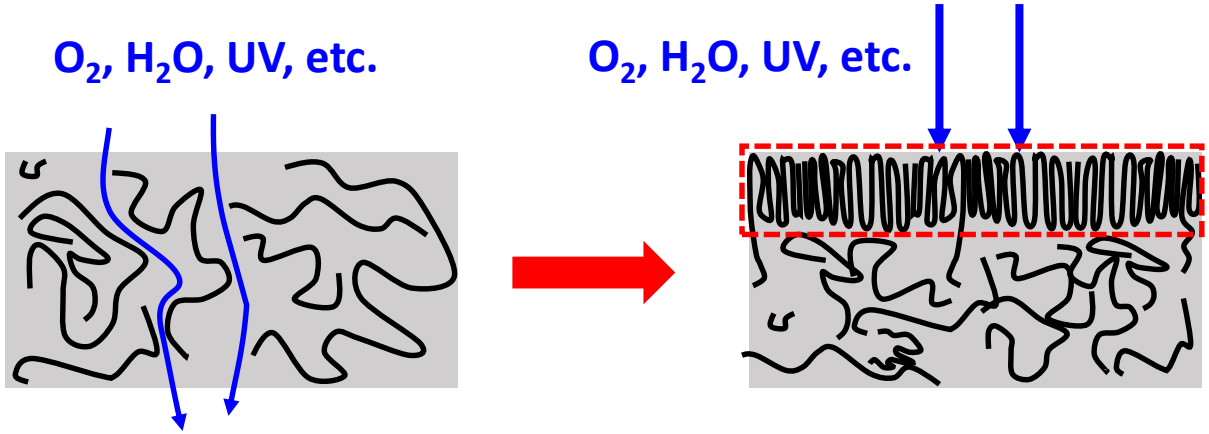

➢ **How to construct a denser barrier layer: crystallization?**

➢ Preparation of surface-crystallized PC

- Amorphous PC
- Surface crystallized PC

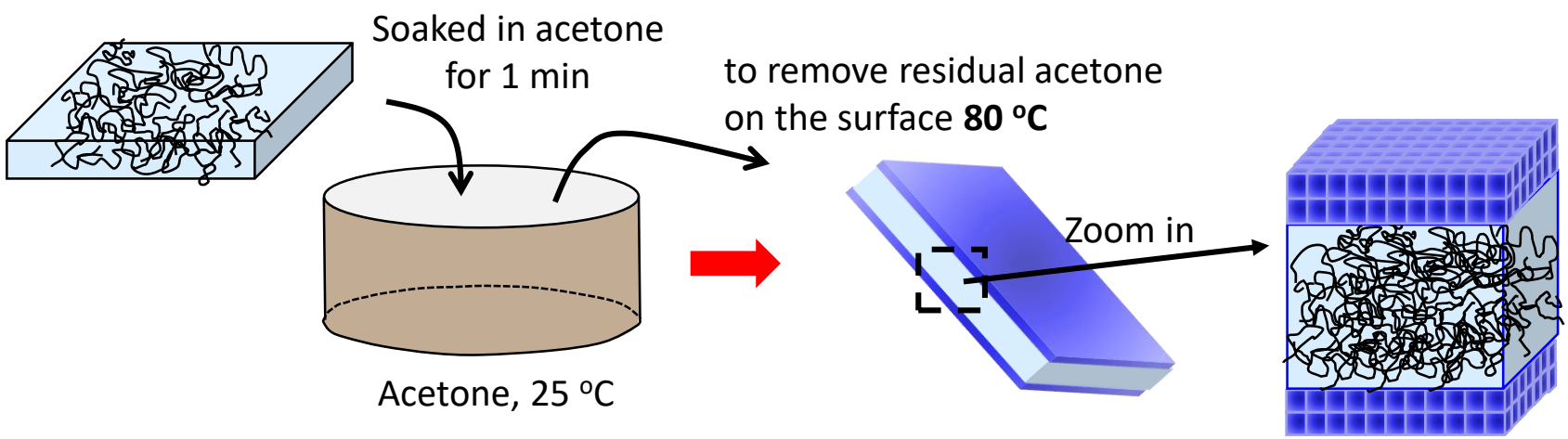

YL Zhou, GX Li, Polymer Degradation and Stability, 2013, 98, 1465

➢ Effects of surface-crystallization on the hydrophobicity

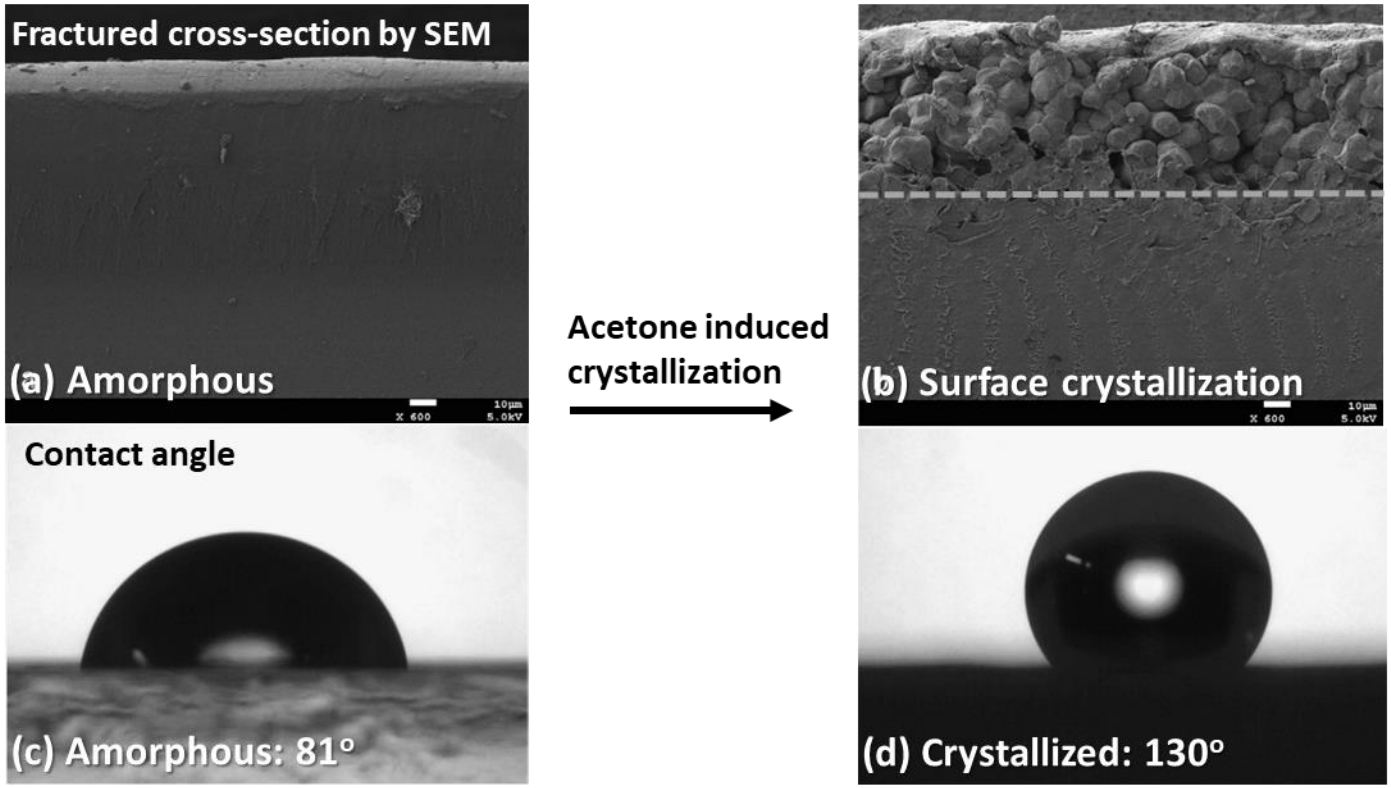

Crystallinity= 4.76 %

Fig. 14 Cross-sectional images and contact angle for neat PC and surface-crystallized PC

- **Hydrophobicity of PC is enhanced obviously with the surface crystallization**

➢ Effects of surface-crystallization on the hydrothermal oxidation stability

Table 2 Reduction in concentration of C=O group （hot water 65 oC ）

	Neat PC	Surface crystallized PC
Reduction in C=O (Hydrolysis for 36 days)	33.9%	23.9%

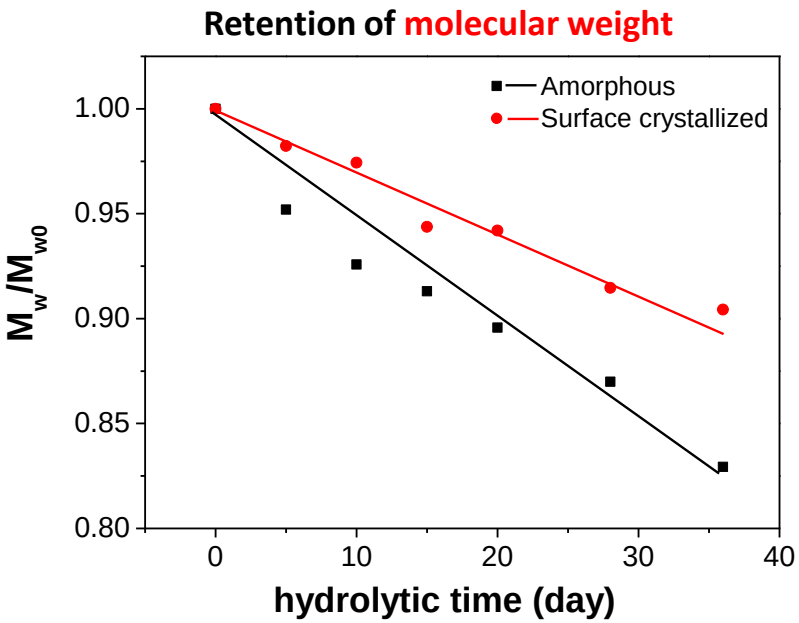

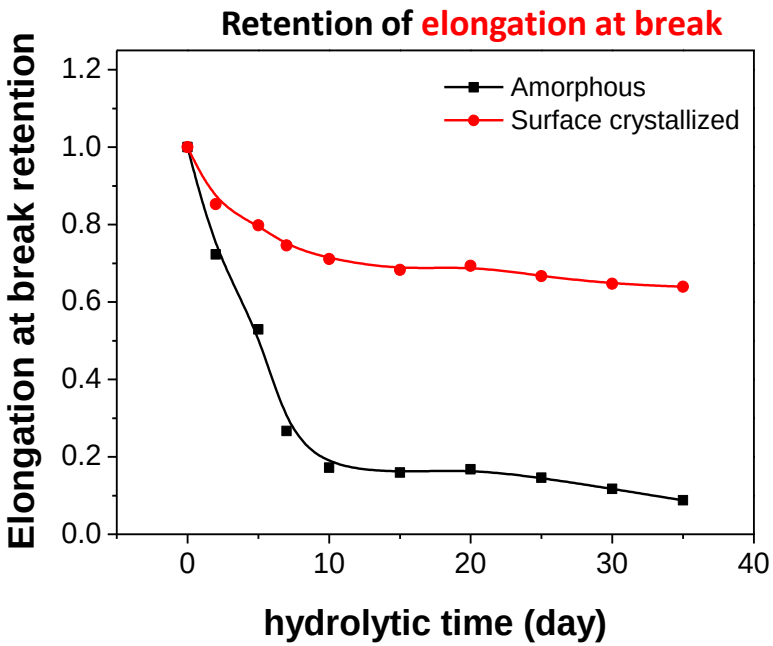

Fig. 15 Retention of molecular weight and elongation at break vs. hydrolytic time for neat PC and surface-crystallized PC

- **Enhancement in the hydrophobicity of surface crystallized PC inhibits the hydrolysis**

Case 2:
Orientated polymer

PA6: Orientation prevented the hydrothermal oxidation

➢ Effect of drawing orientation on crystal structures of PA6

Table 3 Draw ratio against crystallinity

Drawing ratio (%)	Crystallinity (%)	*Orientation factor*
0	39.2	-
200	45.0	0.17
400	45.4	0.18
600	53.6	0.21

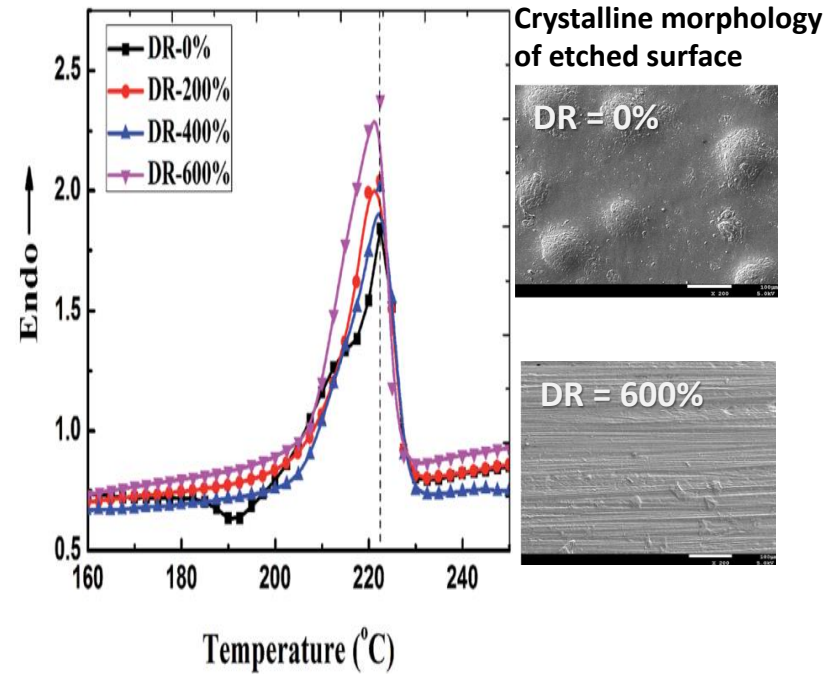

Fig. 16 DSC melting curves and crystal morphology of PA6 and orientated PA6

- **Polymer drawing increases the orientation degree and crystallinity of PA6**

KH Shi, GX Li, Journal of Thermal Analysis and Calorimetry, 2016, 126, 795

➢ Effect of drawing orientation on the hydrophobicity of PA6

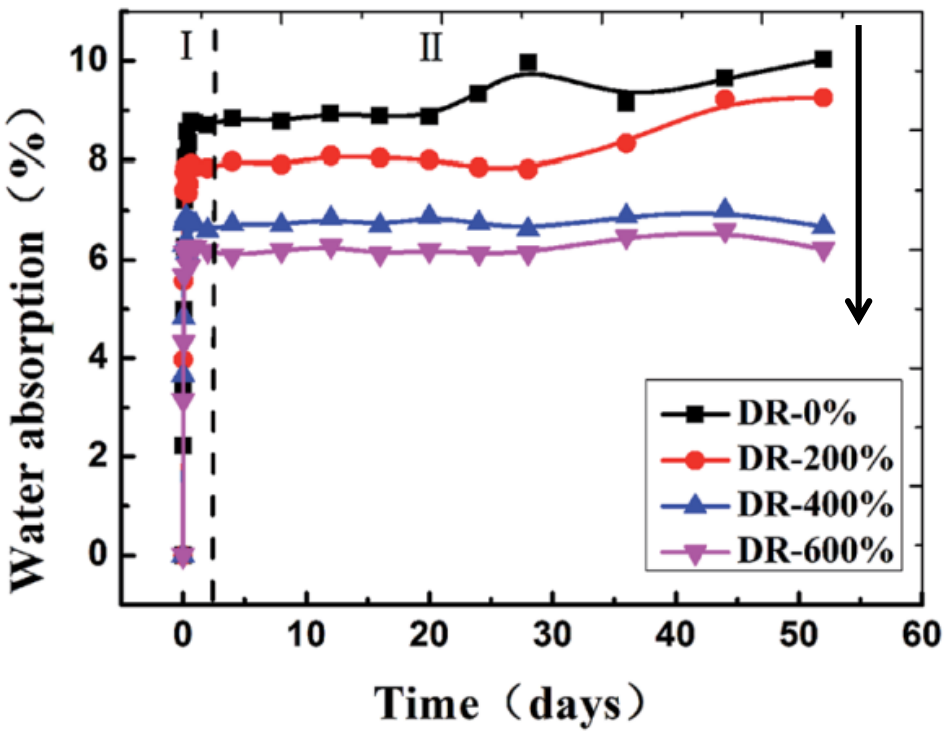

Contact angle

Table 4 **Draw ratio against coefficient of water diffusion**

DR (%)	*D* ($mm^2\ s^{-1}$)
0	9.89×10^{-5}
200	2.40×10^{-5}
400	1.02×10^{-5}
600	0.71×10^{-5}

Fig. 17 **Water absorption** curves of PA6 in hot water at 85 °C

- **With increase of drawing ratio, water absorption decreases ; leading to lower coefficient of water diffusion**

➢ Effect of drawing orientation on surface cracking

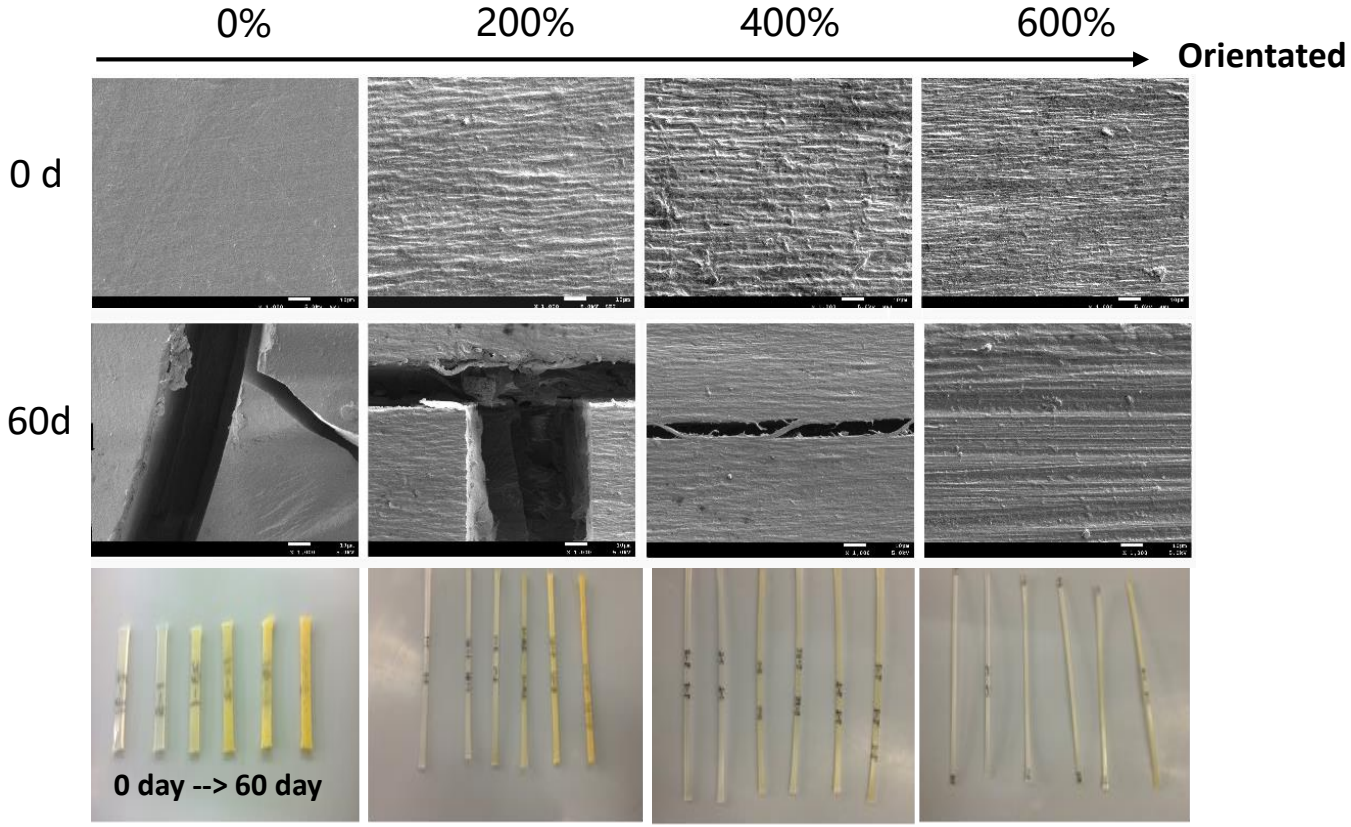

Fig. 18 SEM and photographs of PA6 samples after immersing in hot water (85 °C) for 60 days

- **Polymer orientation suppresses the cracking and yellowing of PA6 during hydrothermal oxidation**

➢ Effect of drawing orientation on tensile strength

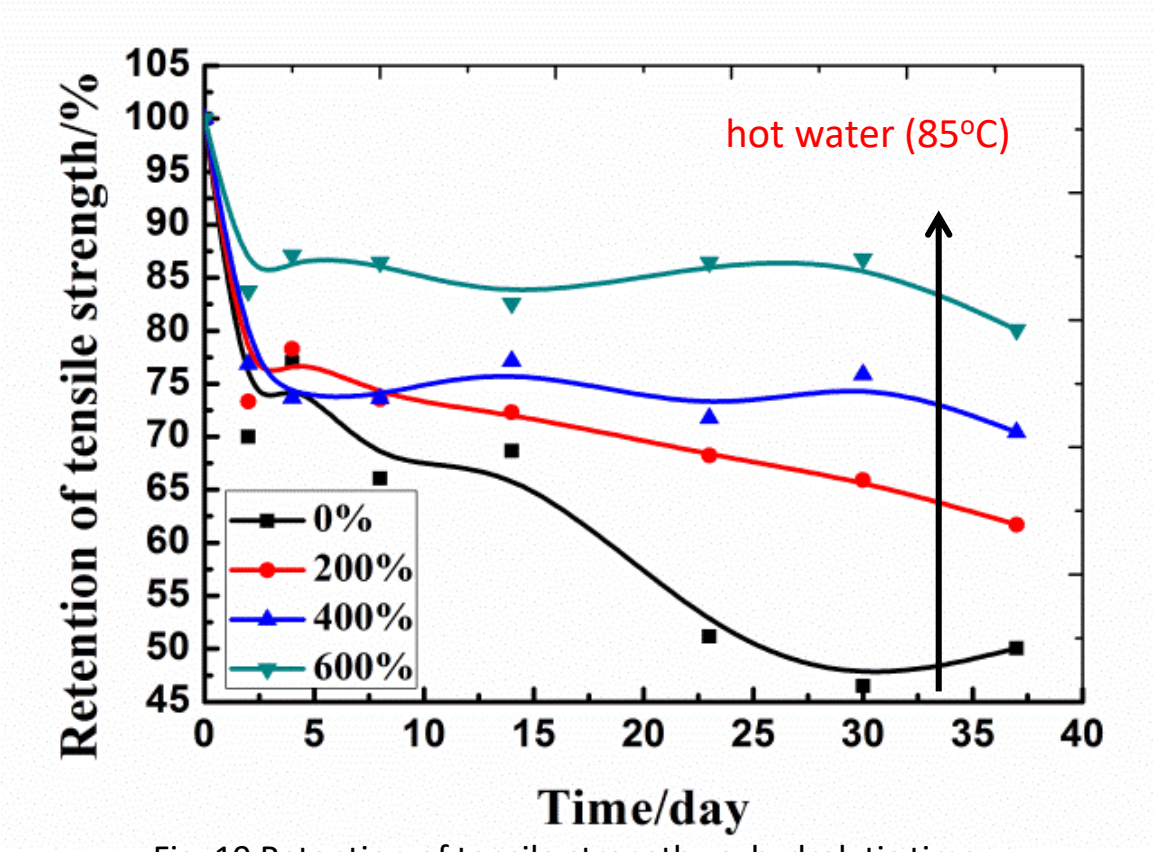

Fig. 19 Retention of tensile strength vs. hydrolytic time

- **The orientation increases the retention of mechanical properties during hydrothermal oxidation**

➢ Effect of drawing orientation on molecular weight

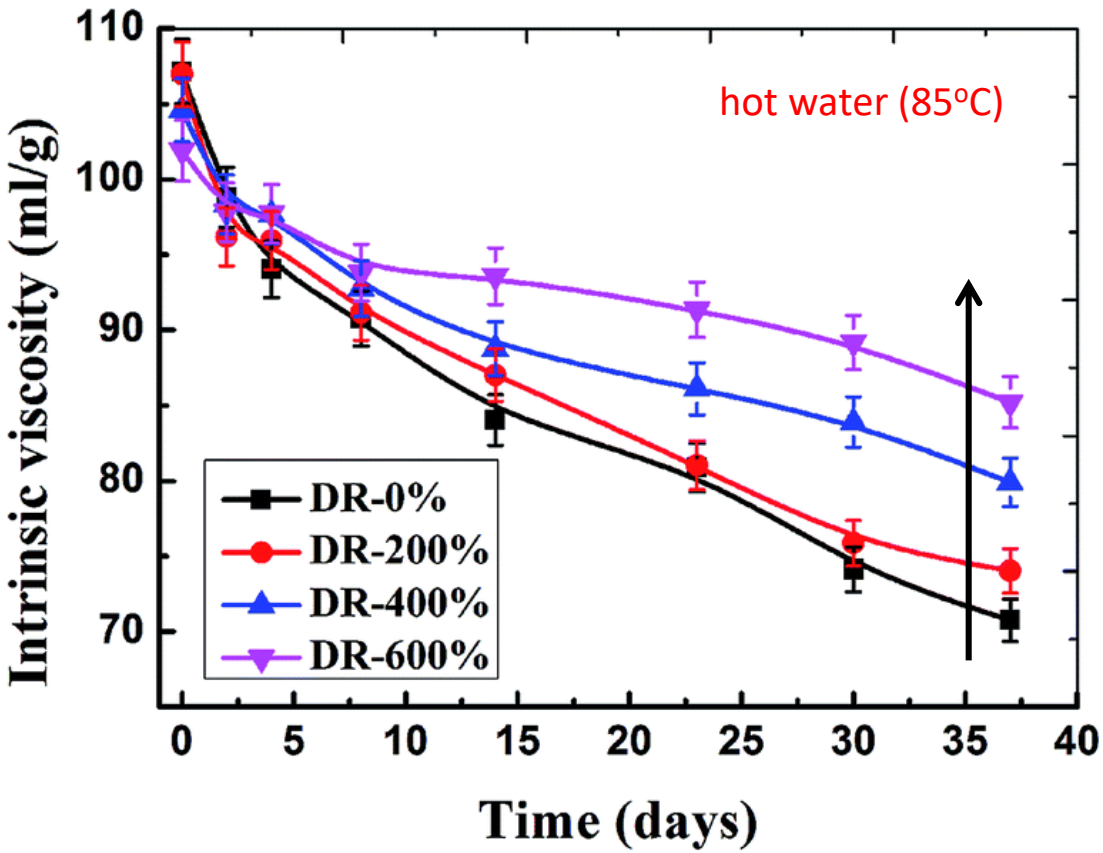

Fig. 20 Intrinsic viscosity vs. hydrolytic time

Table 5 Draw ratio against Hydrolytic rate k_1

- **Auto-catalyzed hydrolytic**

$$\ln\left(\frac{[\eta]}{[\eta]_0}\right) = -k_1 t$$

DR(%)	k_1 ($10^3 \cdot day^{-1}$)
0	10.04
200	8.94
400	6.36
600	3.98

- **Polymer orientation suppresses the decline of molecular weight during hydrothermal oxidation**

Diffusion channel of water

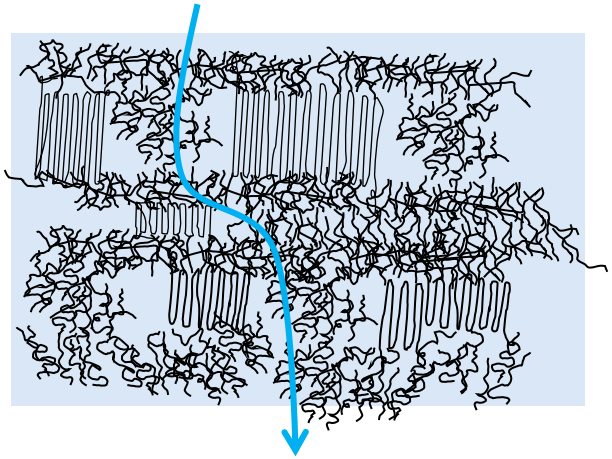

Mechanical drawing

➢Orientation

➢Increase in the crystallinity

Block the diffusion channel of water

➢Lower water absorption

➢Higher hydrophobicity

- **Higher crystallinity and orientation degree of orientated PA6 lowers its water absorption, produced better resistance to hydrothermal oxidation**

Case 3:
Adding barrier filler into polymer matrix

1. Adding oxygen-barrier fillers in polymer matrix

◻ Two dimensional plane graphene nanosheet

➢ **Graphene hindered two critical factors of degradation:**

(1) blocking oxygen diffusion (2) scavenging free radical

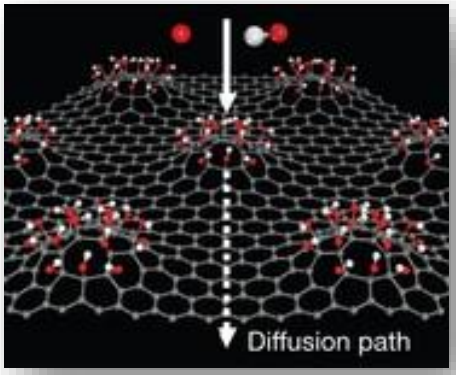

Mesh size: 0.28 nm, O_2 size: 0.296 nm

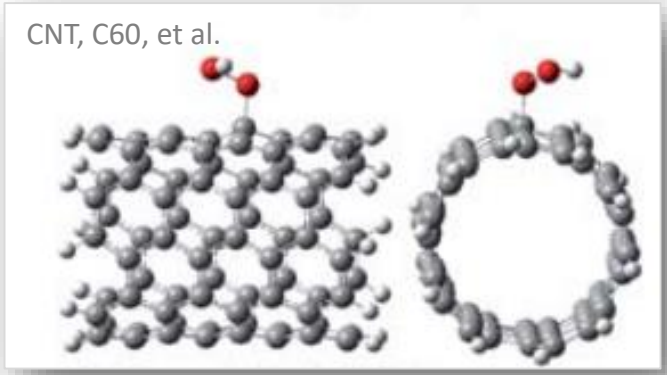

Carbon materials with conjugated double bond

- **Graphene sheets possess great potential in improving the thermal-oxidative stability of polymers**

Compton, *et al. Advanced Materials*, 2010, 22, 4759-4763; Galano. *Nanoscale*, 2010, 2, 373–380

➢ Preparation of crGO/polymer composites

(1) *Preparation of chemically reduced graphene oxide* (*crGO*)

Graphite powders

Graphene oxide (GO)
(a modified Hummers method)

crGO

(2) *Preparation of composites*

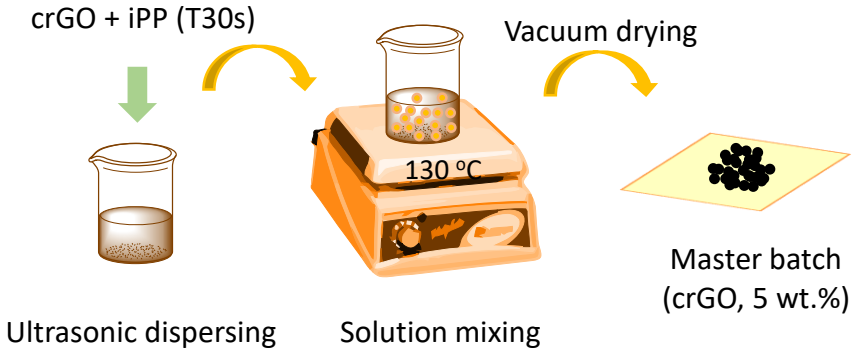

180°C, 10 min
Melt blending

Neat PP
PPR02 (crGO, 0.2 wt.%)
PPR05 (crGO, 0.5 wt.%)
PPR10 (crGO, 1.0 wt.%)
PPR20 (crGO, 2.0 wt.%)
PPR36 (crGO, 3.6 wt.%)

Yang JL, Li GX. *Journal of Materials Chemistry A*, 2013, 37, 11184

➢ Characterization of crGO

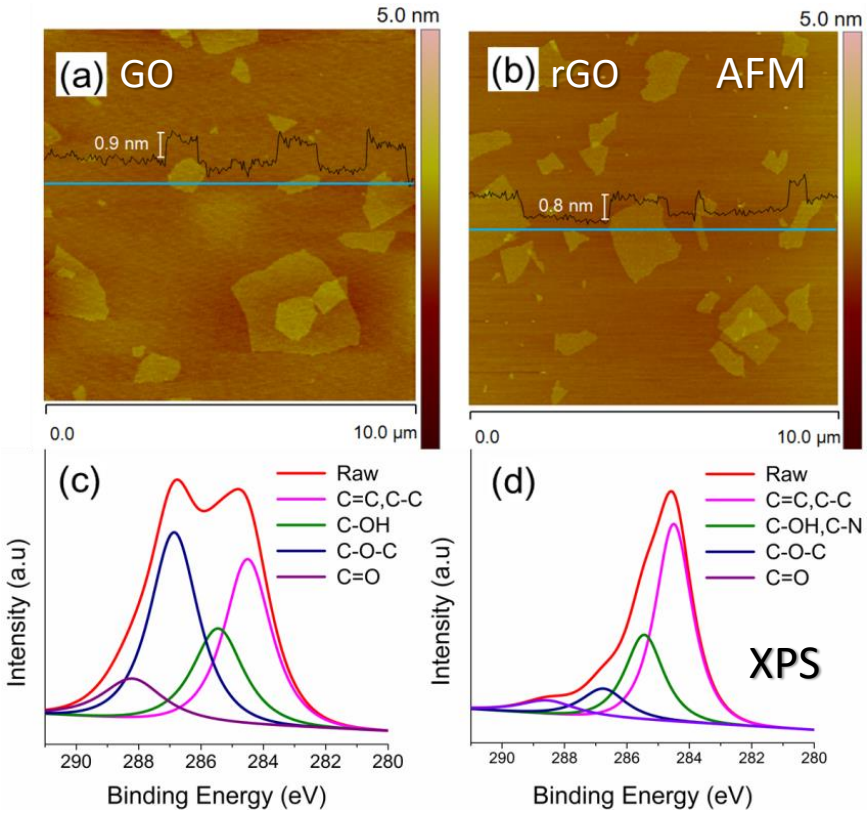

Fig. 21 The AFM, XRD and XPS results of GO and crGO

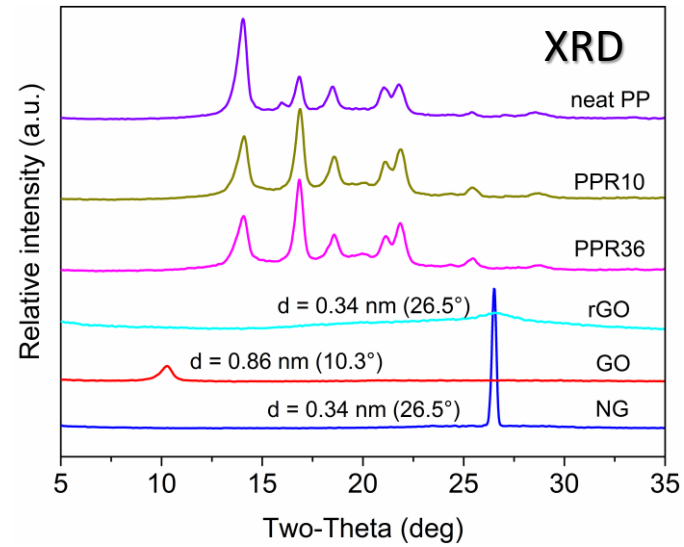

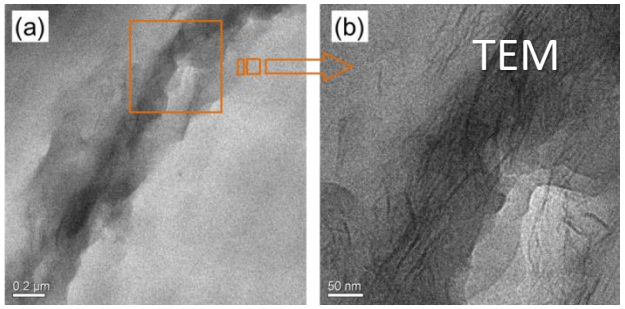

- **crGO is successfully synthesized**

➢ Oxygen permeability and radical scavenging ability of GO

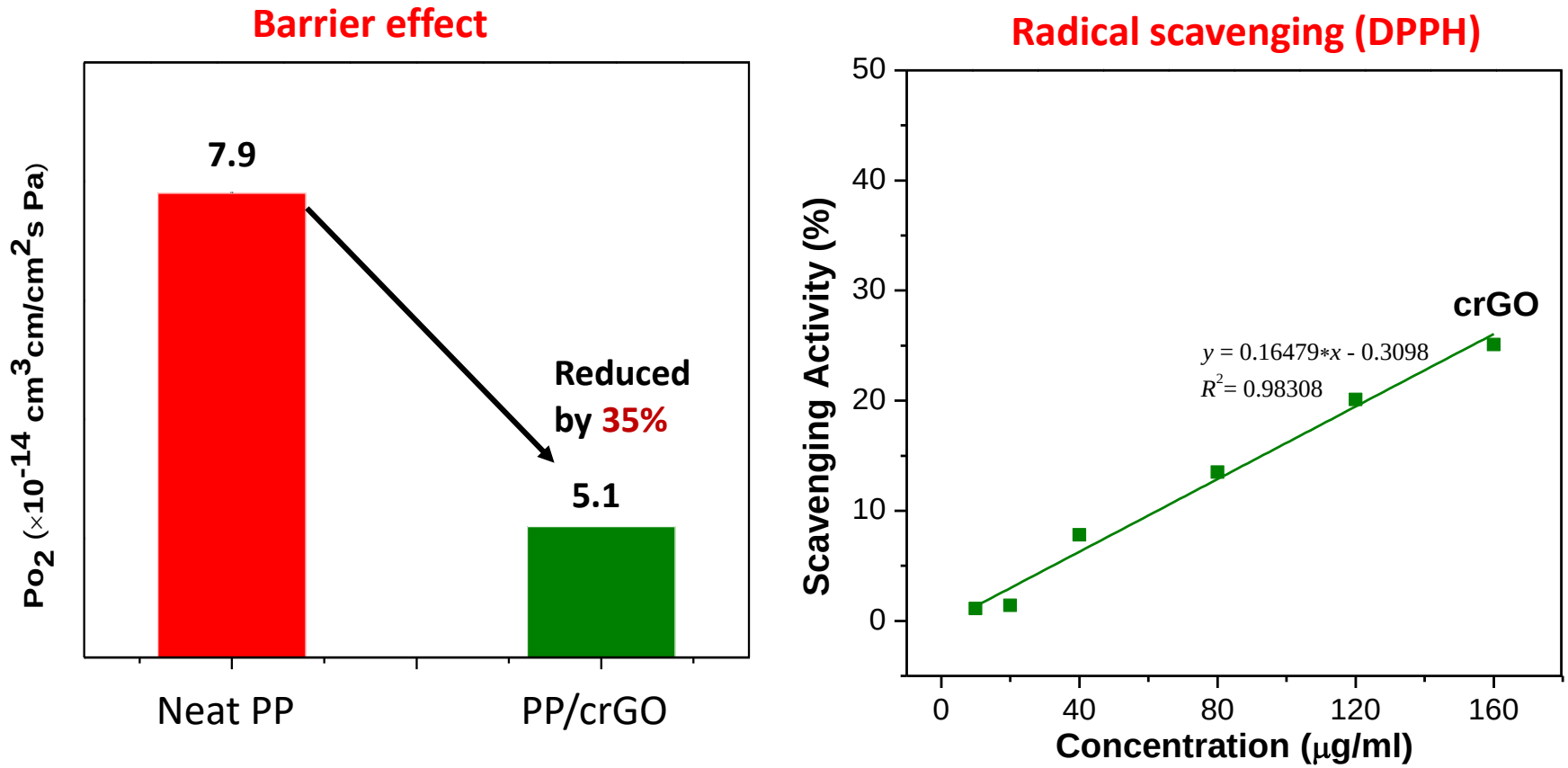

Fig. 22 Oxygen permeability and radicals scavenging ability of GO and crGO. Radical scavenging ability was measured using DPPH (2,2-diphenyl-1-picrylhydrazyl), which is a stable free-radical molecules.

- **PP/crGO composites have much lower oxygen permeability and higher radical scavenging ability**

➢ Thermal-oxidative stability of PP/crGO composites

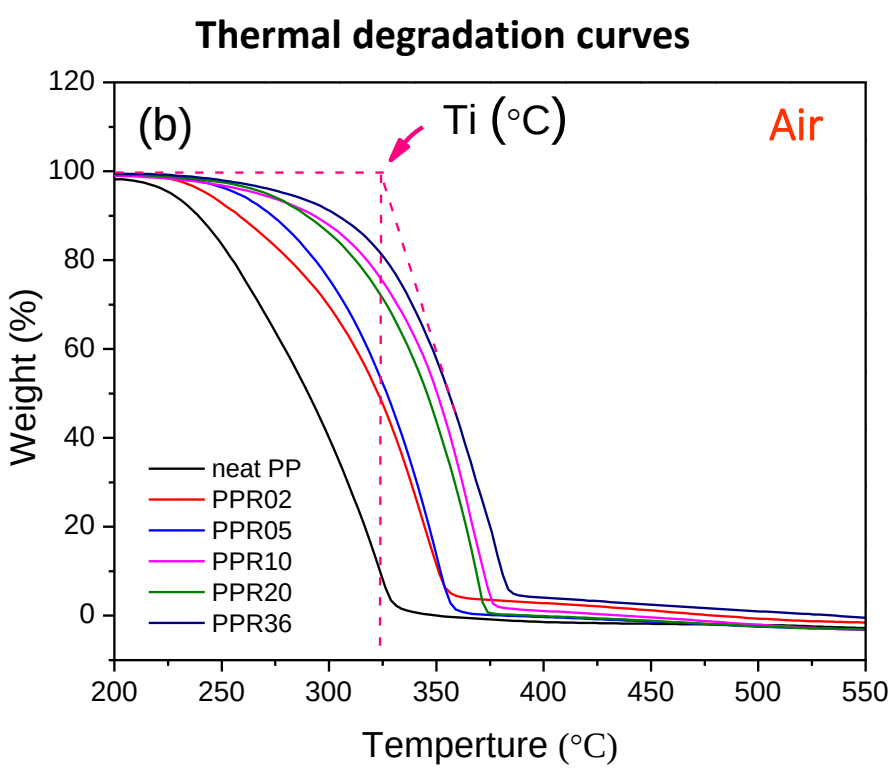

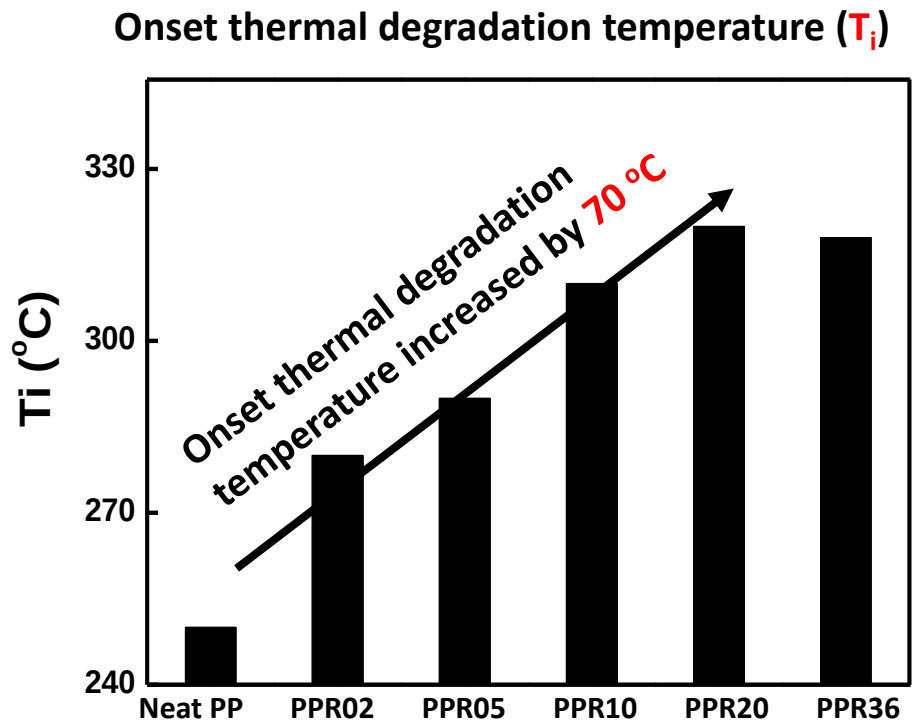

Fig. 23 Thermal degradation curves and thermal degradation temperature of PP/GO and PP/crGO composites

- **crGO suppresses the oxidation of PP in air atmosphere**

➢ Physical mixture of GO/antioxidant (AO) in PP

☐ Preparation of iPP/GO/AO composites

(a) Preparation of GO-coated PP pellets

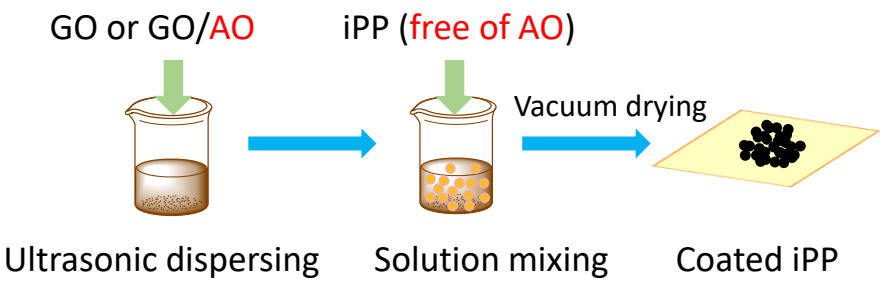

(b) Preparation of GO/iPP composites

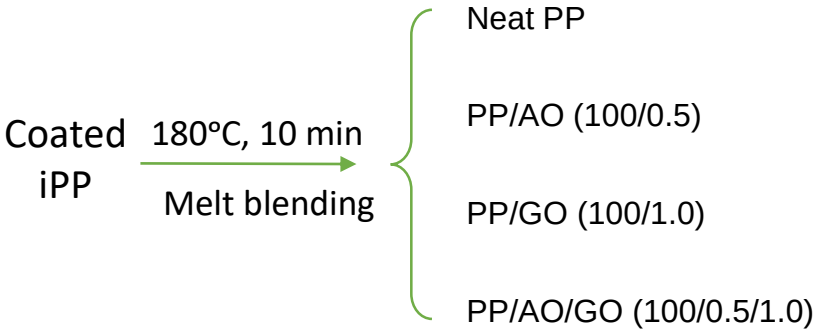

AO:

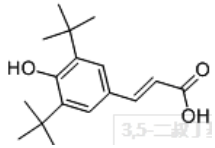

Phenolic antioxidant (3,5-di-tertbutyl-4-hydroxycinnamic acid)

(To avoid the complexity of system , no surface modification or compatibilizer is used)

- **Interaction between AO and GO caused a better dispersion**
- **Oxygen barrier of GO and radical scavenging ability of both GO and AO could generate much better resistance to the degradation**

Yang JL, Li GX. Carbon 2015, 89, 340-349; Journal of Materials Chemistry A, 2013, 1: 11184

➢ Dispersion and oxygen permeability

Better dispersion of GO in iPP

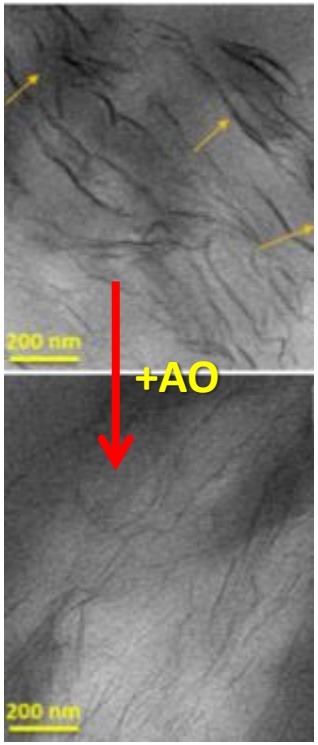

Lower oxygen permeability of PP/GO

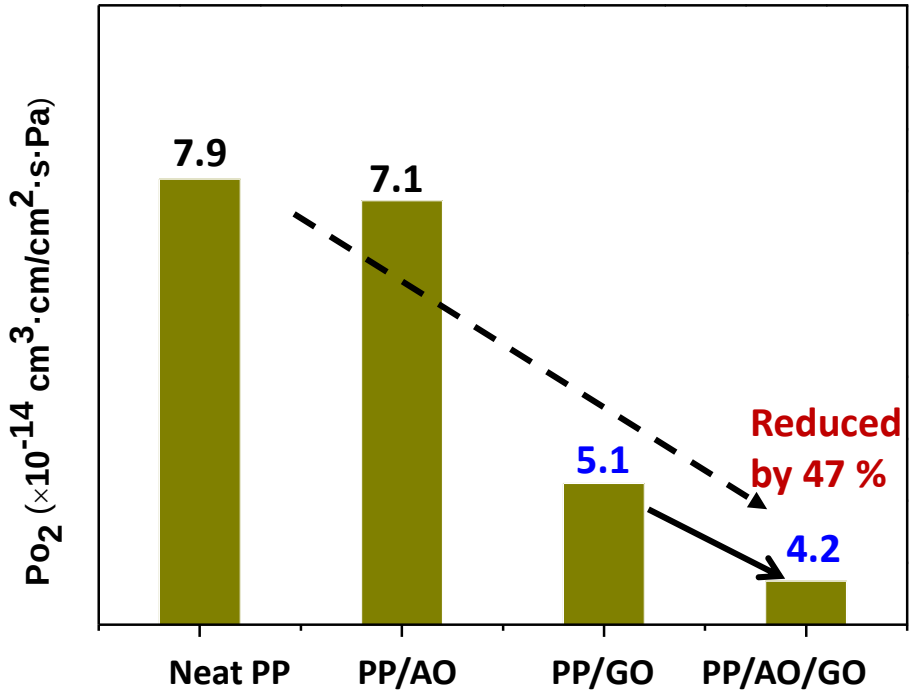

Fig. 24 Dispersion status of GO and oxygen permeability of PP/GO and PP/AO/GO composites

- **Interaction between AO and GO caused better dispersion of GO, which leads to synergistic effects: better oxygen barrier**

➢ Thermal-oxidative stability of PP/AO/GO composites

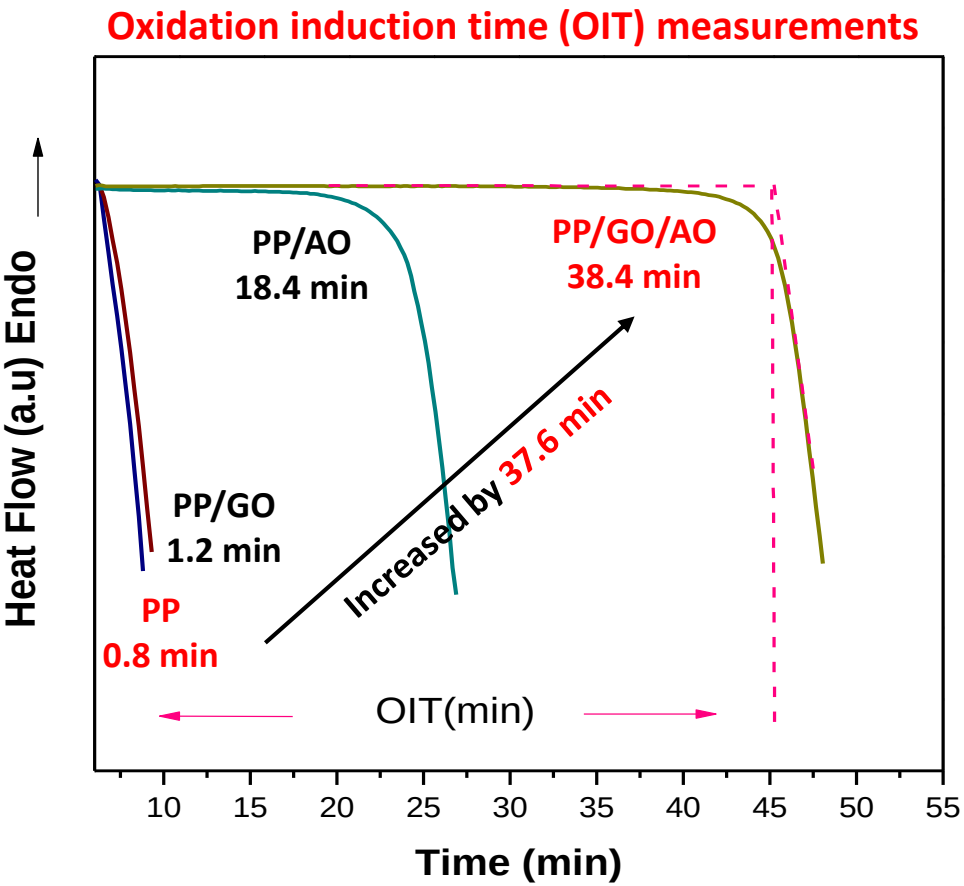

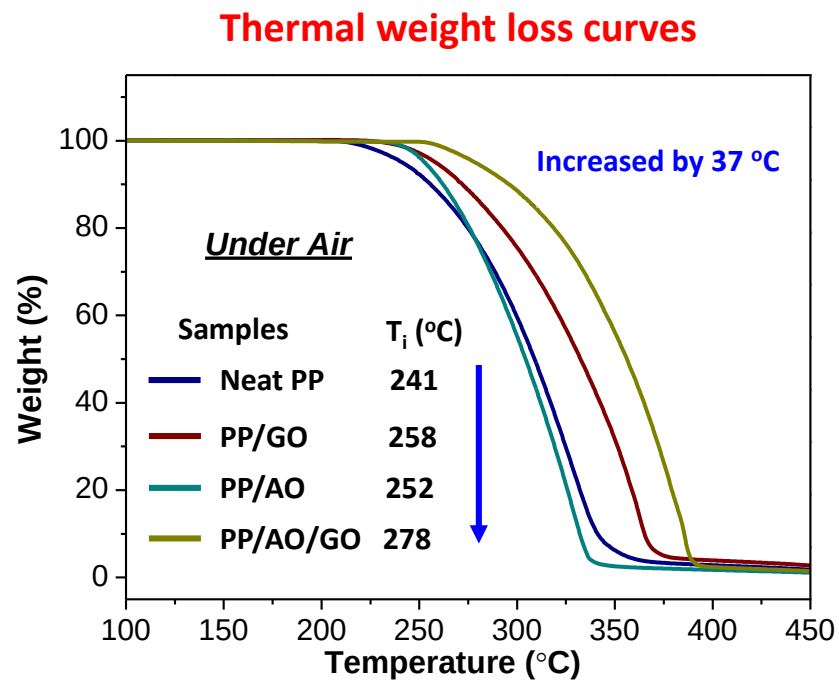

Fig. 25 Oxidation induction time curves and thermal degradation curves of of PP/GO and PP/AO/GO nanocomposites

- **By incorporating mixture of AO/GO: (0.5 wt. % / 1.0 wt. %), OIT and T_i of PP were improved significantly.**

2. Opposite example: to produce a diffusion channel by making surface microcracks

Formulation of PVC material

Component	phr
PVC	100
Lead sulfate tribasic	2
Lead phosphite dibasic	1
Stearic acid (HSt)	0.5

Photo-oxidation experiment

- High-pressure mercury lamp
- 500 W (55W/m^2 @365nm)
- T=50±5°C
- Aging time: 20 d, sampling for every 5 d

- **Aging at constant strain**

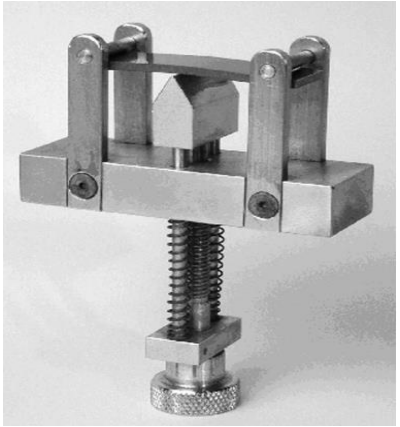

T=50°C

Strain=0-4%

Three-point bending clamp

- **Aging at constant stress**

➢ Stress caused microcracks on the surface of PVC

300x

3000x

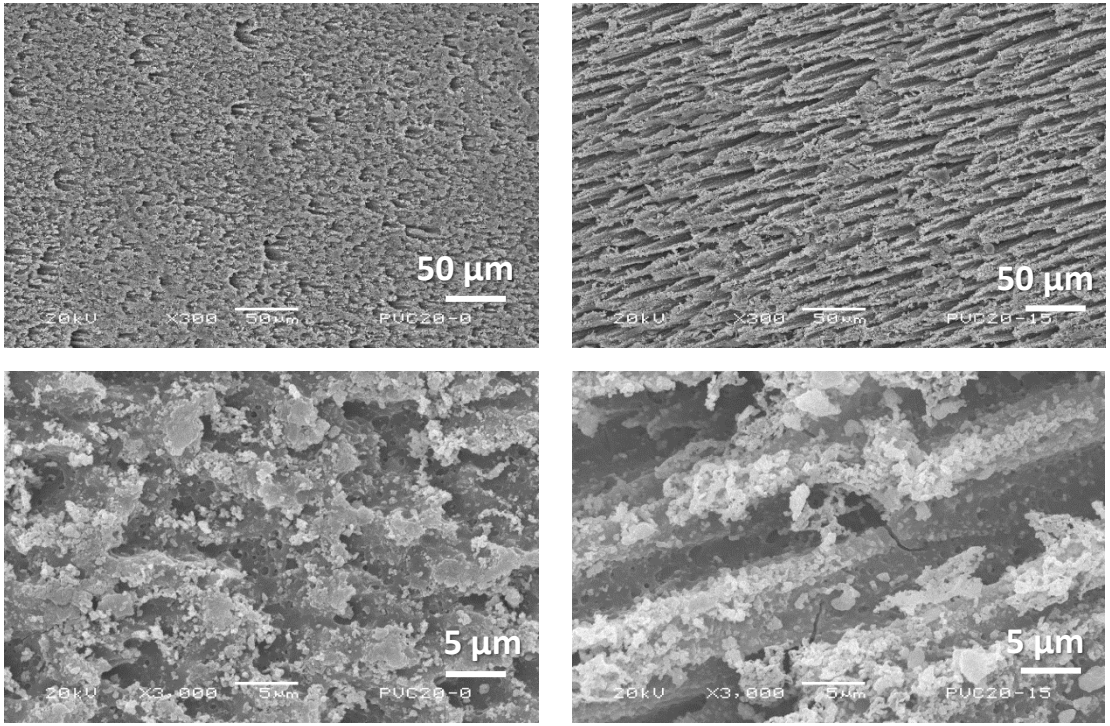

Without stress **With stress**

Aging time: 20 days

Strain=2%

Fig. 26 Surface morphology of PVC before and after degradation

- **Deeper microcracks are formed in stressed samples, facilitating the diffusion of oxygen**

➢ Mass loss of PVC sample under UV exposure

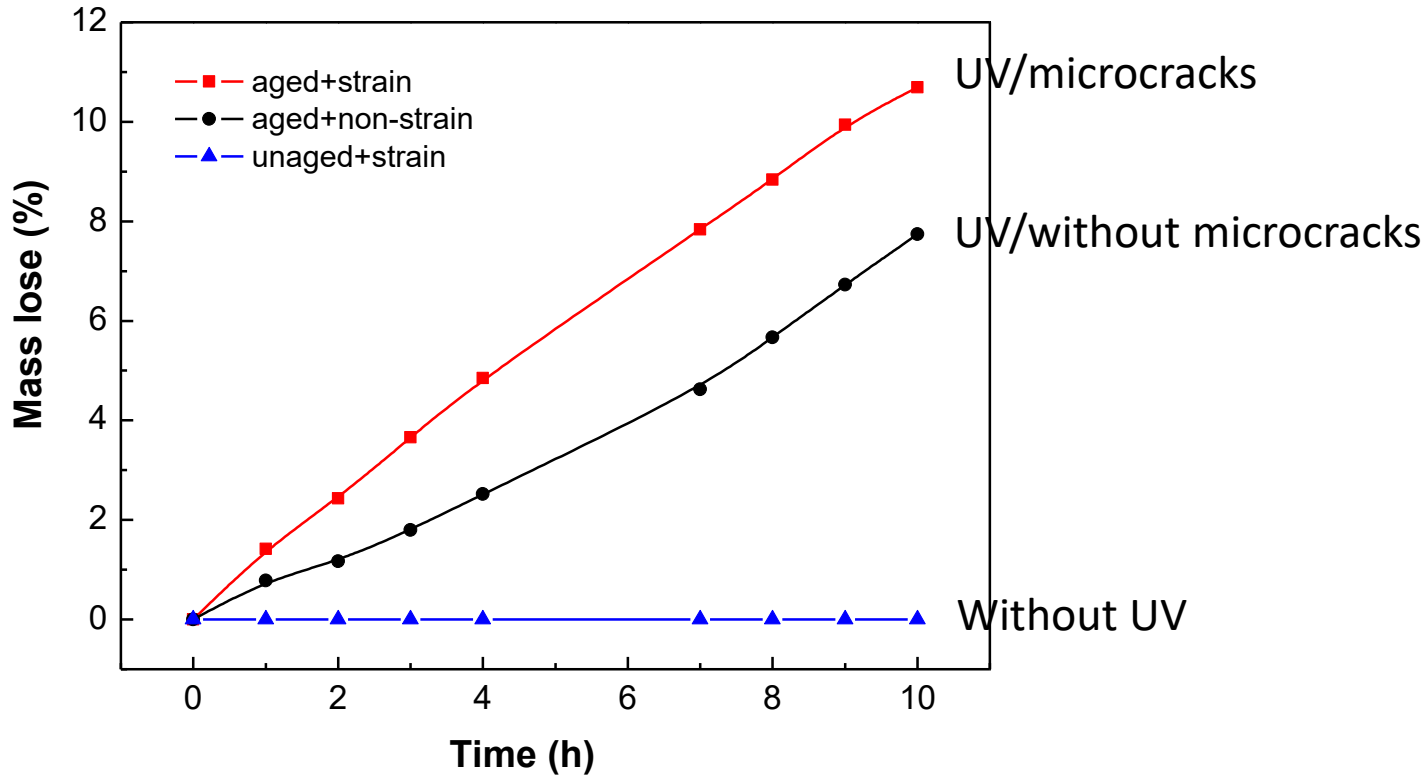

Fig. 27 Mass loss vs. photodegradation time

- **Without UV irradiation, there is no mass loss in stressed sample**
- **After stress induceed cracks, UV leads to more rapid mass loss than the case only UV is involved**

➢ Appearance of sliced samples

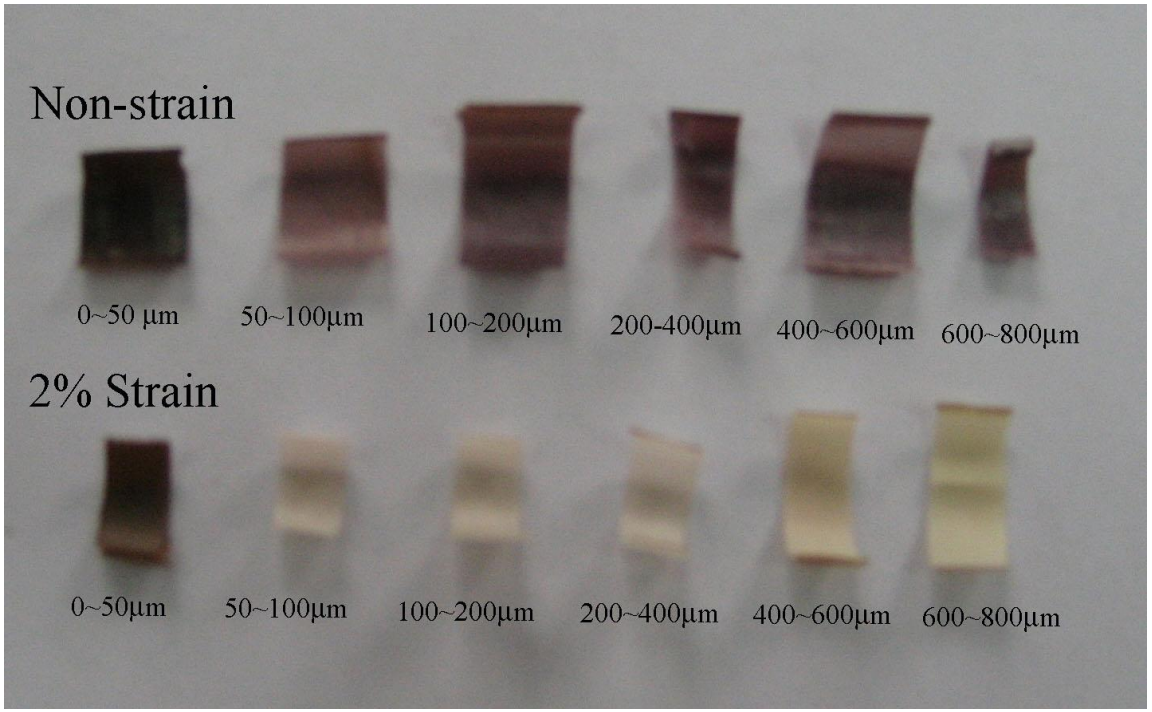

Fig. 28 Color of sliced **sample at different depths** (irradiated for 20 days)

- **The color change caused by chromophore is depth dependent**
- **The stressed samples show a photobleaching effect: darkening color happened only in the surface layer**

➢ Total C=C bonds (n=3~8) by UV-Vis analysis

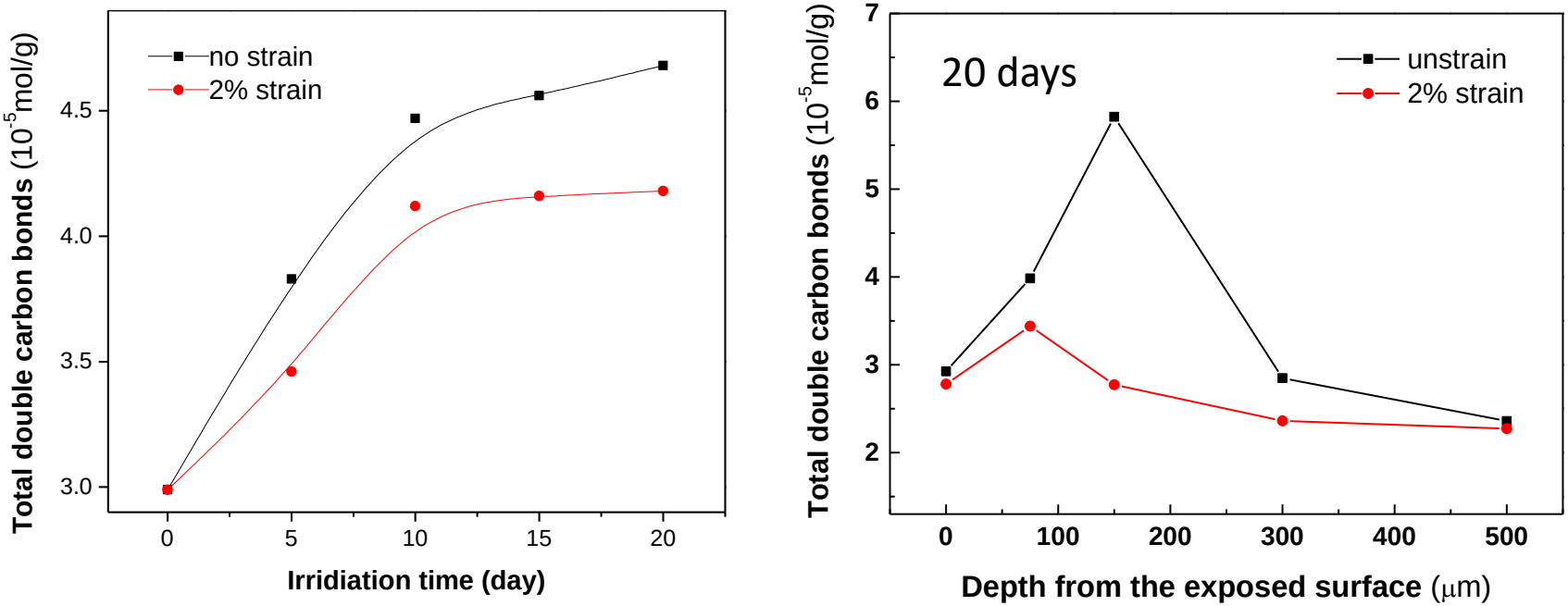

Fig. 29 Total double carbon bonds vs. irradiation time and depth (irradiated for 20 days)

- **Stress promotes the oxidation of C=C bonds and lowers the concentration of double bonds**

- **C=C bonds reach a maximum at subsurface layer due to the competition between oxidation and generation of double bonds**

➢ C=O index by FTIR

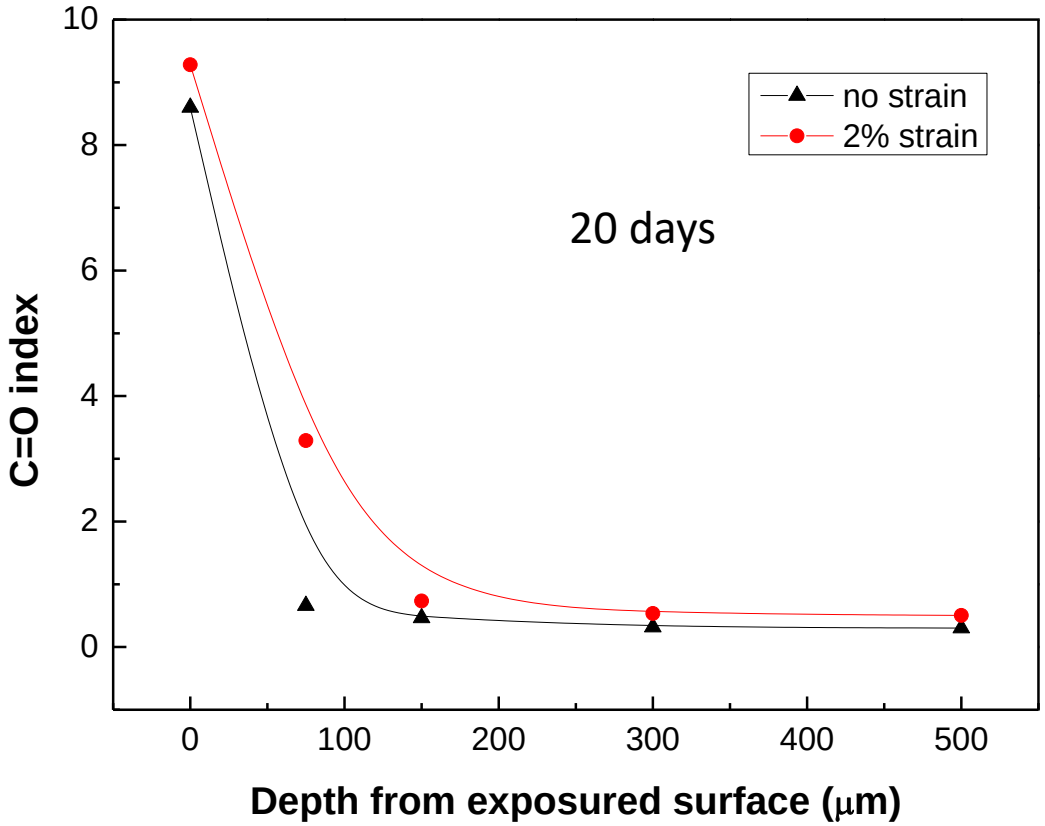

Fig. 30 C=O vs. depth (irradiated for 20 days)

- **Stressed samples have higher content of carbonyl groups**

➢ Impact strength

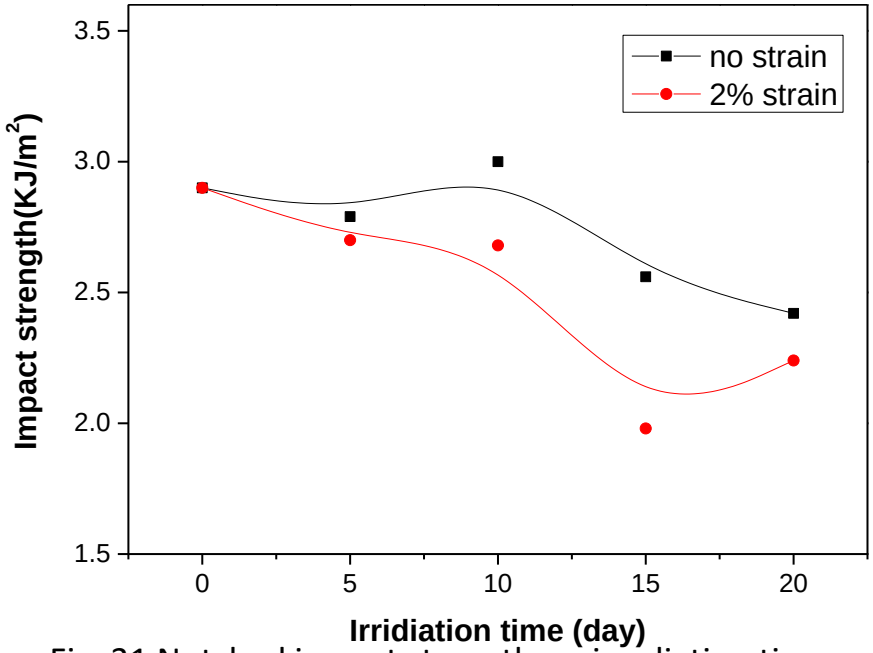

Fig. 31 Notched impact strength vs. irradiation time

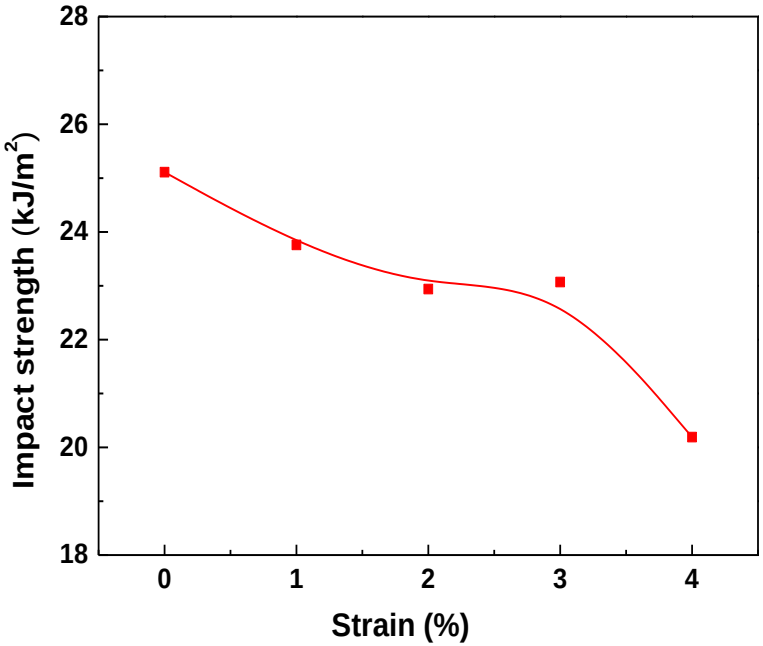

Fig. 32 Notched impact strength vs. strain after 20 days

- **stressed samples have high oxidation-induced degradation, resulting in lower impact strength**

Case 4:
New stabilization methods: novel antioxidant

❑ Synthesis of chemically grafted hindered phenol (HP) with GO

- **Two steps for the synthesis**

(1) GO + $SOCl_2$ ⟶ Activated GO

(2) Activated GO + HP ⟶ GO-HP

(1) Grafting of HP improves the dispersion of GO, which is much better than the physical mixture of GO and AO

(2) GO can immobilize HP, which suppresses the migration of HP (This is a urgent problem for the reliability of long-term service of polymer)

⟵ **Synergistic effects?**

➢ Oxygen permeability of GO-HP

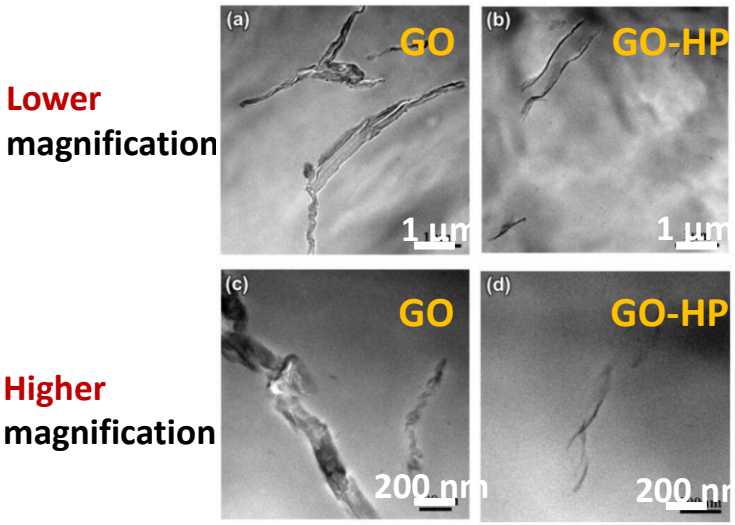

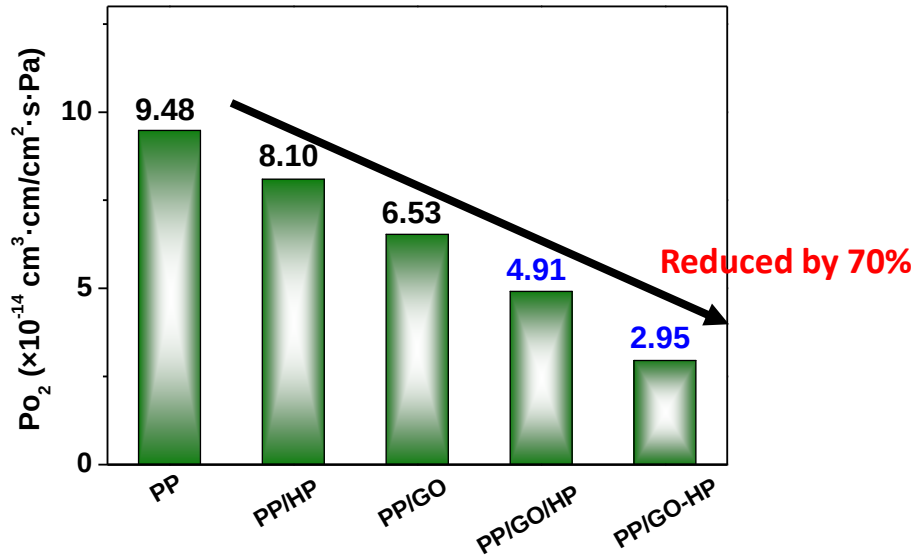

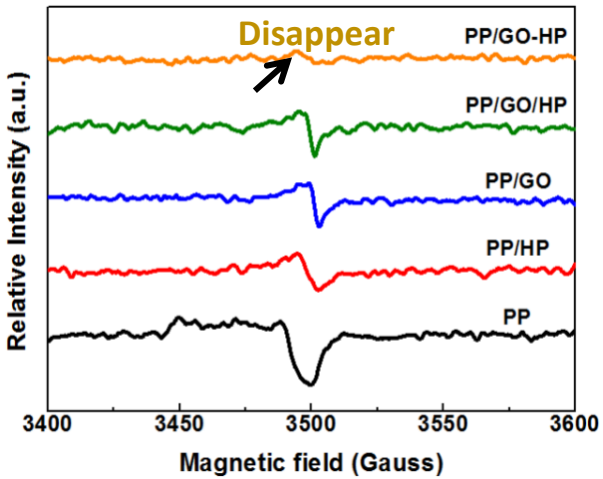

- **PP/GO-HP has much lower oxygen permeability**
- **GO-HP has excellent radical scavenging ability**

Fig. 34 TEM images, oxygen permeability and EPR curves for PP, PP/GO, PP/HP and PP/GO-HP nanocomposites

➢ Photo-oxidation of PP/GO-HP composites

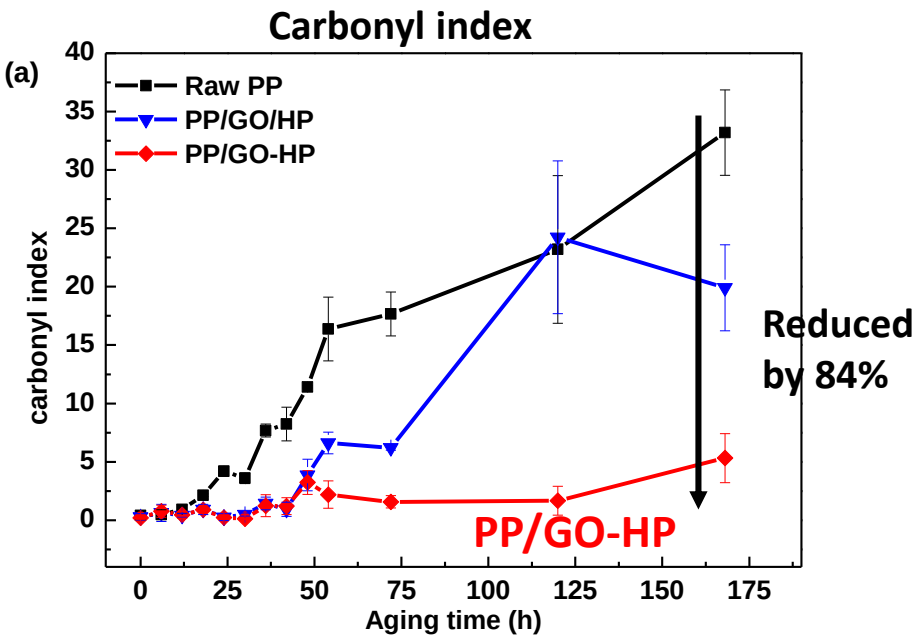

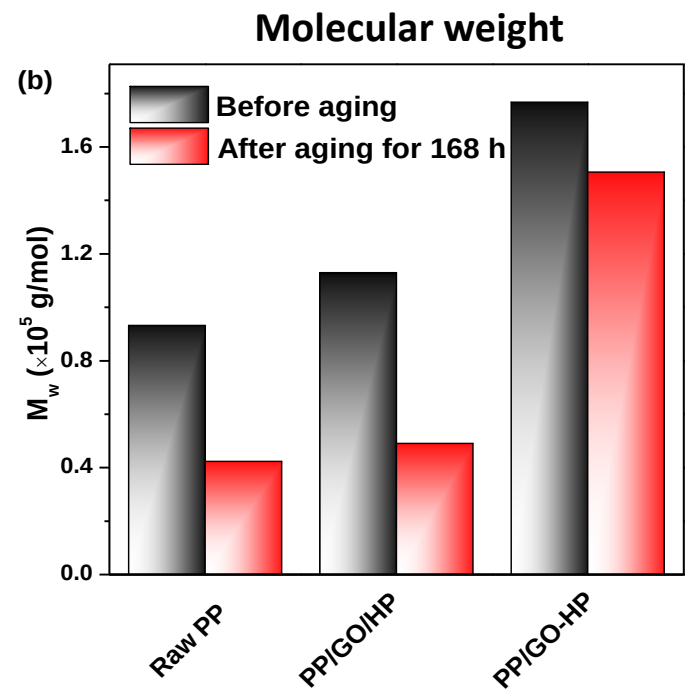

Fig. 35 Carbonyl index and molecular weight for PP, PP/GO, PP/HP and PP/GO-HP nanocomposites **experiencing the same thermal processing procedure** after UV degradation.

- **GO-HP is much more effective to suppressed photo-oxidation than that of the physical mixture**

➢ Thermal oxidation of PP/GO-HP composites

Oxidation induction period (OIT) at 180 °C

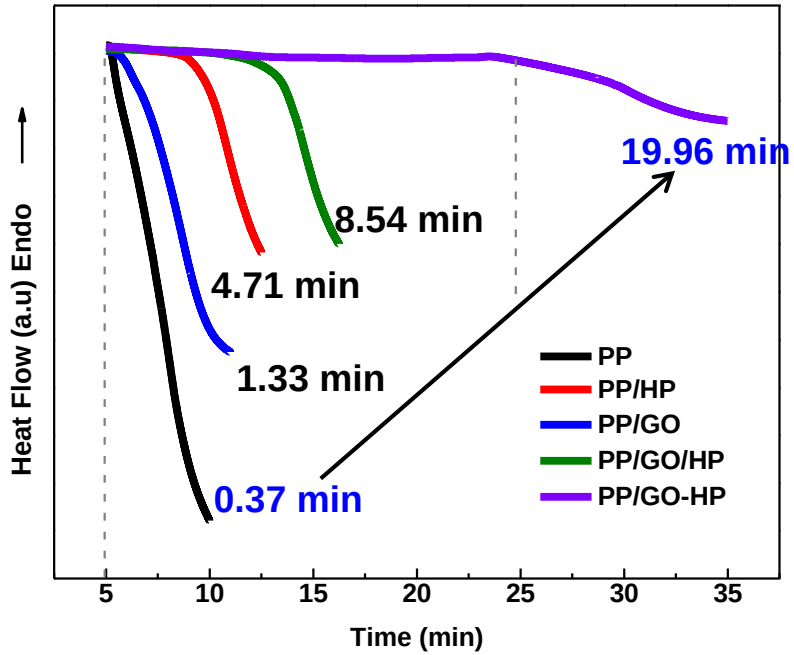

Onset thermal degradation temperature (T_i)

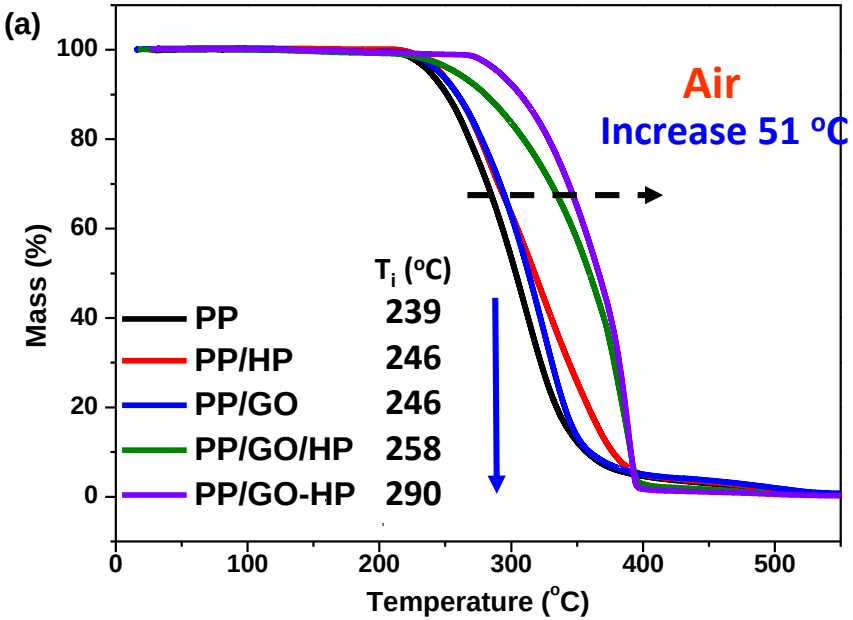

Fig. 36 Oxidation induction period and thermal degradation curves for raw PP, PP/GO, PP/HP and PP/GO-HP nanocomposites

- **Addition of HP-GO improves the thermal-oxidative stability remarkably**

➢ Extraction resistance of GO-HP

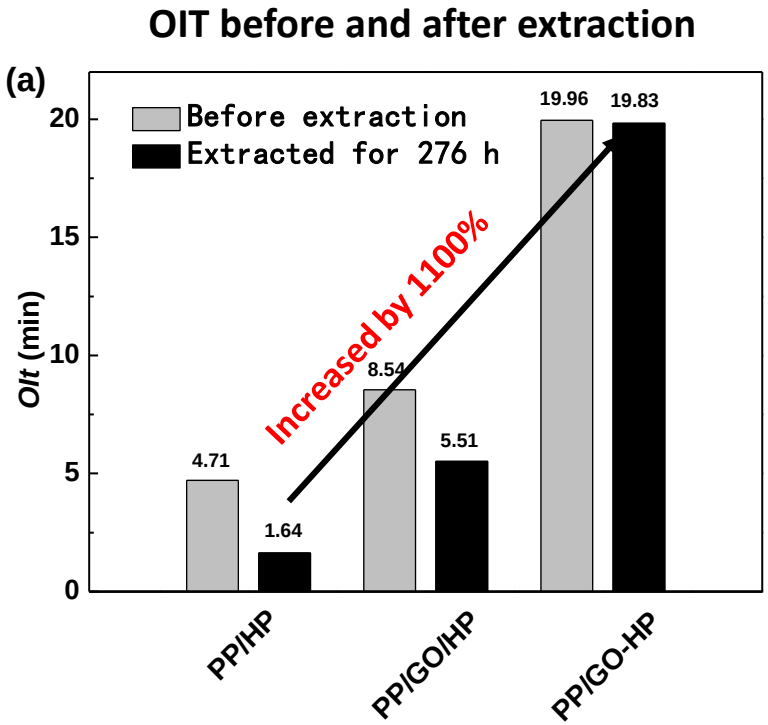

Fig. 37 Oxidation induction period and retention rate for PP, PP/GO/HP and PP/GO-HP nanocomposites after extraction

- **PP/GO-HP effectively reduces the migration and loss of small-molecule antioxidant (long-term stable application)**

➢ Summary of the novel anti-oxidant of GO-HP

- **The grafting HP with GO possessed a high scavenging- radicals ability, strong oxygen barrier property , and excellent anti migration effect which was a major and urgent problem for small molecular antioxidants.**
- **It has much better anti-oxidation effect than that of GO or HP used individually, or that of the physical mixture of GO/HP used**

Case 5:
Outdoor degradation behaviors of different polymers under typical climatic regions in China

➢ The 6 typical climate regions in China

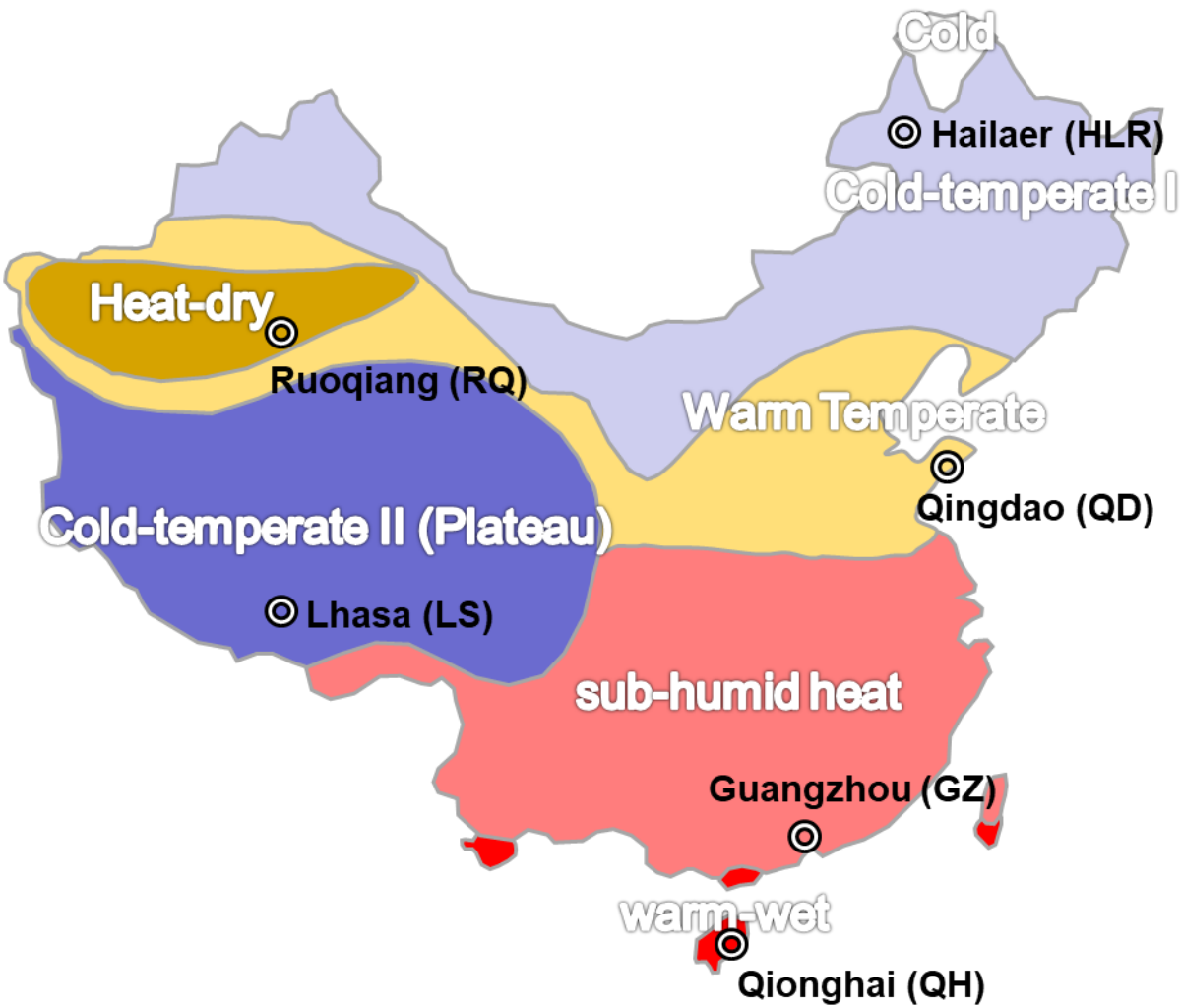

- QH (Hot-wet)
- GZ (sub-humid hot)
- RQ (Hot-dry)
- QD (Warm temperate)
- HLR (Cold-temperate I)
- LS (Cold-temperate II) plateau: Lowest oxygen concentration and highest irradiation

*The classification of climatic types is according to China national standard GB4797 and GB4796-1984

➢ Outdoor weathering stations

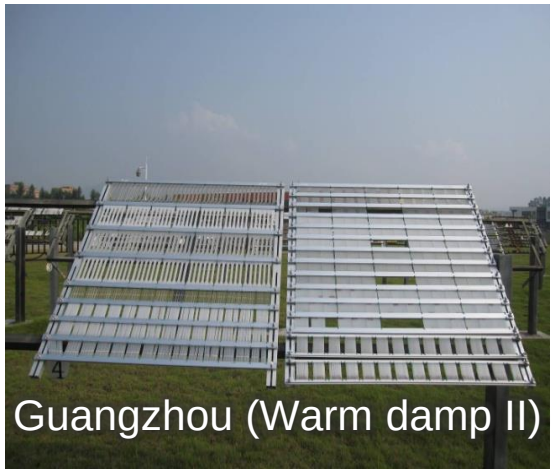

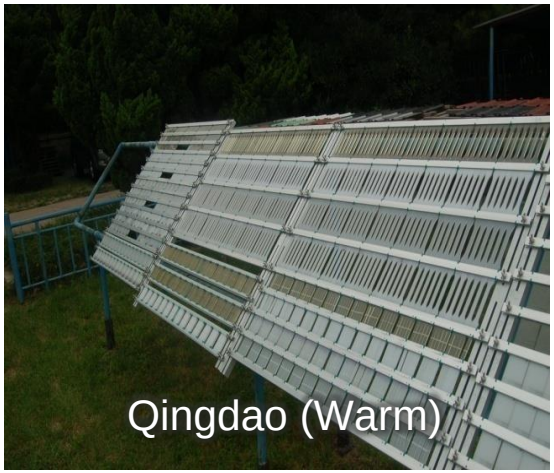

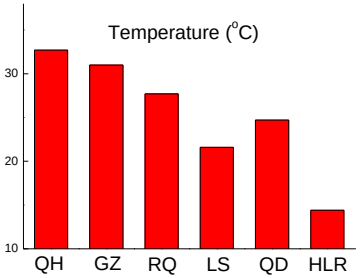

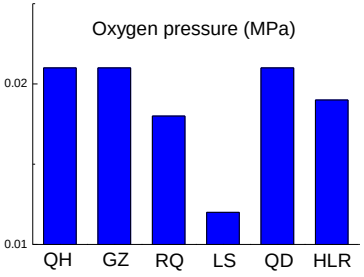

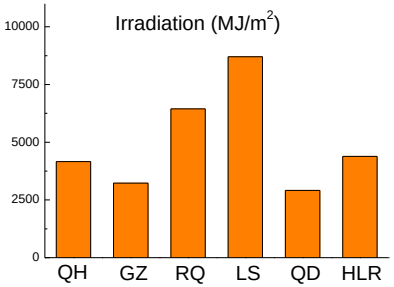

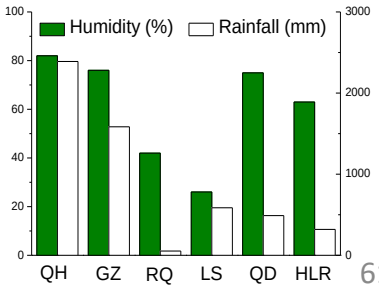

➢ Weathering features for different outdoor stations

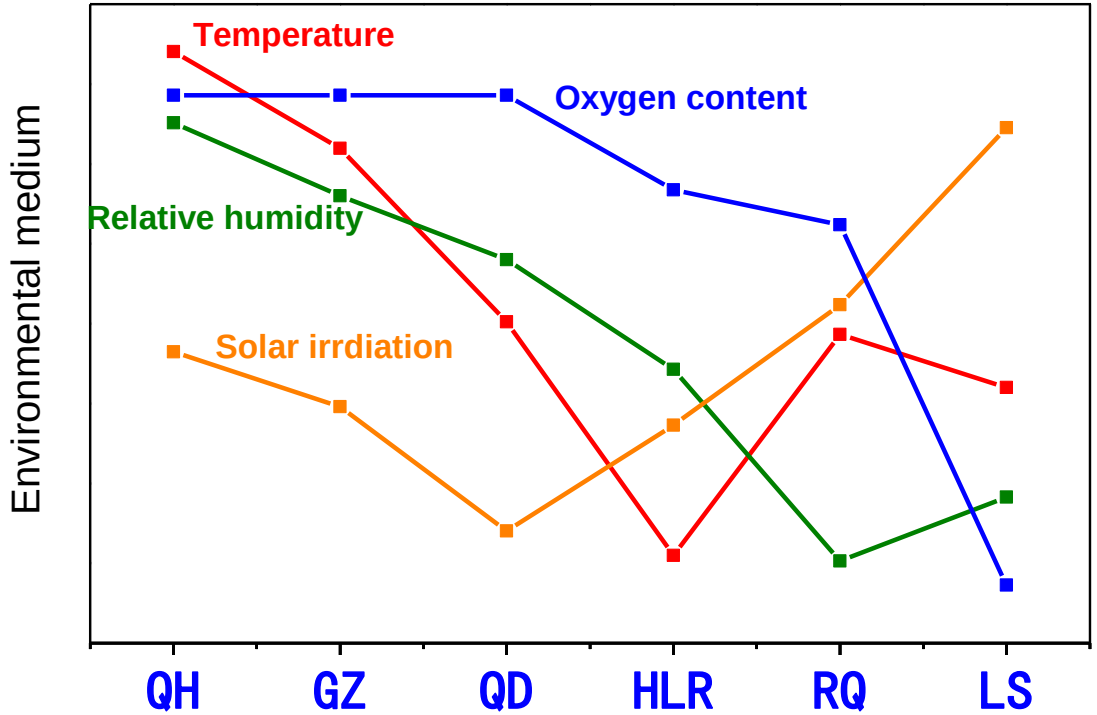

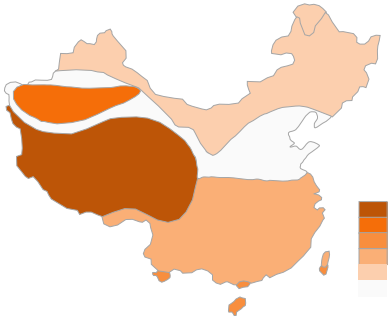

Irradiation (MJ/m²)

Relative humidity (%)

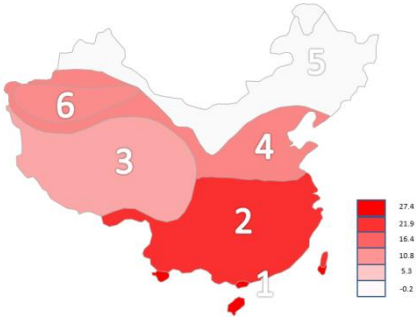

Temperature (°C)

Oxygen content (g/m³)

➢ Samples for field exposure

- Experimental samples: PE, PP, PVC, PS
- Engineering plastic: PA6, PC, ABS
- Coating: Acrylic ester coating
- Rubber: SBR

➢ **Characterization techniques:**

UV-Vis for yellowness index, FTIR for chemical changes, GPC for molecular weight, DSC, WAXS and SAXS for crystal structures, SEM for surface morphology, tensile tests for mechanical properties

➢ Color

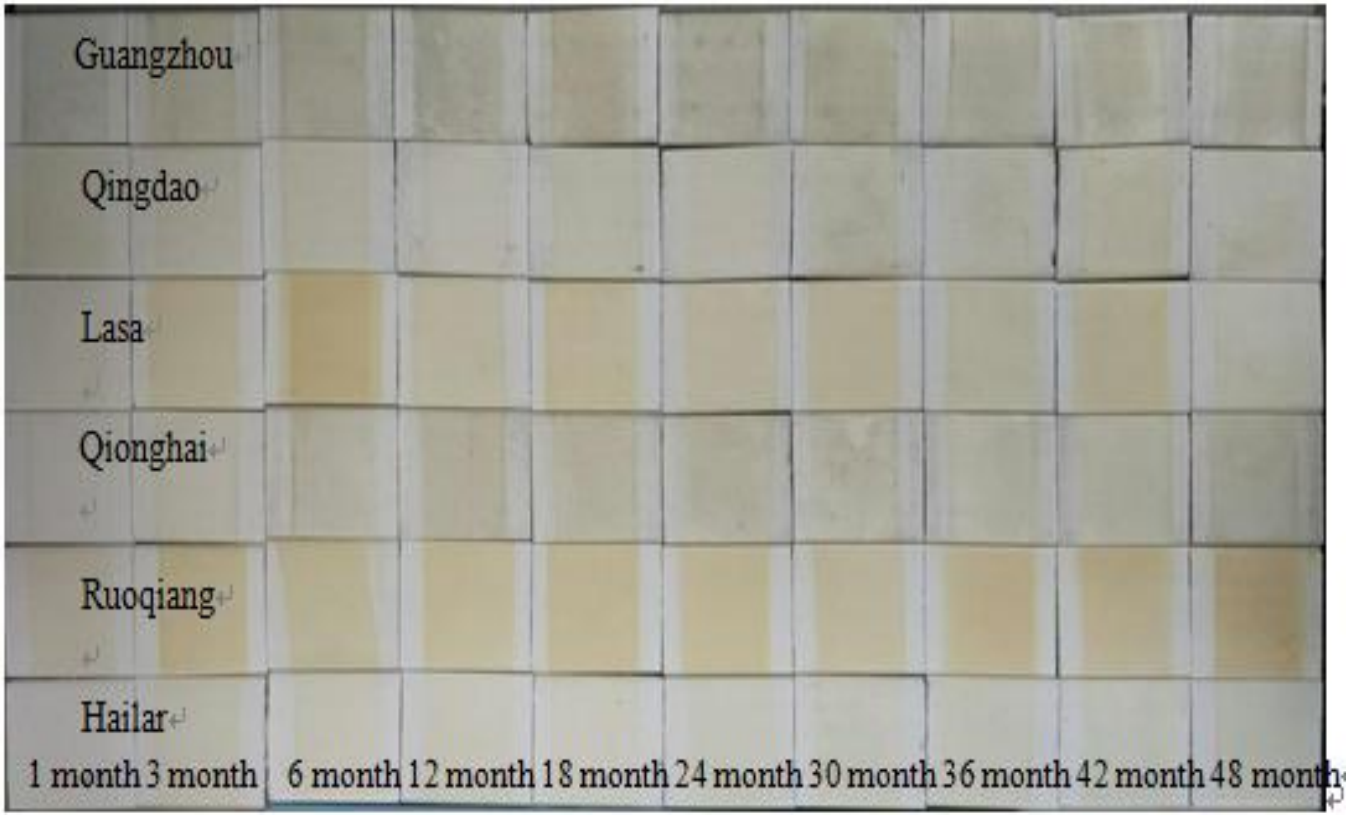

Fig. 38 Digital images showing the color changes vs. aging time for PVC aged under different outdoor climatic conditions

- **Yellowing and darkening of PVC samples occur during aging**

➢ Appearance by SEM

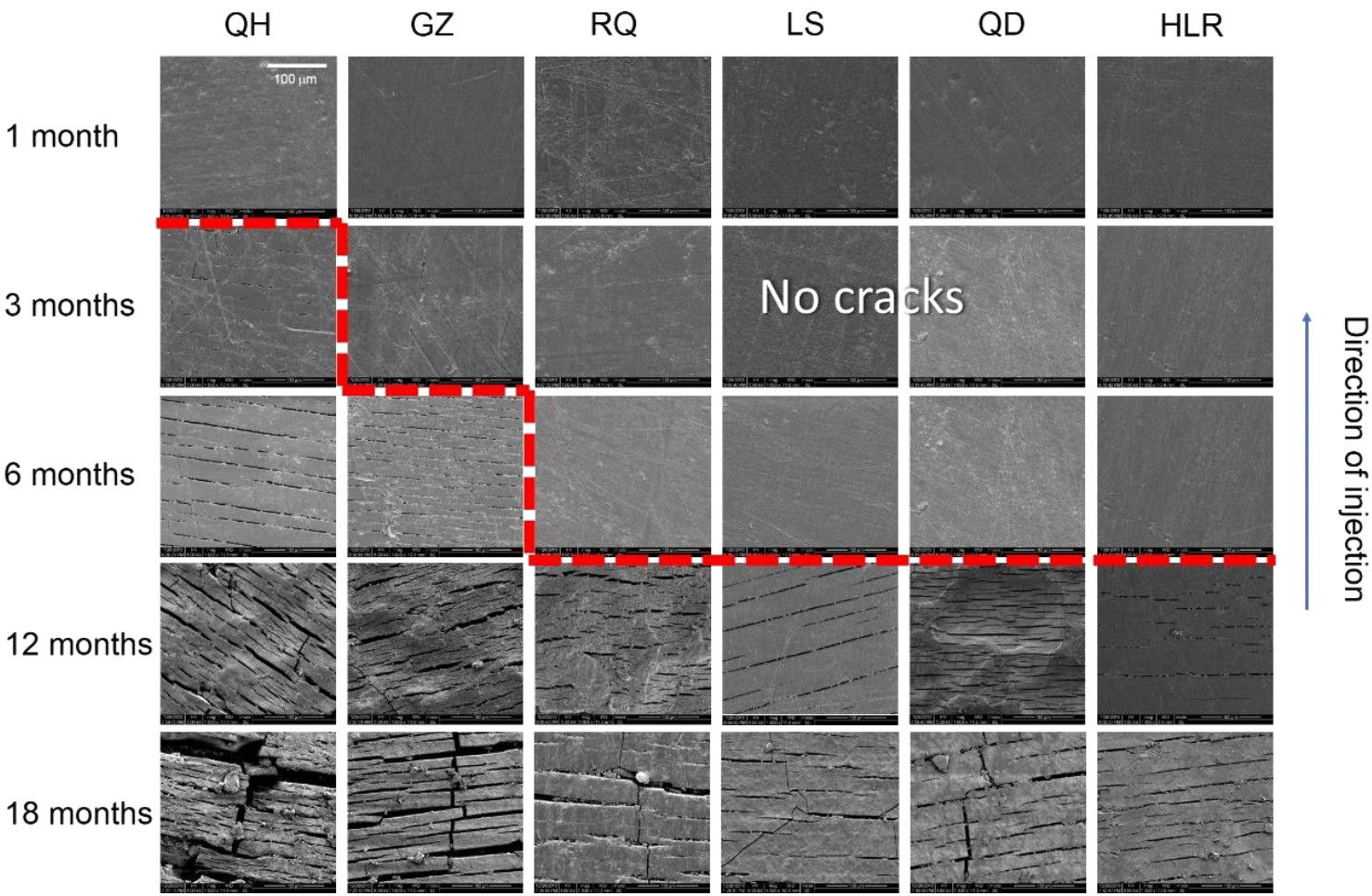

Fig. 39 SEM morphology images vs. aging time for iPP aged under different outdoor climatic conditions

- **Microcracks perpendicular to the injection direction develop during aging**

➢ Mechanical properties

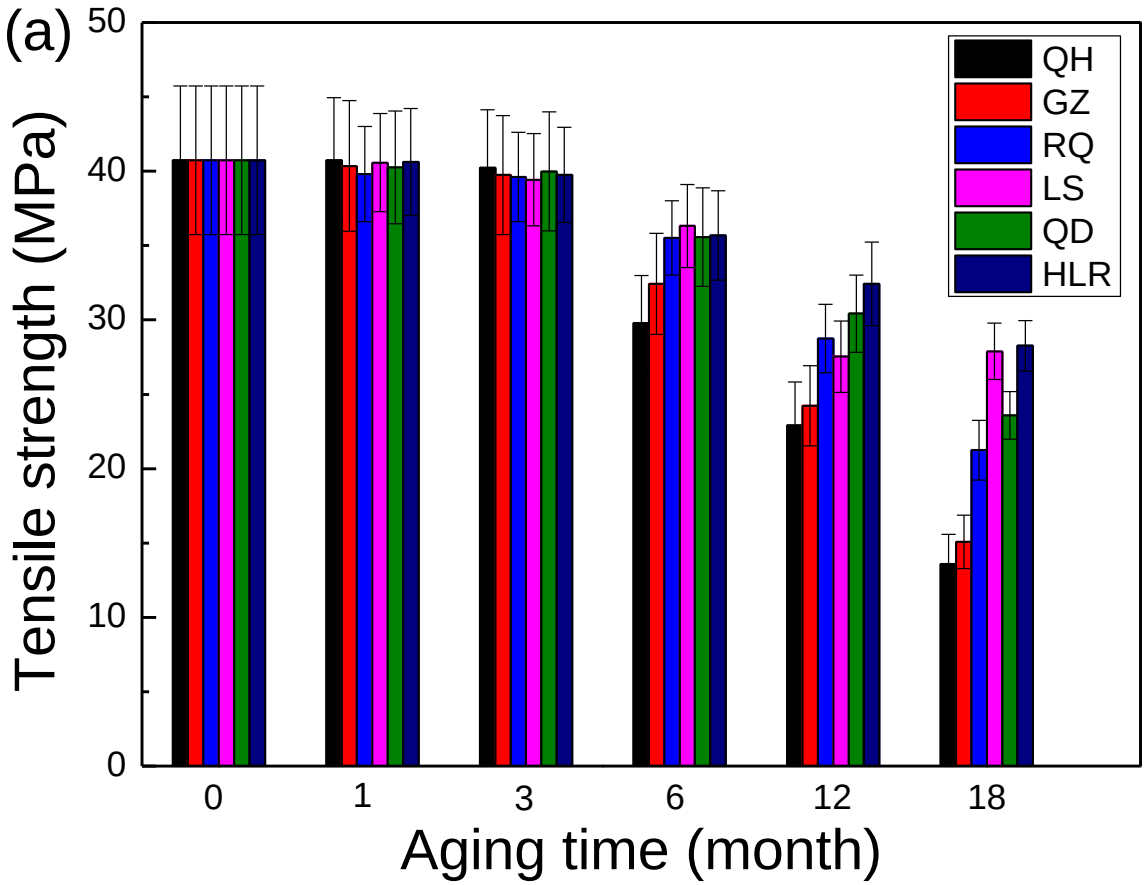

Fig. 41 Tensile strength, flexural modulus and elongation at break vs. aging time for iPP

- **The mechanical properties of iPP deteriorate with exposure time**

➢ Chemical structure

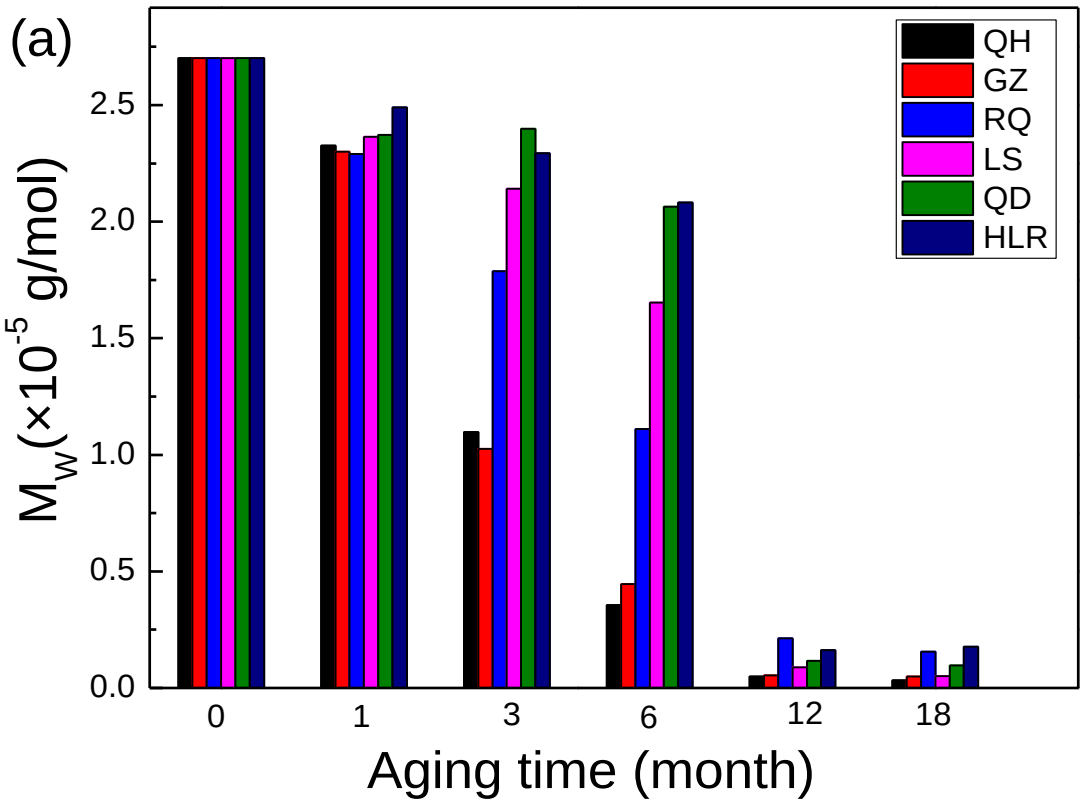

Fig. 43 Molecular weight vs. aging time for iPP

- **Molecular weight of iPP drops gradually with increasing aging time**

Two key issues

Establish a standard method to evaluate the aging degree of polymer materials at different regions

Predict the lifetime of polymers in different regions

1. Establish the measuring standard and map the regional distribution

- **Establishing the relationship between normalized physical quantity *P* and aging time *t*.**

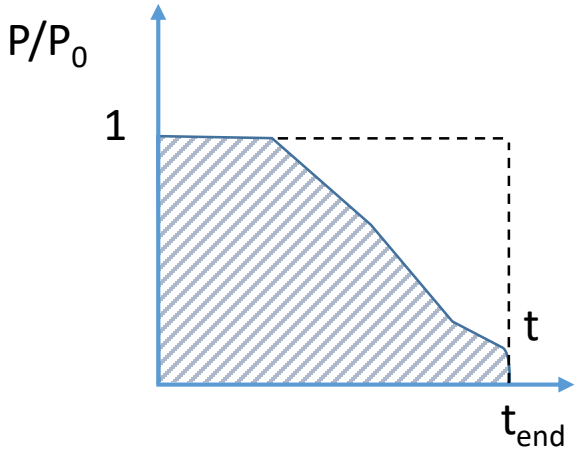

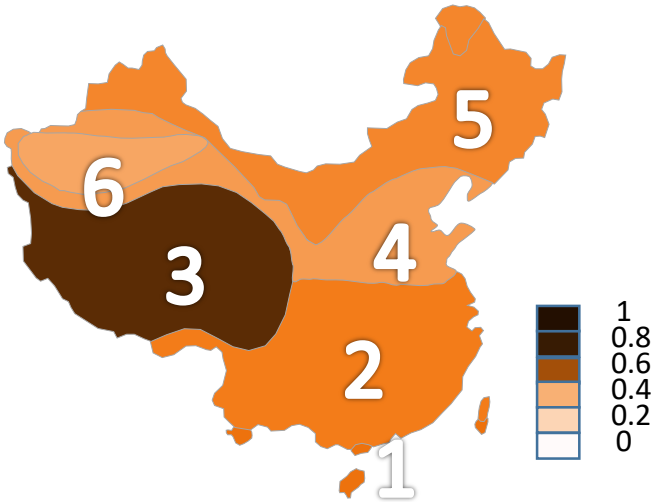

- **Quantitatively converting aging index to intuitive map**

Regional distribution

➢ The aging degree of PE with time at different regions

☐ Elongation at break data of PE at different regions

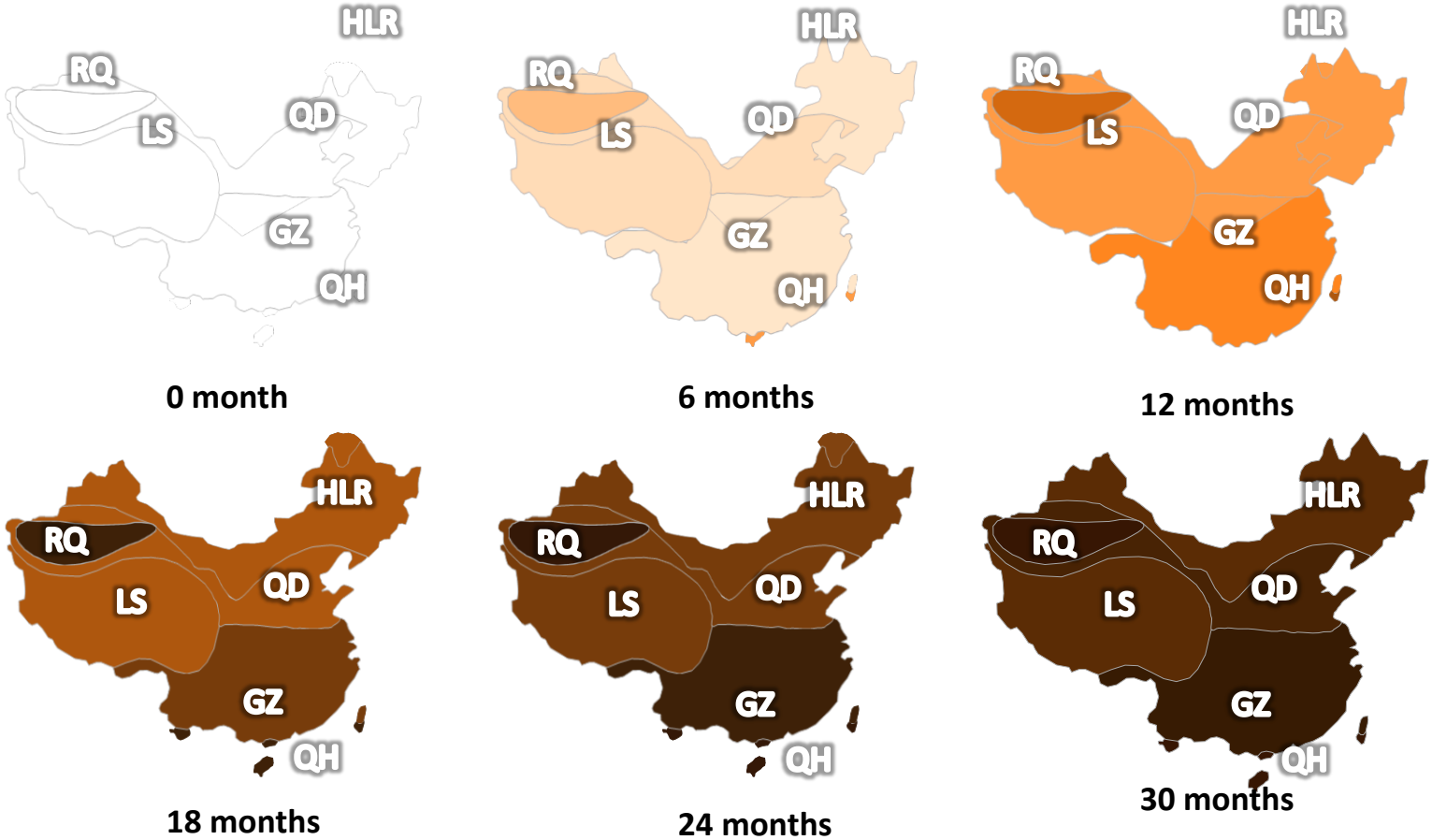

- **With increase of aging time, the aging degree of PE aggravated; aging of PE under heat–dry and humid heat is the severest**

➢ Comparison of elongation at break with yellowness index of PE

☐ **Elongation at break mapping**

☐ **Yellowness index mapping**

(Aging time: 18 months)

- **The sensitivity of different aging indicators of PE is quite different**

➢ The aging degree maps of different raw polymers

- Elongation at break maps

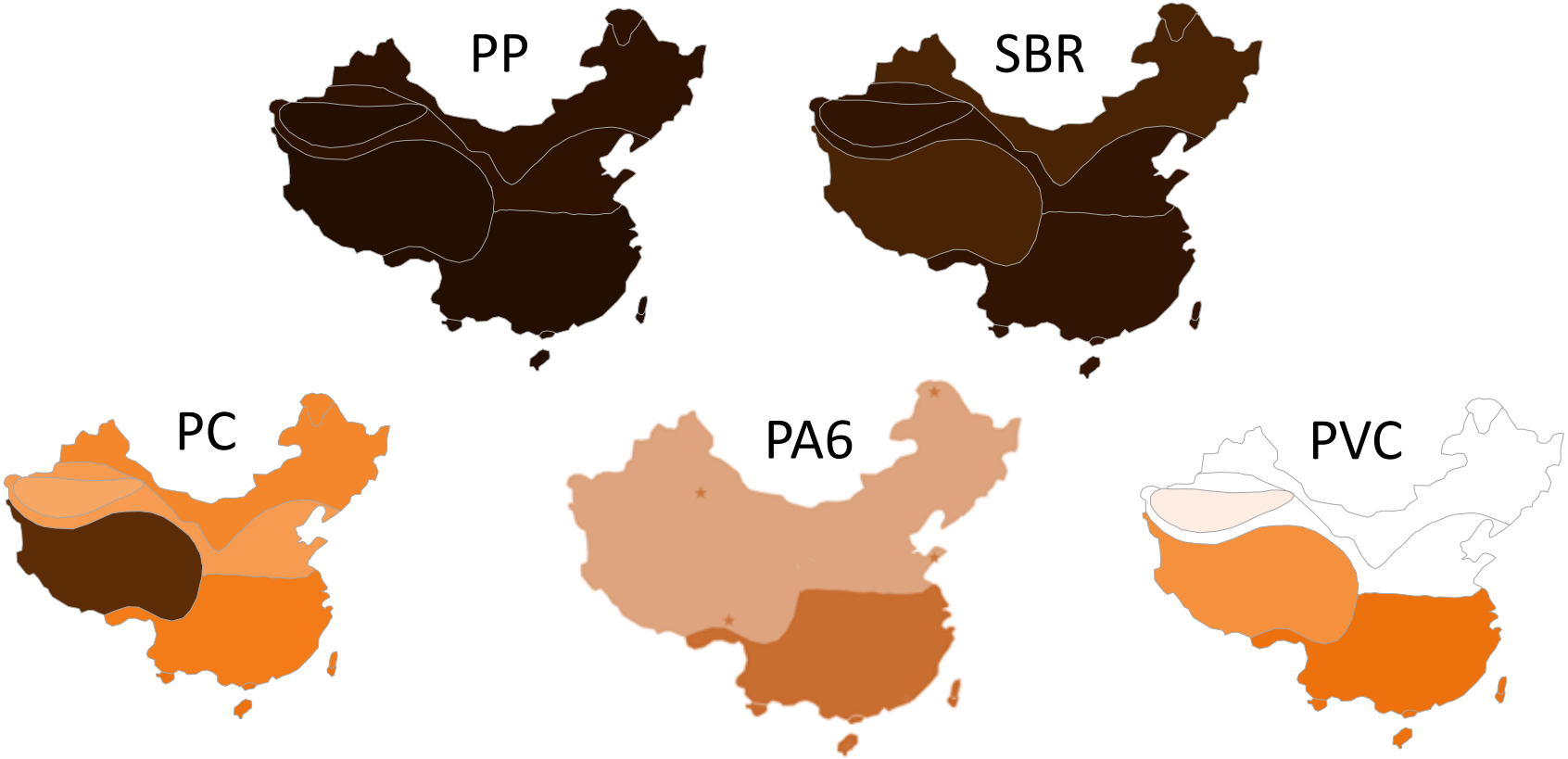

(Aging time: 18 months)

Processed with thermal stabilizer and plasticizer

- **The aging degree of different types of raw polymers varies from sites to sites**

2. Predict the lifetime of iPP based on correlation between indoor and outdoor exposure

- **Comparison of degradation mechanism between indoor and outdoor conditions**

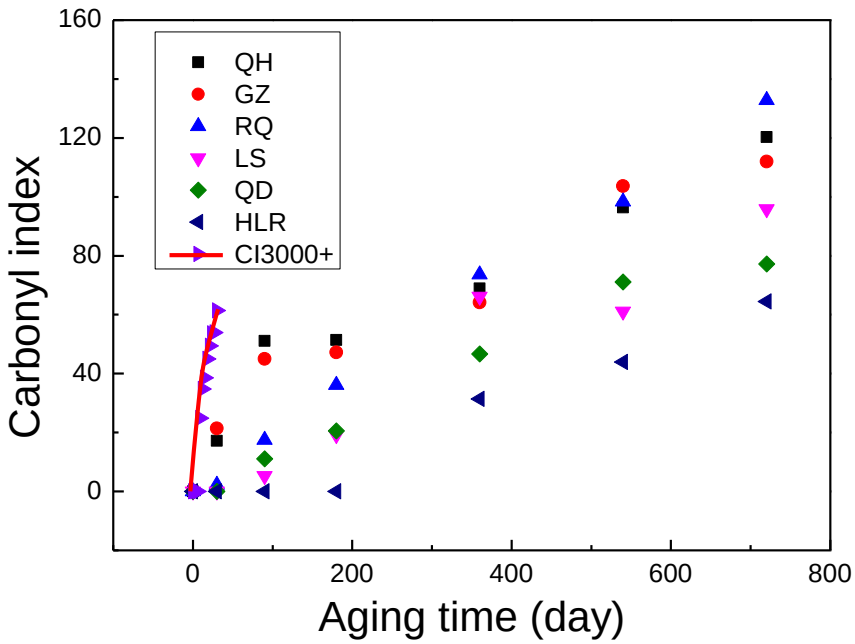

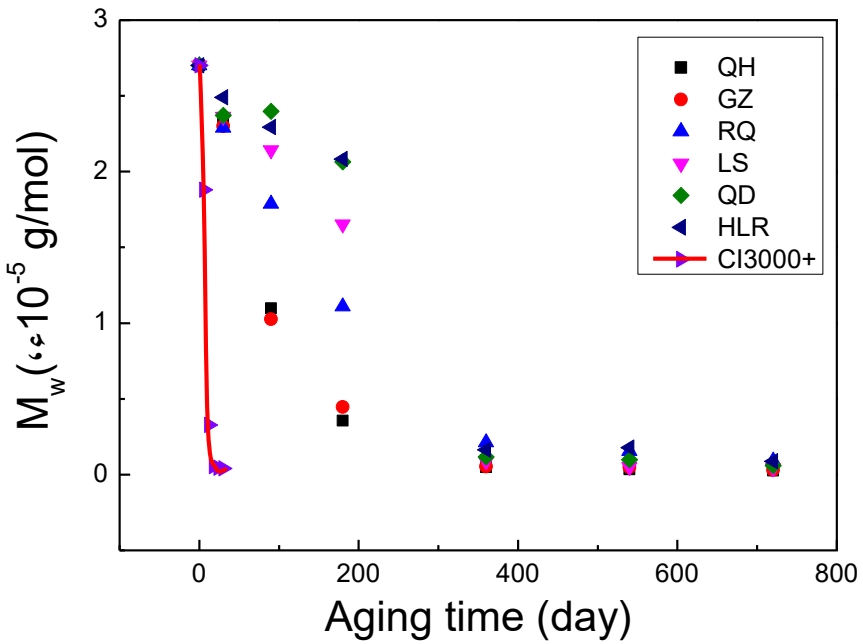

Fig. 44 Carbonyl index and molecular weight vs. aging time for iPP aged under accelerated condition and outdoor conditions

YD Lv, GX Li. *Polymer Degradation and Stability*, 2015, 112, 145

➢ Comparison of the ratio between different degradation products

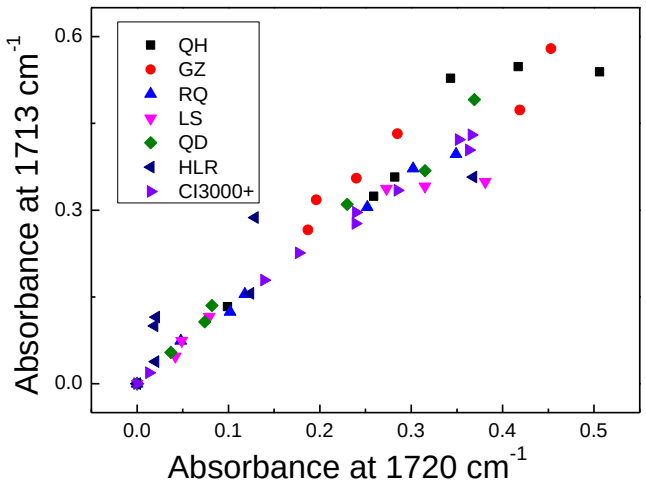

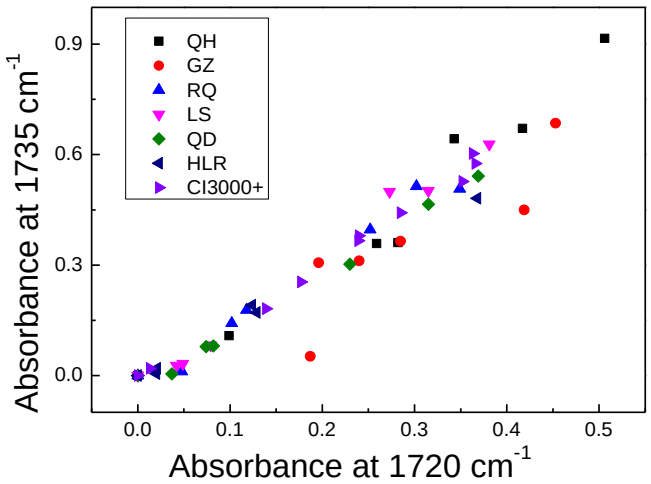

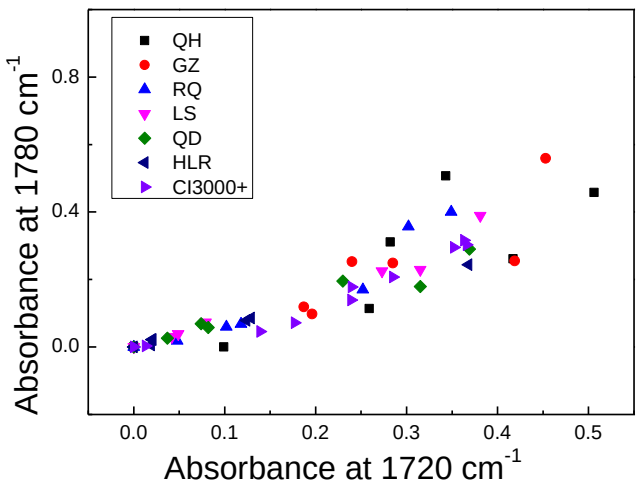

1713 cm^{-1}: Carboxylic acid
1720 cm^{-1}: Ketone
1735 cm^{-1}: Ester
1780 cm^{-1}: Lactone

Fig. 45 Correlation between different degradation products including carboxylic acids, esters as well lactones ketones for all exposure conditions.

- **Accelerated weathering and outdoor weathering show similar carbonyl product concentration ratio, thus a similar degradation mechanism**

➢ A three-parameter equation: considering temperature, irradiation and oxygen concentration

Arrhenius equation(Temperature): $k = Ae^{-E_a/RT}$

Schwarzschild law(Irradiance)

$$k = BI^p$$

Linear law(oxygen concentration)

$$k = CO^q$$

Temperature (T) + Irradiation (I) $k = aI^p e^{-E_a/RT}$

Temperature (T) + Oxygen content (O) $k = bO^q e^{-E_a/RT}$

Temperature (T) + Irradiation (I) + Oxygen content (O)

$$k_{ITO} = a(I)^p e^{\frac{-E_a}{RT}} (O)^q$$

Acceleration factor: $\alpha_{ITO} = \frac{k_{ITO_2}}{k_{ITO_1}} = \left(\frac{I_2}{I_1}\right)^p e^{\frac{-E_a}{R}\left(\frac{1}{T_2}-\frac{1}{T_1}\right)} \left(\frac{O_2}{O_1}\right)^q$

E_a activation energy, R gas constant, *p and q are coefficients related with the materials*, p=0.5~1, q=~1

➢ Lifetime prediction at 6 different sites: carbonyl index

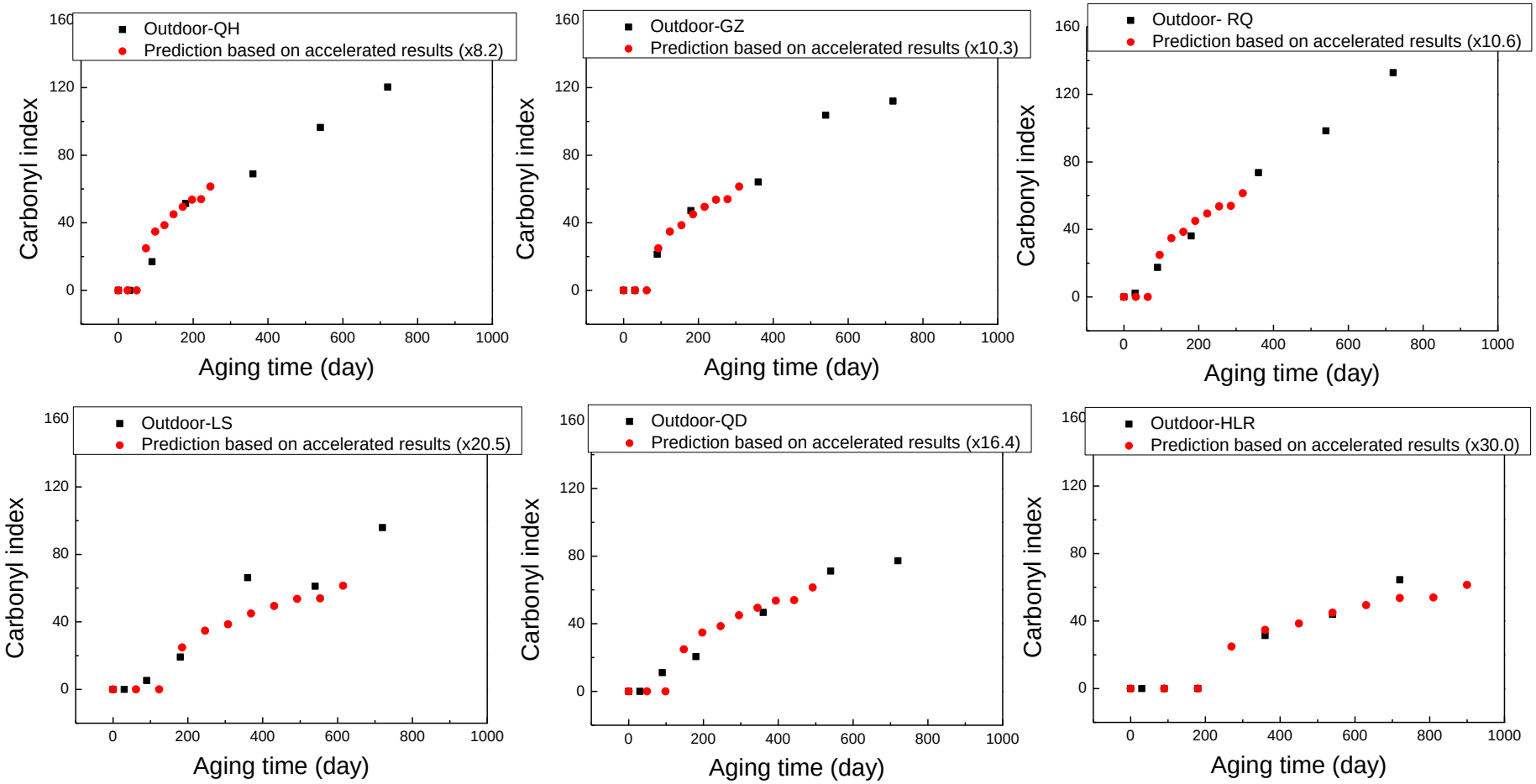

Fig. 46 Comparisons between the outdoor results and the predictions based on the accelerated laboratory results for carbonyl index.

- **Satisfactory predictions based on three-parameter Arrhenius equation are obtained**

➢ Lifetime prediction at 6 different sites : molecular weight

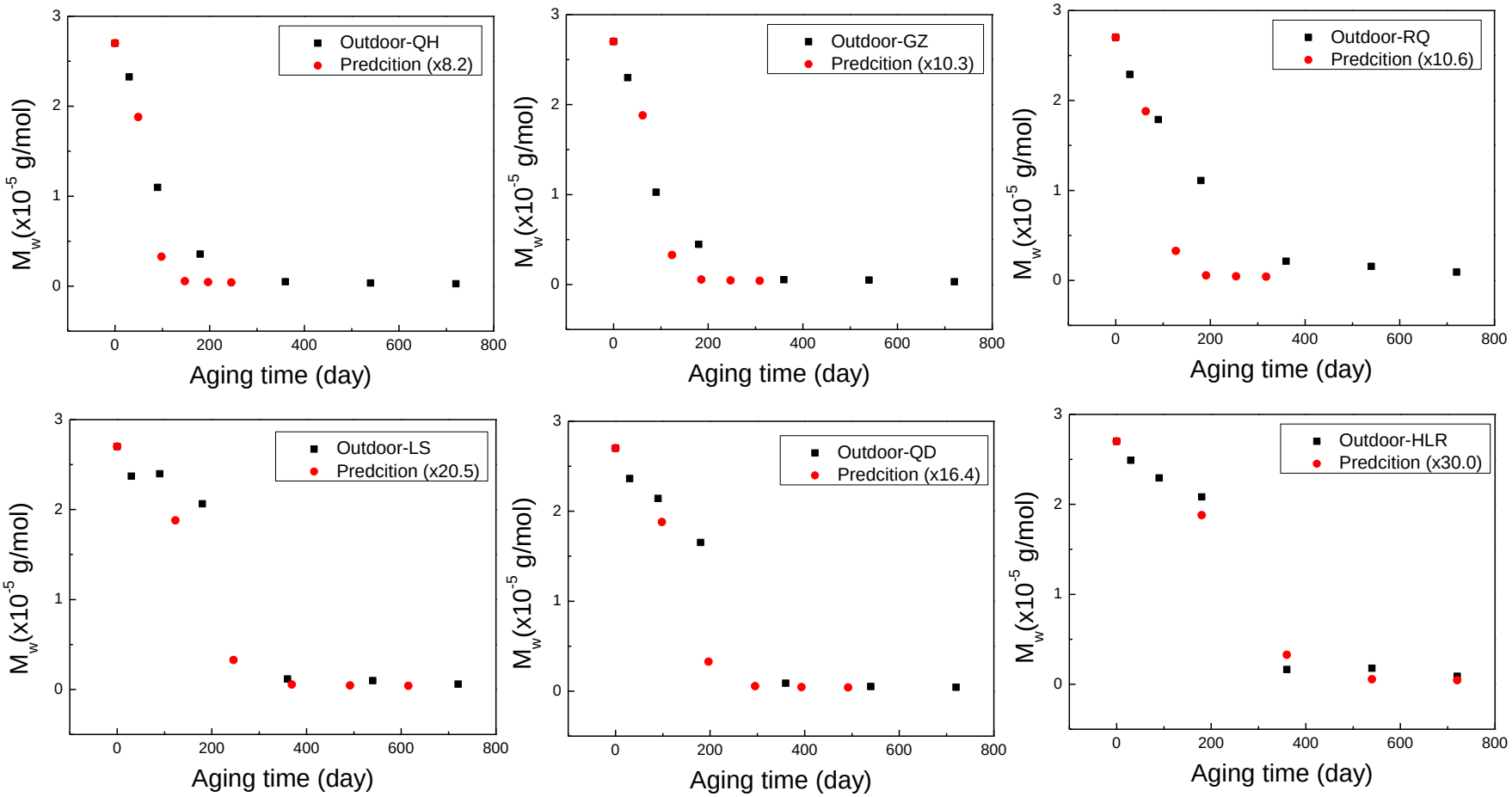

Fig. 47 Comparisons between the outdoor results and the predictions based on the accelerated laboratory results for molecular weight

- **Predictions based on three-parameter Arrhenius equation are satisfactory**

Conclusions

- Controlling the diffusion channel by structuring the aggregations is an efficient way to prevent degradation of polymers. It can effectively block the diffusion channels for aging factors (O_2, H_2O, solvent etc.), which resist the photo- and hydrothermal oxidation process.

- A new stabilization route for polymers was developed by grafting antioxidants onto functionalized graphene, which is better than traditional anti-aging agents in preventing polymer from degradation.

- A method to map the regional distribution of aging degree of different polymers was established, and a three-parameter lifetime prediction model based on Arrhenius equation was successfully constructed, which was well verified by the outdoor data

Acknowledgement

- National Natural Science Foundation of China (NSFC, 51133005, 50533080)
- Foundation for Innovative Research Groups of the NSFC (51421061)
- Dr. Yajiang Huang, Yadong Lv, Junlong Yang
- Graduated students Qiang Liu, Shixiang Liu, Jialu Yao

Thanks for your attention !

Prediction with and without considering the oxygen effects

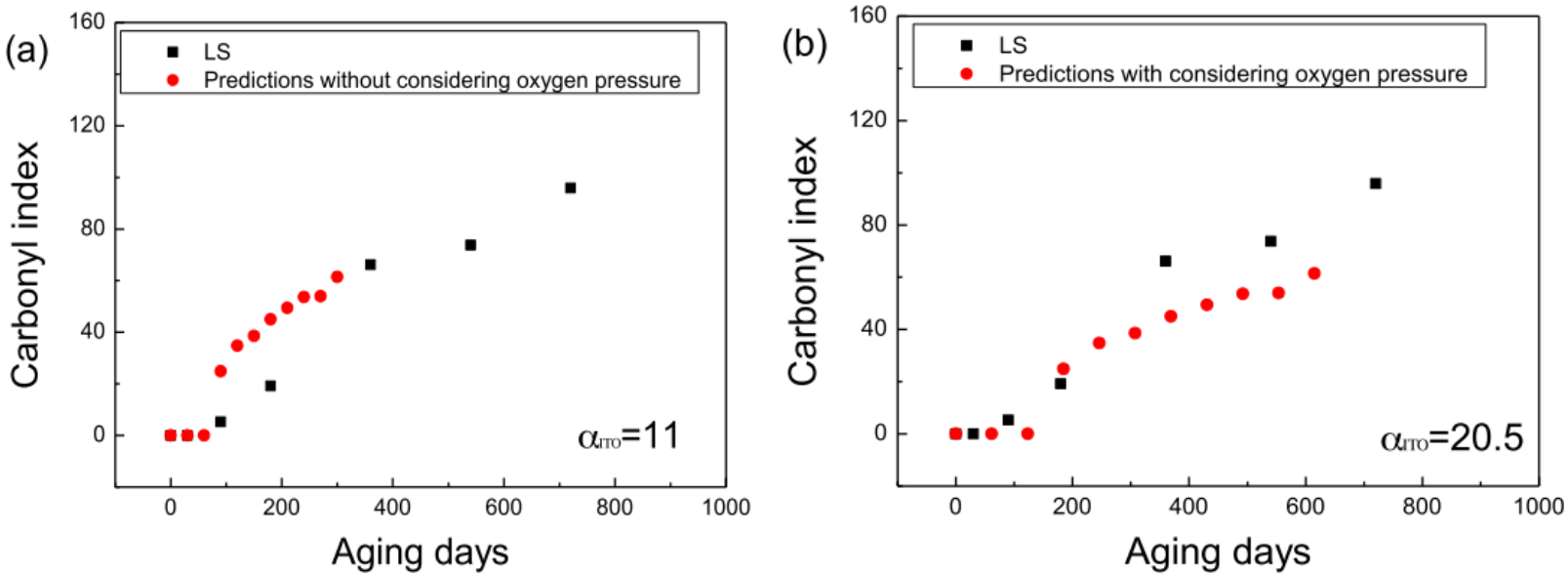

➢ Characterization of GO-HP

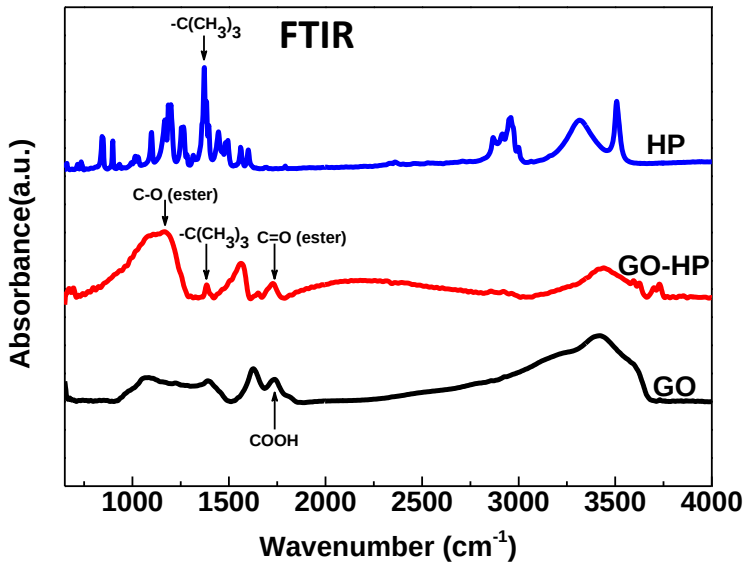

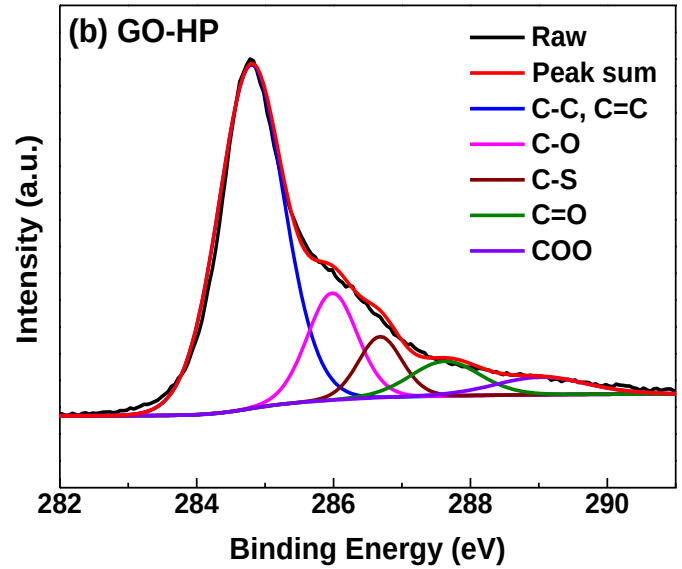

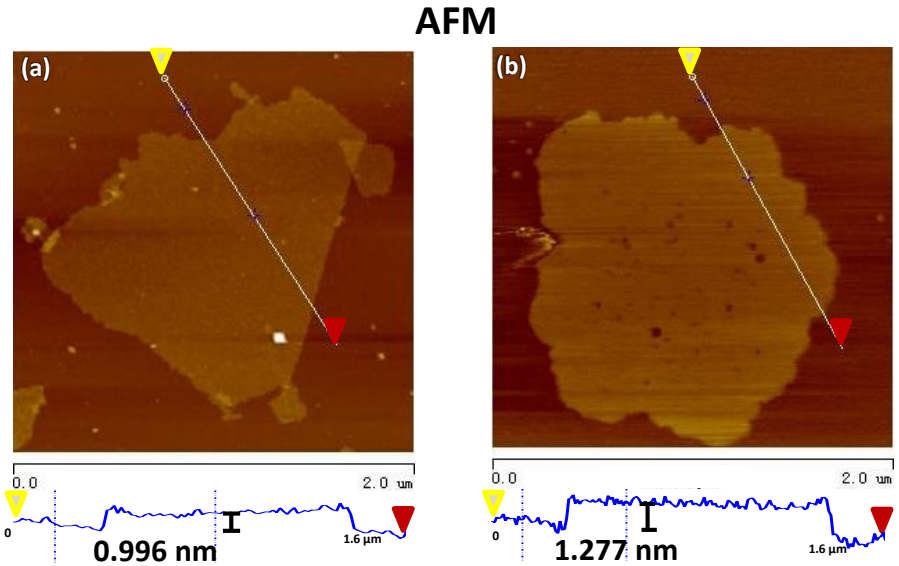

Fig. 33 FTIR curves, XPS curves and AFM height images for GO-HP.

- **Successfully prepared GO-HP**